MECHANISTIC AND ELECTROCHEMICAL STUDIES OF THE REDUCTION OF CARBON DIOXIDE AS CATALYZED BY Ni(I)CYCLAM$^+$

Thesis by

Gabriel Bryan Balazs

In Partial Fulfillment of the Requirements

for the Degree of

Doctor of Philosophy

California Institute of Technology

Pasadena, California

1993

(Defended July 31, 1992)

"There is something fascinating about science. One gets such wholesale returns of conjecture out of such a trifling investment of fact."

Mark Twain "Old Times on the Mississippi"

"The grand aim of science is to cover the greatest number of empirical facts by the logical deduction from the smallest number of hypotheses or axioms."

Albert Einstein, *Life*, January 9, 1950.

Acknowledgements

This section of the thesis is one of the most difficult to write because I have to decide who to include, and who cannot be included because of space limitations. Obviously, a great number of people have influenced and helped me during the past six years, and I apologize to those who "did not make the list."

Professor Fred Anson deserves a great deal of credit for teaching me electrochemistry from ground zero, and for his patience as I pursued other aspects of life (or maybe he didn't know??). Special thanks go to Dr. Henry D. Schreiber, my undergraduate advisor and mentor for many years, as well as a special friend. I am indebted to Professor Dennis Evans for his useful comments, especially with regard to chapter four. One piece of equipment was used extensively for this research, and I have to thank Dr. Dave Malerba for building the damn thing and Tom Dunn for restoring it to a functional state on several occasions. In addition, I give a heartfelt round of applause for all of the support personnel in the chemistry department here at Caltech, especially the secretaries and the guys in the shops.

There are several women in my life who I would like to acknowledge at this point, and all of them are named Susan (Desperately Seeking Susan???) Susan Russell deserves credit for teaching me innocence and discovery. Susan Carlson (and John & Rosalee) showed me the meaning of an adult relationship. She taught me the value of giving and the value of forgiveness, ultimately (I'm sorry about the timing, bones). And of course, Sue Clevenger, the quintessential "bad rabbit." She taught me maturity and a glimpse of the happiness a woman can bring into a man's life. Along the way, I also learned the meaning of the phrase, "Hell hath no fury like a woman scorned." If she had not rode my back to finish school, I would probably still be at Caltech for quite some time.

I have no intention of thanking Budweiser or any other beer, but there are several inanimate objects that deserve acknowledgement. I give thanks to my '69 Fiat and all of the fifteen other vehicles I owned while at Caltech (special thanks to Zeke the Deep Breather) for taking me over 100, 000 miles to who the hell knows where. And I guess I should give thanks to Homer, Marge, Bart, Lisa & Maggie and to Solarian II (yesss...) and Spectre.

I especially want to thank the following people for helping me make it through:

-My parents, without whom I wouldn't be writing this,

-Amy Hoffman, for being a true friend and helping me sort out life, and to Greg for letting her,

-Ken Graham, for his strength and torque wrench and the ability to "go on a mission,"

-David "I don't like perky women" Conrad, for helping me to figure out women (yeah, right),

-John Bart, for "Good Feed,"

-Ramy "That's Greeaattt!!" Farid, for "Pie 'n' Burger."

and to all of the other members (past and present) of the Anson group-Thanks!!

Abstract

A detailed electrochemical investigation of $Ni(cyclam)^{2+}$ and its derivatives is described, especially with regard to the aqueous electrocatalytic reduction of CO_2 at mercury. Detailed chronocoulometric studies which quantify the extent of the adsorption of the active catalytic species $Ni(cyclam)^{+}_{ads}$ are discussed. $Ni(cyclam)^{2+}$ is only weakly adsorbed at mercury and in quantities substantially less than a monolayer. In contrast, $Ni(cyclam)^{+}$ is adsorbed over a wide potential range and the adsorption process occurs in two potential dependent stages. An analysis of the kinetics of the adsorption process is discussed.

In the presence of CO, $Ni(cyclam)^{2+}$ is electrochemically reduced to $Ni(cyclam)^{+}$-CO and $Ni(cyclam)^{0}$-CO. This latter species is insoluble and precipitates on the electrode surface. Both of these species are chemically unstable and slowly react to form $Ni(cyclam)^{2+}$ in the presence of oxidizing agents.

$Ni(cyclam)^{+}_{ads}$ catalyzes the reduction of CO_2 to exclusively CO. In unbuffered solutions, the OH^- ion produced as a result of the reduction of CO_2 can decrease the flux of CO_2 molecules to the electrode surface by direct reaction with CO_2 to form HCO_3^- or CO_3^{2-}, both of which are catalytically inactive towards reduction by $Ni(cyclam)^{+}_{ads}$. In both buffered and unbuffered solutions, the precipitate $Ni(cyclam)^{0}$-CO which is formed on the electrode surface under all conditions where CO_2 is reduced causes a slow passivation of the electrode surface towards further catalytic reduction of CO_2.

The binding of CO_2 and CO to $Ni(cyclam)^{2+}$, $Ni(cyclam)^{+}$, and $Ni(cyclam)^{+}_{ads}$ is discussed. The active catalyst, $Ni(cyclam)^{+}_{ads}$, is able to coordinate CO_2, but not the product of the reduction, CO. Both $Ni(cyclam)^{2+}$ and $Ni(cyclam)^{+}$ are unable to coordinate CO_2 and thus solution species are not important in the catalytic cycle. A comparison of these results with previous studies is given and an overall mechanism for the electrocatalytic reduction of CO_2 is proposed. This mechanism contains several important modifications from earlier studies.

Table of contents

List of Figures

Chapter 1

Chapter 2

Chapter 3

Chapter 3 Figures (cont.)

Chapter 4

Chapter 5

List of Tables

Chapter 2

Chapter 5

Chapter 1

Introduction

This thesis has been organized into five chapters. The current chapter reviews the background literature and the stimulus for the research which is the subject of the thesis. Next, the electrochemistry of the $Ni(cyclam)^+$ catalyst and related compounds at a mercury electrode-water interface is discussed in chapter two. Chapter three discusses the electrochemistry of $Ni(cyclam)^{2+}$ and $Ni(cyclam)^+$ in the presence of CO and CO_2. Chapter four addresses a related area: that of the unusual electrochemistry of the free ligand cyclam at a mercury electrode. Finally, chapter five discusses the mechanism and kinetics of the electrocatalyzed reduction of CO_2 and is also provided as a unifying chapter for the entire thesis.

1.1 *Historical Overview*

The reduction of carbon dioxide is a promising route to the production of organic compounds for energy storage and to the formation of building blocks for more complex molecules. Carbon dioxide is the most abundant form of carbon on the Earth's surface (typical estimates are 10^{17} moles[1]) and is therefore a plentiful resevoir for C_1 compounds. However, the transformation of CO_2 to more reduced forms does not occur readily. Carbon dioxide is a relatively inert molecule[2] and its reduction requires reducing agents which are quite high in energy. Thus, the main thrust of recent research in this area has focused on finding efficient methods for the activation of this molecule towards reduction.

The electrochemical reduction of carbon dioxide at a metal cathode is one method for effecting this transformation. In many instances, the first step of the direct reduction

involves the formation of the radical anion,[3] as shown in Equation (1).

$$CO_2 + e^- \longrightarrow CO_2^-\cdot \qquad (1)$$

In many instances, the kinetics of this reaction are very slow and a large overpotential is required to achieve reasonable current densities. This reduction potential is at least -2.0 V vs SCE in water[4] and -2.2 to -2.6 V vs SCE in non-aqueous solvents.[5] Historically, attempts at CO_2 reduction have involved a protic media with water being the most suitable choice for reasons of versatility, solubility and the availability of a wide body of knowledge of aqueous C_1 chemistry.[1,6] Successful attempts were reported as early as the late nineteenth century.[7] These attempts utilized an electrode of lead or tin or an amalgam of these in an aqueous bicarbonate media. Formic acid was formed with a high faradaic efficiency. Although these systems were selective for the reduction of CO_2 over that of the solvent, the energy input for the reduction was substantial.

Other metal electrodes which have been investigated for the reduction of CO_2 include mercury,[8] copper,[9] and indium.[10] These systems have resulted in a variety of products, including CO, CH_4, C_2H_4, CH_3OH and HCOOH. These electrode systems have been reviewed in several excellent articles.[5,8,11,12] In aqueous systems, or other protic solvents, the major product was formic acid, as given by equation (2).

$$CO_2 + 2H^+ + 2e^- \longrightarrow HCOOH \qquad (2)$$

In addition to formic acid, varying amounts of hydrogen were detected, arising from the reduction of the solvent.[10] The distribution of reduced C_1 products was influenced by the solvent pH, electrode pretreatment and the type of electrode material.

In contrast to reaction (2), the use of aprotic solvents resulted in the formation of oxalic acid or carbon monoxide,[11,12] as given by Equations (3) and (4).

$$2\,CO_2 + 2e^- \longrightarrow (COO)_2^{2-} \qquad (3)$$

$$2\,CO_2 + 2e^- \longrightarrow CO + CO_3^{2-} \qquad (4)$$

Products such as CO can be reduced further to more useful organic compounds by reactions such as the Fischer-Tropsch reaction.[13]

All of these studies of the electrochemical reduction of CO_2 at a metal cathode have suffered from one major problem. Because of the very negative electrode potentials required for reaction (1) to proceed at a significant rate, the competing reduction of the solvent often consumes most of the charge, leading to low faradaic efficiencies. For this reason, the choice of electrodes was limited to those which have a very high overpotential for the reduction of the solvent. Although these procedures were quite selective for the reduction of CO_2 over that of the solvent, the energy input simply made the whole process impractical from anything other than a laboratory viewpoint. In addition to these problems, environmental concern over the toxicity of heavy metals has led to increased attention on alternative electrode systems.

1.2 *Transition Metal Catalysis*

In the last decade, attention has been focused on the use of transition metal compounds as catalysts to alleviate the problems of selectivity and activation mentioned above. The use of a catalyst with the electrode system lowers the activation energy for the reduction and allows the reactions to occur at a potential closer to the thermodynamic value, thus lowering the energy input. In addition, the use of a catalyst allows the tailoring of the system to favor the reduction of CO_2 over that of the solvent. In an electrocatalytic

reaction, the catalyst must have a means of transfering the electron(s) to the substrate; this is typically done by direct coordination of the substrate to the catalyst. Because of the relative inertness of the CO_2 molecule, and its high lability, only a modest body of coordination literature exists in comparison with that available for other ligands.[2,14] Carbon dioxide is a weakly electrophilic ligand and tends to form complexes with very basic, coordinately unsaturated metal centers. Its ability to engage in insertion reactions with organometallic compounds has been well documented.[15]

Many transition metal complexes have exhibited catalytic activity towards the electrochemical reduction of CO_2.[16] The substrate, CO_2, usually bonds directly to the metal center, and the electron transfer steps occur from electrode to catalyst to substrate, leading to the final product(s). Phosphine complexes have been widely used as catalysts for the hydrogenation of olefins,[17] but relatively little has been done with regard to CO_2 reduction. Those systems which have been investigated include phosphine complexes of rhodium[18] and palladium;[19] the main products were formate ion and CO, respectively. These reactions were done in organic solvents with a carbon electrode potentiostated at -1.5 V vs Ag/AgCl. Unfortunately, the palladium system suffered from rapid degradation of the catalyst. Other catalysts include complexes containing bipyridine ligands,[16,20] with transition metal centers of the Group VIII metals, such as nickel, cobalt, rhodium, ruthenium, iridium and osmium. Research on transition metal complexes of phthalocyanines and porphyrins has produced a large body of literature with regard to CO_2 reduction.[21] These complexes drastically reduce the overpotential required, and a variety of products from CO to HCOOH are formed. However, hydrogen evolution was still a problem, and many of the catalysts exhibited very short lifetimes.

One subset of these complexes which has been shown to be especially promising is the complexes of non-porphyrinic tetraaza macrocycles, especially those of cobalt and nickel.[22] Considerable literature is available on the chemistry of these complexes, and they

have been shown to be efficient catalysts for a variety of reactions.[16] These complexes have the advantage of being exceptionally stable, and in many cases the binding of various substrates to them is also favorable. Through changes in the degree of unsaturation of the ligand and variations in any pendant groups, one can tune the redox potential of the central metal atom,[23] and thus optimize the performance of the catalyst-substrate system.

1.3 *Ni(cyclam)$^+$ As Electrocatalyst*

One compound in particular, Ni(cyclam)$^{2+}$, (cyclam = 1,4,8,11-tetraazacyclotetradecane, Figure 1.1) has been shown to be a catalyst for the photochemical[24,25] and electrochemical reduction[26-29] of CO_2, the reduction of NO_3^-[30] and N_2O[31], and the reduction of a variety of hydrocarbon substrates.[32] Since the initial report of this catalyst,[26] several papers have appeared discussing further mechanistic[27-29] and theoretical[33] studies.

In the initial reports, Ni(cyclam)$^+$ was shown to be an effective and selective catalyst for the electrochemical reduction of CO_2 to CO in water at mercury electrodes at potentials much less negative than those which are required for the uncatalyzed reduction.[26,27] Current efficiencies for the conversion of CO_2 to CO of greater than 99% were achieved, with only a minimal amount of hydrogen formation detected. Catalytic reduction currents were observed at potentials as positive as -1.0 V vs NHE. In the more detailed study,[27] Sauvage *et al.* proposed the mechanistic cycle shown in Figure 1.2. Ni(cyclam)$^{2+}$ in solution is reduced and adsorbed at a mercury electrode in a concerted process, leading to the active catalyst, $Ni(cyclam)^+_{ads}$. This adsorbed Ni(I) complex binds CO_2 through an oxidative addition step, forming a Ni(III)cyclam -CO_2 adduct at the electrode surface. After the protonation of this adduct, an additional electron is shuttled through the adsorbed catalyst to the substrate. Hydroxide ion is released and the Ni(II)cyclam^{2+}-CO complex remains on the surface. However, Ni(II)cyclam^{2+}-CO is not

stable either on the mercury surface or in solution and thus CO and $Ni(cyclam)^{2+}$ dissociate and are desorbed from the electrode surface. $Ni(cyclam)^{2+}$ is again reductively adsorbed, completing the cycle. The overall reaction is expressed in Equation (5); the potential given is the standard thermodynamic potential.

$$CO_2 + 2\,e^- + H^+ \longrightarrow CO + OH^- \quad -0.52 \text{ V vs NHE} \quad (5)$$

It was proposed that the only active catalyst was the adsorbed form of $Ni(cyclam)^+$ and that $Ni(cyclam)^+$ in solution was of minor importance. The evidence for this assertion was the weak dependence of the catalytic reduction current on the bulk solution $Ni(cyclam)^{2+}$ concentration, and the observation that the catalysis occurs several hundred millivolts positive of the potential at which $Ni(cyclam)^{2+}$ is reduced to $Ni(cyclam)^+$ in solution. Recent studies, both experimental[28,29] and theoretical,[33] have added to the evidence that the active catalyst is the adsorbed $Ni(cyclam)^+$ species. It is believed that the mercury electrode acts as an axial ligand and a sixth coordination site is then open to bind CO_2. The presence of the mercury electrode "ligand" evidently fulfills a vital role, as the $Ni(cyclam)^+$ in solution has little or no catalytic activity.

Figure 1.1 Structure of $Ni(cyclam)^{2+}$.

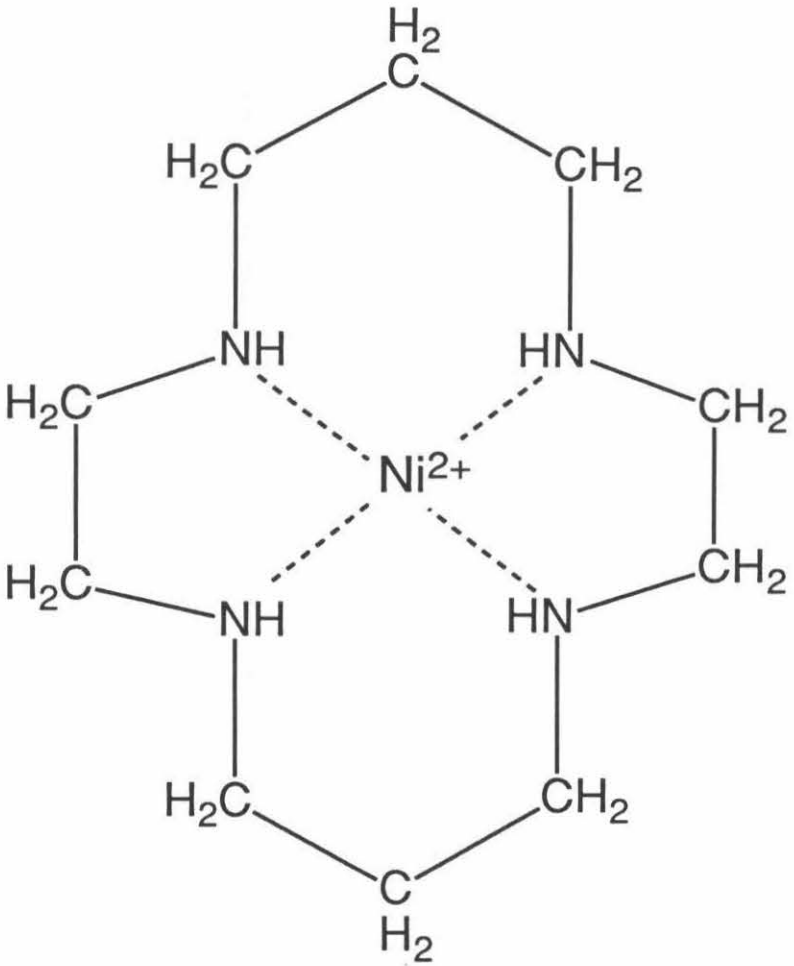

Figure 1.2 Postulated mechanistic cycle for the aqueous electrocatalytic reduction of CO_2 to CO by $Ni(cyclam)^{2+}$ (from reference 27).

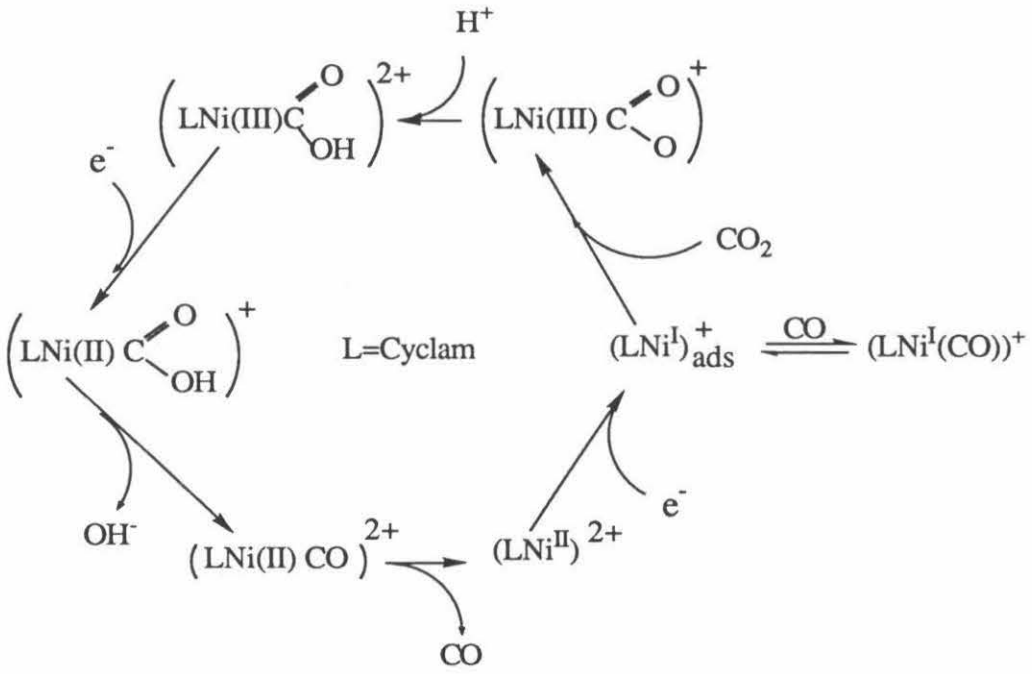

1.4 *Stimulus for this Study*

Following the initial report[34] of the synthesis of Ni(cyclam)$^{2+}$, many investigations of the chemistry of this complex have appeared in the literature.[35-38] A variety of studies has been done on the structural configuration of the ligand around the Ni(II) atom, both in the crystalline state[35] and in solution,[36,37] and of the dynamics of the equilibrium between the different configurational isomers.[36] In addition, the coordination environment and ligand field of the complex have received extensive study.[38] These topics will be discussed in more detail in chapter two.

Despite these advances in the understanding of the solution chemistry of Ni(cyclam)$^{2+}$, relatively little work has been done on the electrochemistry of the complex, in particular with regard to the mechanistic cycle[27] proposed for the electrochemical reduction of carbon dioxide. Although some work has been done on the chemistry of the intermediates in the proposed mechanistic cycle, e.g., Ni(I)cyclam^{+}-CO compounds in non-aqueous solvents,[39] their chemistry at a mercury-water interface has received little attention.[28] Several points in the proposed mechanistic scheme are somewhat implausible, or at best require additional clarification. The presence of a Ni(III) species on the electrode surface at -1.3 V and an exact description of the binding of substrate and product to the catalyst are areas which need to be addressed. In addition, a detailed electrochemical study of the catalyst itself at a mercury-water interface is necessary to draw conclusions regarding the overall mechanistic scheme of the electrocatalyzed reduction.

Chapter 1 References

1. Stumm, W.; Morgan, J.J.; Aquatic Chemistry: An Introduction Emphasizing Chemical Equilibria in Natural Waters; Wiley and Sons: New York, 1981.

2. Collman, J.P.; Hegedus, L.S.; Norton, J.R.; Finke, R.G.; Principles and Applications of Organotransition Metal Chemistry; University Science Books: Mill Valley, CA, 1987, p. 204.

Sneeden, R.P.A. in Comprehensive Organometallic Chemistry, Wilkinson, G.; Stone, F.G.A; Abel, E.W., Eds., Pergamon: New York, 1982; Vol. 8, Chap. 50.

3. Bard, A.J. (Ed.); Encyclopedia of Electrochemistry of the Elements, Vol. 7; Dekker: New York, 1976.

4. Jordan, J.J.; Smith, P.T. *Proc. Chem. Soc.* **1960**, 246.

Greener, E.P., Ph.D. Thesis, Southampton University, 1970.

5. Eggins, B.R.; McNeill, J. *J. Electroanal. Chem.* **1983**, *148*, 17.

6. Kern, D. M. *J. Chem. Ed.* **1960**, *37*, 14.

7. Royer, E. *Compt. Rend.* **1870**, *70*, 731.

Coehn, A.; Jahn, S. *Chem. Ber.* **1905**, *38*, 4138.

8. Russell, P.G.; Kovac, N.; Srinivasan, S.; Steinberg, M. *J. Electrochem. Soc.* **1977**, *124*, 1329.

Paik, W.; Andersen, T.N.; Eyring, H. *Electrochim. Acta* **1969**, *14*, 1217.

Kolthoff, L.; Jordan, P. *J. Am. Chem. Soc.* **1952**, *74*, 570, 4801.

Teeter, R.E.; Van Rysselberghe, P. *J. Chem. Phys.* **1954**, *22*, 759.

Gressin, J.C.; Michelet, L.; Nadjo, L. Savéant, J.M. *Nouv. J. Chim.* **1979**, *3*, 545.

9. Udupa, K.S.; Subramanian, G.S.; Udupa, H.V.K. *Electrochim. Acta* **1971**, *16*, 1593.

Hori, Y.; Murata, A.; Takahashi, R.; Suzuki, S. *J. Am. Chem.Soc.* **1987**, *109*, 5022.

Kyriacou, G.; Anagnostopoulos, A. *J. Electroanal. Chem.* **1992**, *322*, 233.

10. Kaiser, V.; Heitz, E. *Ber. dB. Gesellschaft*, **1973**, *77*, 818.
11. Ulman, M.; Aurian-Blajeni, B.; Halmann, M. *CHEMTECH*, **1984**, 235.
12. Vassiliev, Y.B.; Bagotzky, V.S.; Osetrova, N.V.; Khazova, O.A.; Mayorova, N.A. *J. Electroanal. Chem.* **1985**, *189*, 271.
13. Ref. (2), pp 653-660.
14. Darensbourg, D.J.; Kudaroski, R.A. *Adv. Organomet. Chem.* **1983**, *22*, 129.
    Floriani, C.J. *Pure Appl. Chem.* **1982**, *54*, 59.
    Ibers, J. A. *Chem. Soc. Rev.* **1982**, *11*, 57.
15. Behr, A.; Carbon Dioxide Activation by Metal Complexes; VCH Press: Germany, 1988.
16. Collin, J.-P.; Sauvage, J.-P. *Coord. Chem. Rev.* **1989**, *93*, 245.
    Tsai, J.-C.; Nicholas, K.M. *J. Am. Chem. Soc.* **1992**, *114*, 5117.
    Sullivan, B.P.; Bruce, M.R.M.; O'Toole, T.R.; Bolinger, C.M.; Megehee, E.; Thorp, H.; Meyer, T.J., in Catalytic Activation of CO_2, Ayers, W.A., Ed.; ACS Symp Ser. 363, ACS: Washington, 1988.
17. Ref. (2), p. 530.
18. Slater, S.; Wagenknecht, J.H. *J. Am. Chem. Soc.* **1984**, *106*, 5367.
19. DuBois, D.L.; Miedaner, A.; Haltiwanger, R.C. *J. Am. Chem. Soc.* **1991**, *113*, 8753.
    DuBois, D.L.; Meidaner, A. *J. Am. Chem. Soc.* **1987**, *109*, 113.
20. Danielle, S.; Ugo, P.; Bontempelli, G.; Fiorani, M. *J. Electroanal. Chem.* **1987**, *219*, 259.
    Ishida, H.; Fujiki, K.; Ohba, T.; Ohkubo, K.; Tanaka, K.; Terada, T.; Tanaka, T. *J. Chem. Soc., Dalton Trans.* **1990**, 2155.
    Keene, F.R.; Creutz, C.; Sutin, N. *Coord. Chem. Rev.* **1985**, *64*, 247.
    Hawecker, J.; Lehn, J.M.; Ziessel, R. *Helv. Chim. Acta* **1986**, *69*, 1990.

Bruce, M.R.M.; Megehee, E.; Sullivan, B.P.; Thorp, H.; O'Toole, T.R.; Downart, A.; Meyer, T.J. *Organometallics* **1988**, *7*, 238.

21. Lieber, C.M.; Lewis, N.S. *J. Am. Chem. Soc.* **1984**, *106*, 5033. Kapusta, S.; Hackerman, N. *J. Electrochem. Soc.* **1984**, *131*, 1511. Hammouche, M.; Lexa, D.; Momenteau, M. Savéant, J.-M. *J. Am. Chem. Soc.* **1991**, *113*, 8455. Meshitsuka, S.; Ichikawa, M.; Tamaru, K. *J. Chem. Soc., Chem. Commun.* **1974**, 158. Takahashi, K.; Hiratsuka, K.; Sasaki, H.; Toshima, S. *Chem. Lett.* **1979**, 305. Becker, J.Y.; Vainas, B.; Eger, R.; Kaufman, L. *J. Chem. Soc., Chem. Commun.* **1985**, 1471. Atoguchi, T.; Aramato, A.; Kazusaka, A.; Enyo, M.*J. Electroanal. Chem.* **1991**, *318*, 309.

22. Fischer, B.; Eisenberg, R. *J. Am. Chem. Soc.* **1980**, *102*, 7361. Pearce, D.J.; Pletcher, D. *J. Electroanal. Chem.* **1986**, *197*, 317.

23. Busch, D.H.; Pillsbury, D.G.; Lovecchio, F.V.; Tait, A.M.; Hung, Y.; Jackels, S.; Rakowski, M.C.; Schammel, W.P.; Martin, L.Y. in Electrochemical Studies of Biological Systems, Sawyer, D.T., Ed.; ACS Symp. Ser. 38., Washington, 1977.

24. Petit, J.-P.; Chartier, P.; Beley, M.; Sauvage, J.-P. *New J. Chem.* **1987**, 11, 751.

25. Grant, J.L.; Goswami, K.; Spreer, L.O.; Otvos, J.W.; Calvin, M. *J. Chem. Soc., Dalton Trans.* **1987**, 2105. Craig, C.A.; Spreer, L.O.; Otvos, J.W.; Calvin, M. *J. Phys. Chem.* **1990**, *94*, 7957.

26. Beley, M.; Collin, J.-P.; Ruppert, R.; Sauvage, J.-P. *J. Chem. Soc., Chem. Commun.* **1984**, 1315.

27. Beley, M.; Collin, J.-P.; Ruppert, R.; Sauvage, J.-P. *J. Am. Chem. Soc.* **1986**, *108*, 7461.

28. Fujihira, M.; Hirata, Y.; Suga, K. *J. Electroanal. Chem.* **1990**, *292*, 199.

29. Fujihira, M.; Nakamura, Y.; Hirata, Y.; Akiba, U.; Suga, K. *Denki Kagaku* **1991**, *59*, 532.

30. Taniguchi, I.; Nakashima, N.; Matsushita, K.; Yasulouchi, K. *J. Electroanal. Chem.* **1987**, *224*, 199.

31. Taniguchi, I.; Shimpuku, T.; Yamashita, K.; Ohtaki, H. *J. Chem. Soc., Chem. Commun.* **1990**, 915.

32. Koola, J.D.; Kochi, J.K. *Inorg. Chem.* **1987**, *26*, 908.
Becker, J.Y.; Kerr, J.B.; Pletcher, D.; Rosas, R. *J. Electroanal. Chem.* **1981**, *87*, 117.

33. Sakaki, S. *J. Am. Chem. Soc.* **1992**, *114*, 2055.

34. Bosnich, B.; Tobe, M.L.; Webb, G.A. *Inorg. Chem.* **1965**, *8*, 1102, 1109.

35. Bosnich, B.; Mason, R.; Pauling, P.J.; Robertson, G.B.; Tobe, M.L. *Chem. Commun.* **1965**, *6*, 97.

36. Connolly, P.J.; Billo, E.J. Inorg. Chem. 1987, 26, 3224.

37. Adam, K.R.; Antolovich, M.; Brigden, L.G.; Lindoy, L.F. *J. Am. Chem. Soc.* **1991**, *113*, 3346.

38. Barefield, E.K.; Bianchi, A.; Billo, E.J.; Connolly, P.J.; Paoletti, P.; Summers, J.S.; Van Derveer, D.G. *Inorg. Chem.* **1986**, *25*, 4197.
Thöm, V.J.; Fox, C.C.; Boeyens, J.C.A.; Hancock, R.D. *J. Am. Chem. Soc.* **1984**, *106*, 5947.
Pell, R.J.; Dodgen, H.W.; Hunt, J.P. *Inorg. Chem.* **1983**, *22*, 529.

39. Gagné, R.R.; Ingle, D.M. *J. Am. Chem. Soc.* **1980**, *102*, 1444.
Gagné, R.R.; Ingle, D.M. *Inorg. Chem.* **1981**, *20*, 420.

Chapter 2

Electrochemistry of Ni(cyclam)$^{2+/+}$ and its Derivatives at a Mercury Electrode

2.1 *Introduction*

In previous studies of the electrochemical reduction of CO_2 catalyzed by Ni(cyclam)$^{2+}$ at a mercury electrode, it was proposed that the active catalyst is Ni(cyclam)$^{+}$ adsorbed at the mercury surface.[1-4] In this heterogeneous catalytic system, the presence of the mercury electrode is necessary not only to provide the electrons for the reduction, but also to activate Ni(cyclam)$^{+}$ so that it functions as a catalyst. This behavior is in contrast to that which would occur in an homogeneous system. An investigation of the mechanism of the Ni(cyclam)$^{+}$ electrocatalytic system must therefore address both the electrochemistry of the Ni(cyclam)$^{+}$ catalyst at the mercury surface, as well as the electrochemistry of Ni(cyclam)$^{2+/+}$ in solution insofar as this latter species has a direct influence on the surface catalyst activity through the equilibrium between the two.

In the initial reports of the electrocatalytic reduction of CO_2 by Ni(cyclam)$^{2+}$, Sauvage *et al.* made no attempt to assess quantitatively the adsorption process.[1,2] In a subsequent work in this area,[3] it was reaffirmed that the active catalyst was $Ni(cyclam)^{+}_{ads}$ and it was concluded that both Ni(cyclam)$^{2+}$ and Ni(cyclam)$^{+}$ are adsorbed on mercury; the exact species present being determined by the potential of the mercury electrode. These qualitative studies were done using traditional electrochemical methods and are subject to different interpretations. The subject of this chapter is a detailed, quantitative investigation of the nature of the adsorbed catalyst. Much of this chapter is based on a recent publication by this author.[5]

2.2 *Experimental*

2.2.1 Materials

Cyclam (Aldrich) was recrystallized from *p*-dioxane. Tetramethylcyclam (TMC, Aldrich), was used as received. Ni(cyclam)Cl_2 and Ni(cyclam)$(ClO_4)_2$ were prepared according to the method of Bosnich *et al.*[6] Each was recrystallized twice from methanol/diethyl ether and dried *in vacuo* at 60°C for 24 hours. The synthesis of *trans* I Ni(TMC)$(ClO_4)_2$ and of *trans* III Ni(TMC)$(ClO_4)_2$ were performed following literature procedures.[7,8] Ni(dimethylcyclam)$(ClO_4)_2$ and Ni(monomethylcyclam)$(ClO_4)_2$ were provided by an undergraduate researcher; these were synthesized following literature procedures.[8,9] *Cis*-Ni(cyclam)Cl_2 and α-Ni(cyclam)$(ClO_4)_2$ were prepared according to the method of Billo.[10] $KClO_4$ was prepared by the addition of $HClO_4$ to a solution of KOH. The product was recrystallized twice from water and dried *in vacuo* at 80°C for 24 hours. Tetraethylammonium perchlorate (TEAP, Southwest Analytical) was recrystallized from water and dried *in vacuo* at 80°C for 24 hours. All aqueous solutions were prepared from analytic grade reagents; distilled water was further purified by passage through a Barnstead Organopure contaminant removal system. Buffered solutions were either acetate, borate or an appropriate concentration of HCl or KOH; $KClO_4$ was added if necessary to provide a total ionic strength of 0.1 M. Dimethyl Formamide (DMF) and Acetonitrile (MeCN) were used immediately as received from Burdick and Jackson. Prepurified argon was bubbled through a solution of V(II) to remove residual oxygen.

2.2.2 Electrochemical Measurements

Triply distilled Hg (Bethlehem Instrument Co.) was used in a Brinkman model #410 Hanging Mercury Drop Electrode (HMDE). The surface area of this electrode was 0.027 cm^2 as determined by weight, averaging a large number of drops. Controlled potential reductions were performed with a mercury pool electrode (surface area of 4 cm^2) instead of the HMDE. Most aqueous experiments were done in 0.1 M $KClO_4$ as supporting electrolyte; non-aqueous experiments were done in 0.1 M TEAP. A conventional two compartment electrochemical cell was employed. Solutions were dearated by bubbling with argon for at least 15 minutes prior to each experiment and a blanket of argon was kept over the solution during the course of the experiments.

Cyclic voltammograms were obtained with a Princeton Applied Research (PAR) Model 173 Potentiostat and a PAR Model 175 programmer. For normal pulse polarography a dropping mercury electrode (DME) was employed with a PAR Model 174 potentiostat. The flow rate of the DME was typically 1 mg/sec which provided a drop area of 0.85 mm^2 for drop times of 1 second. Chronocoulometric and chronoamperometric experiments were done with a previously described computer-controlled instrument.[11]

All experiments were carried out at ambient laboratory temperature, 22 ±2 °C. All potentials were measured with respect to a saturated calomel reference electrode (SCE).

2.2.3 NMR Measurements

Proton Nuclear Magnetic Resonance was performed in D_2O using a Bruker AM-500 instrument with a 5 mm probe.

2.3 *Results*

2.3.1 Cyclic Voltammetry of $Ni(cyclam)^{2+}$

A cyclic voltammogram of $Ni(cyclam)^{2+}$ in 0.1 M $KClO_4$ is shown in Figure 2.1. The lower trace is that of the pure supporting electrolyte alone. The magnitude of the cathodic peak current corresponds to a one-electron reduction of $Ni(cyclam)^{2+}$ to $Ni(cyclam)^{+}$. The ratio of cathodic to anodic peak currents is somewhat less than unity and the peak separation is greater than the 59 mV expected for a Nernstian couple. An approximate formal potential for the $Ni(cyclam)^{2+/+}$ couple of -1.56 V was derived from the average of the two peak potentials. The couple exhibits normal diffusional behavior as can be seen from the linearity of a plot of peak current versus $(\text{scan rate})^{1/2}$ (Insert in Figure 2.1). In addition, $Ni(cyclam)^{+}$ is a catalyst for the evolution of hydrogen[12] as is evidenced by the anodic shift of the solvent background response in the presence (upper trace) and absence (lower trace) of $Ni(cyclam)^{2+}$.

A small prepeak is present in the voltammogram near -1.3 V. The position and shape of the prepeak depended upon the concentration of $Ni(cyclam)^{2+}$. As the concentration is increased from 0.05 mM to 1 mM, the peak potential shifts approximately 100 mV positive and the peak becomes broader. However, the integrated charge under this peak remains constant at 0.3 to 0.5 $\mu C\ cm^{-2}$. This peak has been observed in previous studies[1-4,13] and has been attributed to the reduction of $Ni(cyclam)^{2+}$ in solution to $Ni(cyclam)^{+}$ adsorbed on the electrode surface. A somewhat different origin for this prepeak is proposed in this study (see section 2.4.5).

Figure 2.1 Cyclic voltammogram of a 0.2 mM solution of $Ni(cyclam)^{2+}$ at a hanging mercury drop electrode. Scan rate is 100 mV s^{-1}. Supporting electrolyte is 0.1 M $KClO_4$. Lower trace is supporting electrolyte only. Insert is peak current versus $(scan\ rate)^{1/2}$.

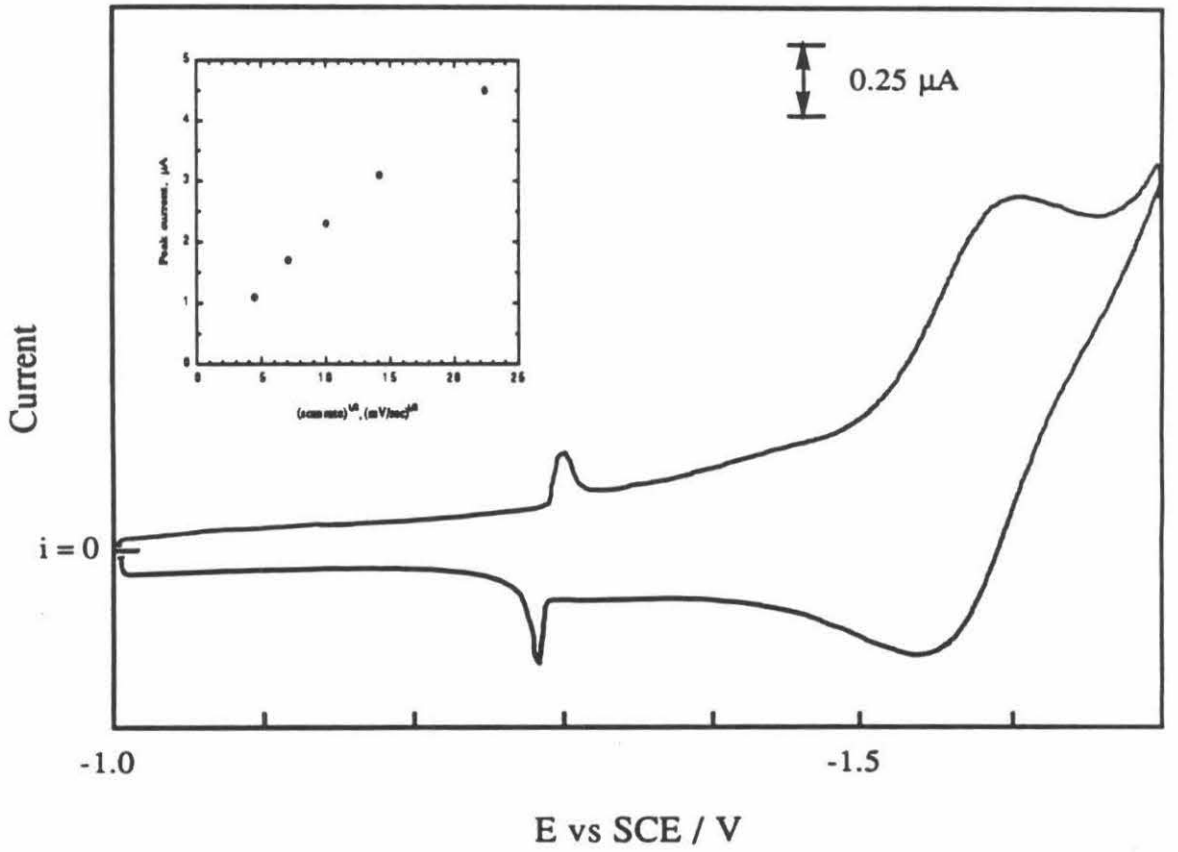

2.3.2 Normal Pulse Polarography of Ni(cyclam)$^{2+}$

Normal pulse polarograms[14] for solutions of Ni(cyclam)$^{2+}$ recorded from an initial potential of -1.0 V exhibited the features expected on the basis of the cyclic voltammetry although the prepeak near -1.3 V was not as prominent and the reduction wave at -1.6 V was only partially resolvable from the background response. These differences resulted from the shorter measurement times employed in normal pulse polarography. In addition to these responses, normal pulse polarograms recorded at high sensitivity revealed the presence of a faradaic process commencing at potentials as positive as -0.5 V. The normal pulse polarograms shown in Figure 2.2 were obtained with three different pulse widths, i.e., the times allowed to elapse following the step change in electrode potential before the current was recorded. The plateau currents decrease with sampling times more quickly than would be expected for diffusion limited currents. A Cottrell plot of current vs (time)$^{-1/2}$ is shown in the insert in Figure 2.2. The line drawn between the origin and the point corresponding to the largest current (shortest time before current sampling) has a slope (0.048 μA $s^{1/2}$) which is much smaller than that calculated for the diffusion limited reduction of the Ni(cyclam)$^{2+}$ at the dropping mercury electrode (0.22 μA $s^{1/2}$). The currents at longer sampling times fall below the line, indicating that the current is also not limited by the diffusion of a minor solution component to the electrode surface. This behavior is consistent with an electrode reaction whose rate is less than diffusion-controlled and whose extent is limited by the available area of the electrode.

Figure 2.2 Normal pulse polarograms at a DME for a 0.2 mM solution of $Ni(cyclam)^{2+}$ at three different pulse widths. The lowest curve was the response of 0.1 M $KClO_4$ only. The insert is a plot of the plateau current versus (pulse width)$^{-1/2}$. The line is drawn from the origin to the point for the largest current.

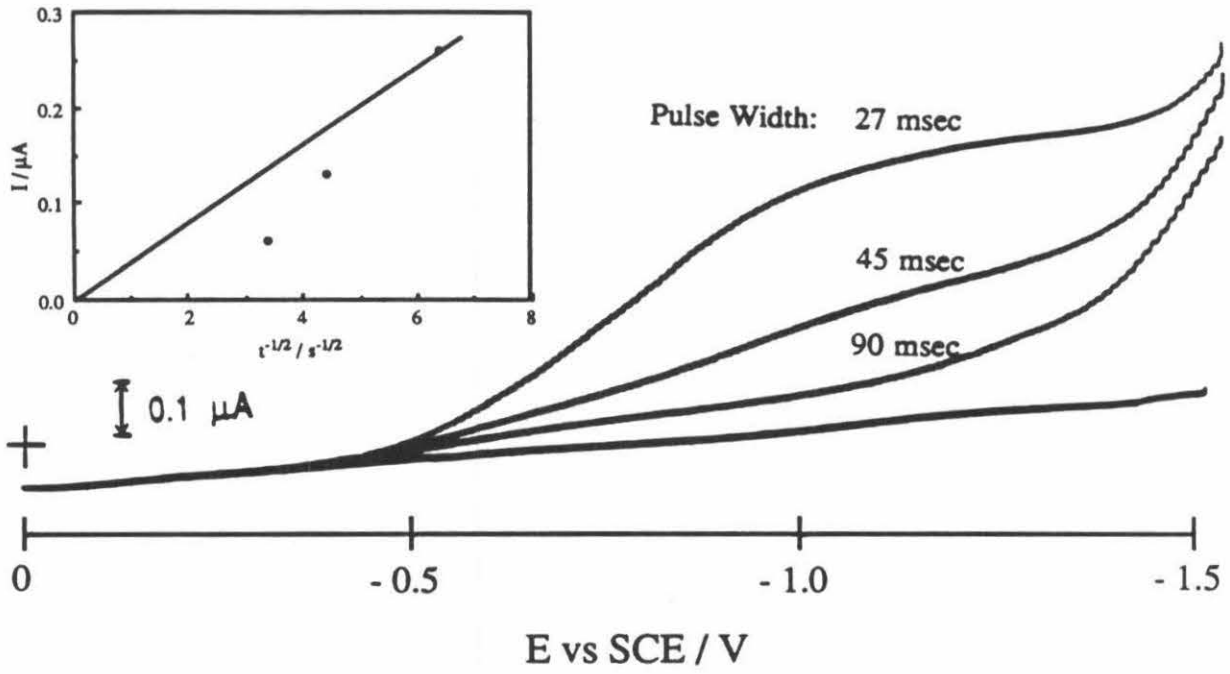

2.3.3 Cyclic Voltammetry of Ni(cyclam)$^{2+}$ Derivatives

The cyclic voltammograms of two configurational isomers, *cis*-Ni(cyclam)$^{2+}$ and α-(Trans IV) Ni(cyclam)$^{2+}$, in 0.1 M $KClO_4$ (buffered at pH 3) and in 4.0 M KCl respectively, are shown in Figure 2.3. The use of a low pH in the former solution and a high ionic strength in the latter was necessary to prevent the isomerization[15] of the species back to the more thermodynamically stable form[6] (*trans* III Ni(cyclam)$^{2+}$) during the course of the experiment. As was observed with Ni(cyclam)$^{2+}$, *cis*-Ni(cyclam)$^{2+}$ exhibits a one-electron reduction corresponding to the formation of the monovalent species; the formal potential for the couple is -1.54 V. In contrast to the electrochemically reversible behavior of Ni(cyclam)$^{2+}$ and *cis*-Ni(cyclam)$^{2+}$, α-Ni(cyclam)$^{2+}$ exhibits an irreversible reduction at -1.64 V. The magnitude of the cathodic peak current corresponds to the expected value for a one-electron reduction.

The presence of methyl groups on the cyclam ring drastically reduces the ability of the ligand to interconvert between different configurational isomers;[8,16-17] it is therefore possible to isolate two of the isomers and investigate them separately. The cyclic voltammograms of *trans* I and *trans* III Ni(TMC)$^{2+}$ in 0.1 M $KClO_4$ are shown in Figure 2.4. In both cases, the magnitudes of the peak currents correspond to the one-electron reduction of the complex to Ni(TMC)$^{+}$. A peak separation of close to 59 mV and a one-to-one ratio of cathodic to anodic peak current indicate that the reduction is reversible, in contrast to the quasi-reversible electrochemistry of Ni(cyclam)$^{2+}$. From the average of the cathodic and anodic peak potentials, formal potentials of -1.02 and -1.07 V were assigned for the *trans* I and *trans* III Ni(TMC)$^{2+/+}$ couples, respectively. In addition, both *trans* I and *trans* III Ni(TMC)$^{2+}$ cyclic voltammograms exhibited a prominent prepeak approximately 160 mV positive of the main wave; this wave was attributed to the reduction of Ni(TMC)$^{2+}$ in solution to Ni(TMC)$^{+}$ adsorbed on the electrode surface. The integrated area under these prepeaks was in both cases equal to the charge expected for the reduction

Figure 2.3 Cyclic voltammetry at a HMDE of 0.5 mM solutions of *cis*-Ni(cyclam)$^{2+}$ in 0.1 M $KClO_4$ (buffered at pH 4). Scan rate is 100 mV sec^{-1}.

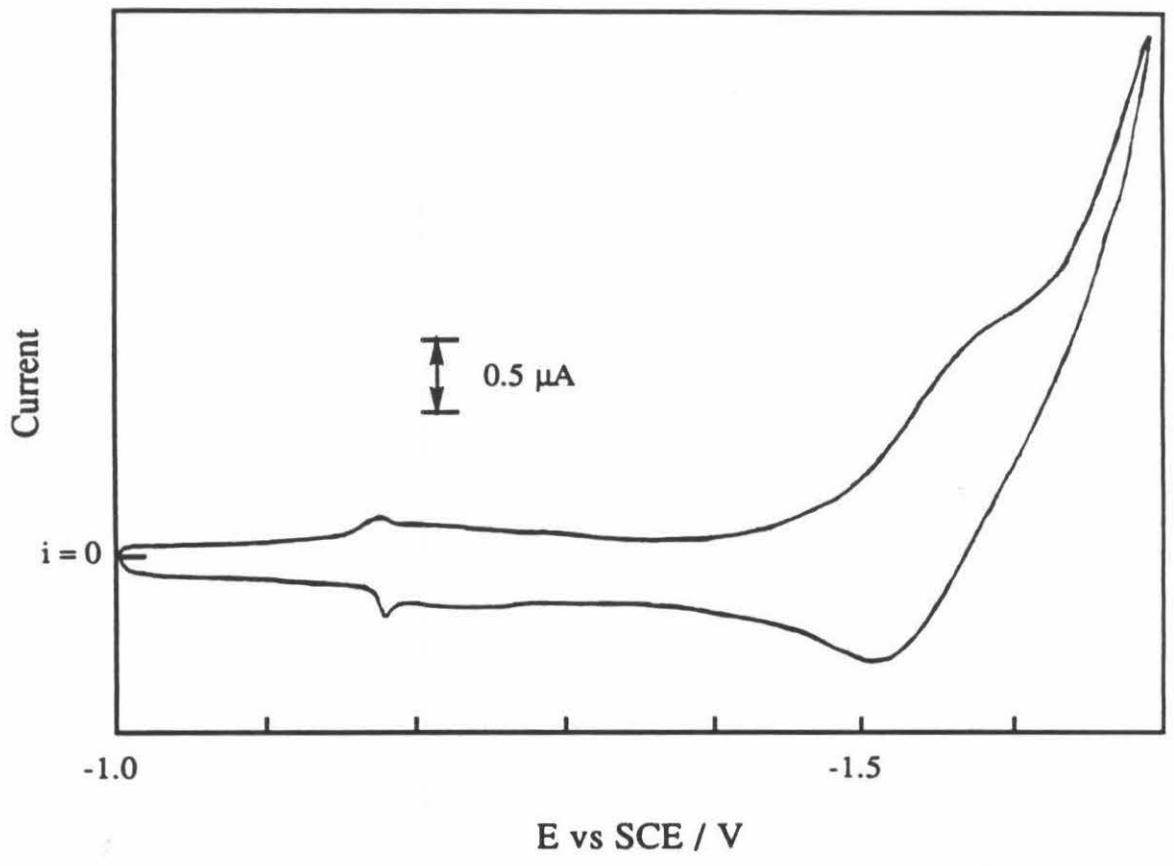

Figure 2.4 Cyclic voltammograms of 0.2 mM solutions of *trans* I $Ni(TMC)^{2+}$ (dashed line) and of *trans* III $Ni(TMC)^{2+}$ (solid line) in 0.1 M $KClO_4$. Scan rate is 100 $mVsec^{-1}$.

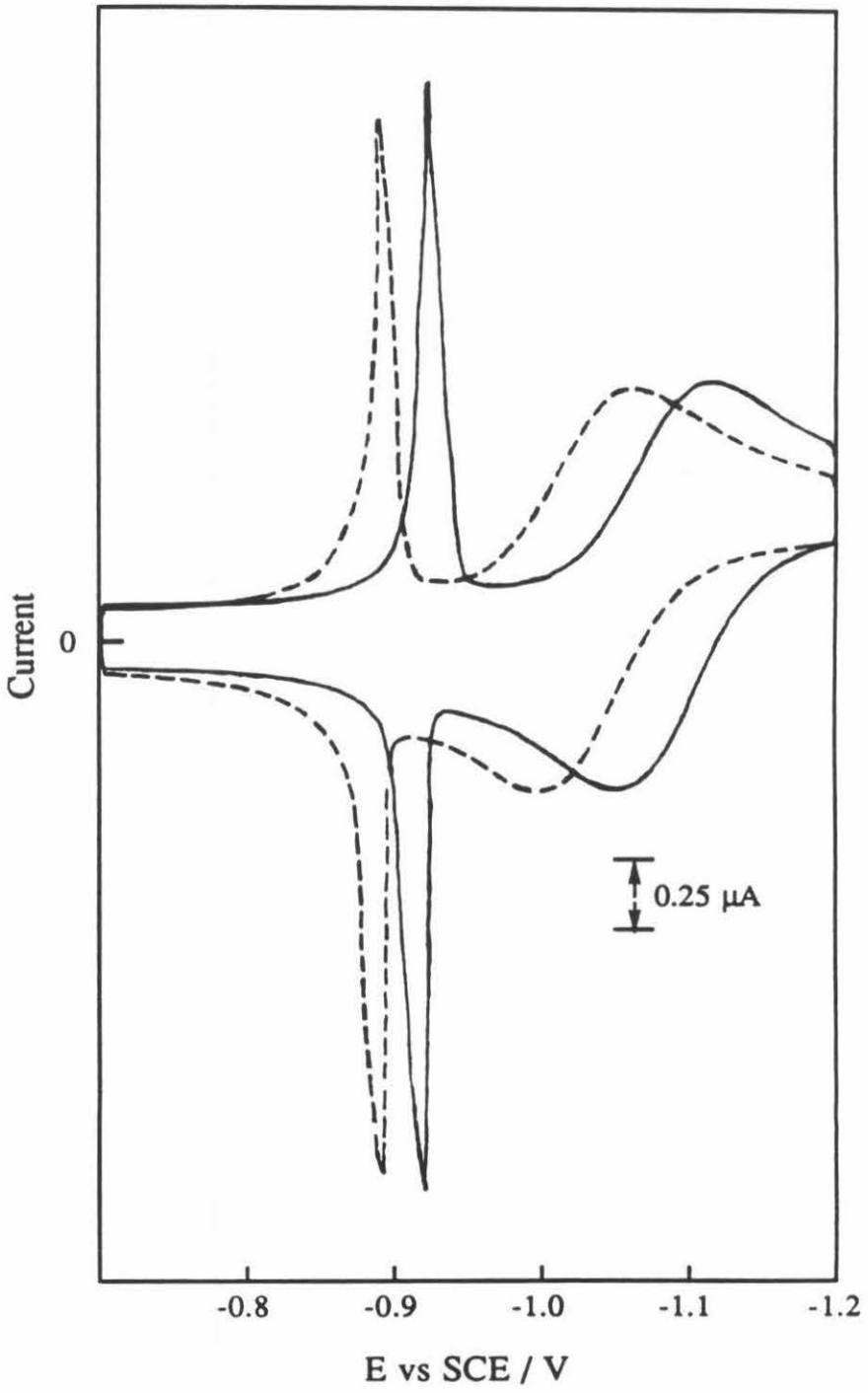

of a monolayer of molecules on the surface (calculated from the area occupied by a single molecule to be 12 $\mu C\ cm^{-2}$). The cyclic voltammetry of $Ni(MMC)^{2+}$ and $Ni(DMC)^{2+}$ was also investigated.[16] Their behavior is similar to that of the tetramethylated cyclam; the addition of each methyl group onto the cyclam ring shifts the formal potential (both prepeak and main wave) approximately 150 mV positive, and increases the prominence of the prepeak. A summary of the electrochemical behavior of the methylated cyclams and of $Ni(cyclam)^{2+}$ and its isomers is given in Table 2.1.

2.3.4 Electrocapillary Curves for Hg in the Presence of $Ni(cyclam)^{2+}$

To examine the possible adsorption of $Ni(cyclam)^{2+}$ and or $Ni(cyclam)^{+}$ on mercury, the natural drop time of a dropping mercury electrode was measured as a function of the electrode potential. It is well known that the adsorption of molecules at a mercury surface results in a lowering of the surface tension of the mercury[18] and decreases the natural drop time. The resulting electrocapillary curves are shown in Figure 2.5. Between -0.1 and -0.5 V, the drop times are changed very little by the addition of $Ni(cyclam)^{2+}$. However, at potentials negative of -0.5 V there is a definite decrease of the drop time in the presence of $Ni(cyclam)^{2+}$. The deviation observed at 0 V was less reproducible and may be untrustworthy. From these results, it may be concluded that $Ni(cyclam)^{2+}$ or $Ni(cyclam)^{+}$ or both appear to be adsorbed on mercury at potentials negative of -0.6 V. These results are in reasonable agreement with those reported recently by Fujihira *et al.*[3]

Figure 2.5 Natural drop times for a dropping mercury electrode in 0.1 M $KClO_4$ (open circles) and in 0.1 M $KClO_4$ + 1 mM Ni(cyclam)$^{2+}$ (closed squares). The bars indicate the range of values obtained in repetitive measurements.

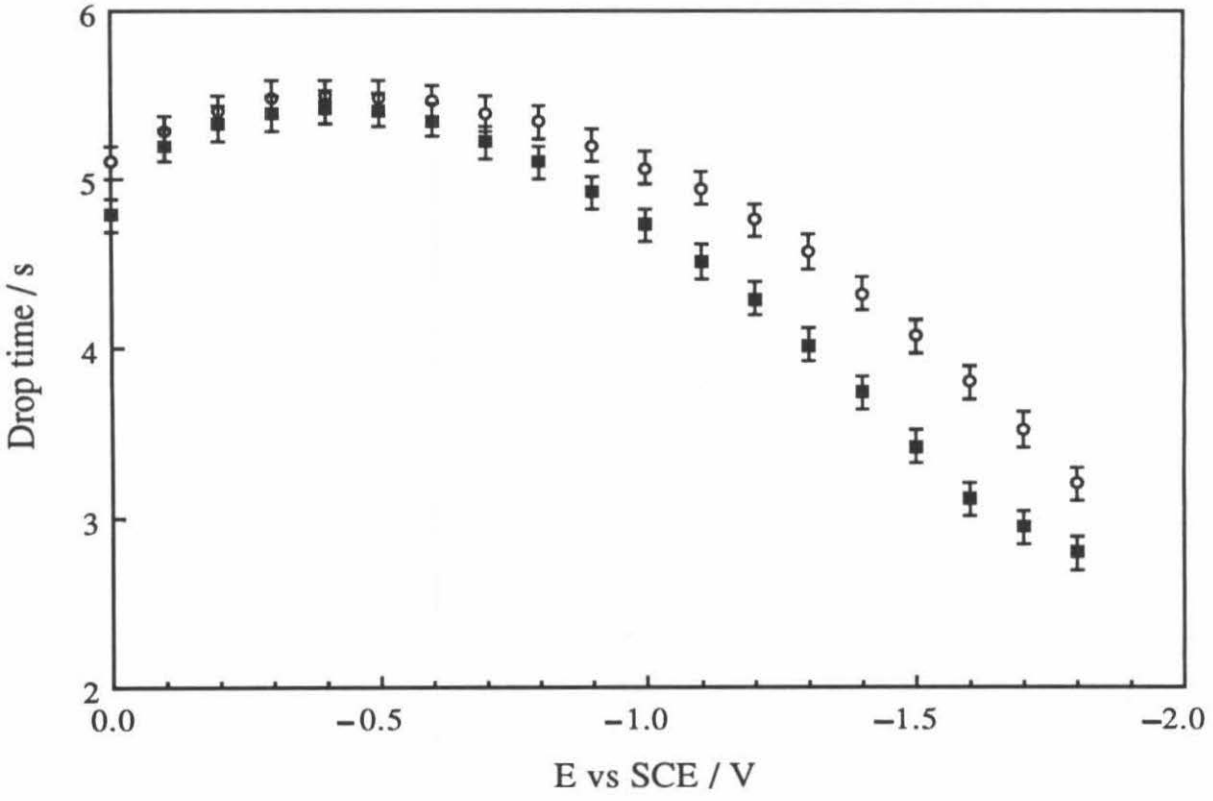

2.3.5 Fundamentals of Single-step Chronocoulometry

The chronocoulometric technique[19,20] is well suited to the evaluation of the quantities of electroactive reactants adsorbed on electrodes. If the potential of the electrode is held at a value where no redox reactions of either surface or diffusing species occurs, and the potential is then stepped to a value where the reduction or oxidation of the species is diffusion controlled, the charge versus time relationship is described by Equation (1).

$$Q_{pot.\ step} = \frac{2nFAD^{1/2}C^*}{\pi^{1/2}} t^{1/2} + nFA\Gamma + Q_{d.l.} \qquad (1)$$

The charge passed during the potential step is thus separated into three components: the faradaic charge for the reduction/oxidation of any diffusing species (first term), the faradaic charge due to the reduction/oxidation of any species adsorbed on the surface (second term), and the capacitive charge required to charge the double layer during the potential step (third term). If the charge passed after the potential step is plotted versus $(time)^{1/2}$, the slope of the resultant line will depend solely on the mass transfer of the solution species to the electrode, and the intercept will be the sum of the faradaic charge due to the electroactive species adsorbed on the surface and the double layer charging. If the amount of charge passed during a similar potential step in the absence of any electroactive species is subtracted, then the resultant intercept is representative of the quantity of electroactive reactant present on the electrode surface.

2.3.6 Adsorption of Ni(cyclam)$^{2+}$ and Ni(cyclam)$^{+}$ as Measured by Chronocoulometry

In order to measure the possible adsorption of Ni(cyclam)$^{2+}$, the electrode potential was stepped from various initial values to -1.6 V, and the resultant charge recorded as a function of time. Similar potential steps in the pure supporting electrolyte defined the quantity of charge involved in double layer charging, i.e., the third term of Equation (1). From the difference in intercepts of the chronocoulometric plots in the presence and absence of Ni(cyclam)$^{2+}$, an estimate of the quantity of Ni(cyclam)$^{2+}$ adsorbed at each initial potential was calculated. The double-potential step chronocoulometric procedure[20-22] was not employed because of the difficulties introduced by the adsorption of Ni(cyclam)$^{+}$ at -1.6 V. The results are summarized in Table 2.2. The differences in intercepts are very small (the experimental uncertainty is ± 1.5 μC cm^{-2}) for initial potentials from 0 to -0.9 V. The negative values of ΔQ obtained with the 1 mM solution at the most positive initial potentials are attributable to the effects of uncompensated resistance, resulting in erroneous charge measurements. These effects are most severe when large potential steps are applied with relatively high reactant concentrations. Between -1.0 and -1.3 V there was a small but reproducible increase in the difference of intercepts of the chronocoulometric plots in the presence of 0.2 mM Ni(cyclam)$^{2+}$ which indicated weak adsorption of this complex. At more negative potentials and at a higher concentration of Ni(cyclam)$^{2+}$ the difference in intercepts was no longer present, a result which suggests that the preferential adsorption of another species prevents the adsorption of Ni(cyclam)$^{2+}$.

The electrocapillary data in Figure 2.5 demonstrate significant adsorption of some species at all potentials between -0.6 and -1.6 V. If this species is not Ni(cyclam)$^{2+}$, except between -1.0 and -1.3 V, the likely alternative is Ni(cyclam)$^{+}$. However, this interpretation would require that the adsorbed Ni(cyclam)$^{+}$ be formed at potentials as

positive as -0.6 V, a potential which is almost one volt more positive than the formal potential of the $Ni(cyclam)^{2+/+}$ couple in solution (Table 2.1).

Unadsorbed $Ni(cyclam)^{+}$ is intrinsically unstable in aqueous media; it reacts with protons or water resulting in the evolution of H_2. However, the rate of this reaction is sufficiently slow in neutral solutions to allow $Ni(cyclam)^{2+}$ to be reductively generated at the surface of mercury electrodes and its electrooxidation subsequently examined by stepping the electrode to potentials positive of -1.4 V. In a series of chronocoulometric measurements, the initial electrode potential was adjusted to values between -1.6 and -0.1 V and the potential stepped to 0 V. The electrode was held at the initial potential for at least 30 seconds before each step to assure that the equilibrium quantity of $Ni(cyclam)^{+}$ was adsorbed. For initial potentials between -1.4 and -1.6V, increasing quantities of the $Ni(cyclam)^{2+}$ in the vicinity of the electrode were reduced to $Ni(cyclam)^{+}$ during the waiting period. The differences in the intercepts of the anodic charge vs $(time)^{1/2}$ plots were much larger than were observed (see Table 2.2) for the experiments of the same potential steps in the opposite direction. Table 2.3 summarizes the measured differences in intercepts. Estimates of the quantities of adsorbed $Ni(cyclam)^{+}$ can be obtained from the values of ΔQ listed in Table 2.3 if it is assumed that the double layer capacitance of the mercury/solution interface is not changed substantially by the adsorption of $Ni(cyclam)^{+}$. In cases where reactant adsorption does alter the double layer capacitance, the double potential-step chronocoulometric technique[20-22] can provide a more accurate estimate of the quantity of reactant adsorbed. The results of such double potential-step experiments for a 0.2 mM solution of $Ni(cyclam)^{2+}$ are summarized in Table 2.4. The values obtained for the quantities of $Ni(cyclam)^{+}$ adsorbed are only slightly different from those resulting from the single-step experiments in Table 2.3. In the presence of higher concentrations of $Ni(cyclam)^{2+}$, the results of double potential-step chronocoulometric experiments were complicated by contributions from both the oxidatively desorbed $Ni(cyclam)^{2+}$ and the

original $Ni(cyclam)^{2+}$ in solution during the reverse potential steps. For this reason, single-step experiments such as those in Table 2.3 were utilized to obtain estimates of the quantities of adsorbed $Ni(cyclam)^{+}$.

The values of the slopes of the chronocoulometric plots for both the forward and reverse potential steps are also included in Table 2.4. The notably larger slopes for the reverse steps when the initial (and final) potential is sufficiently negative to cause the reduction of $Ni(cyclam)^{2+}$ to $Ni(cyclam)^{+}$ in solution (i.e., -1.6 and -1.5 V) are the expected result. These larger slopes arise from the larger concentration of reducible $Ni(cyclam)^{2+}$ generated in the solution at the electrode surface by the instantaneous oxidation and desorption of the $Ni(cyclam)^{+}_{ads}$ at the beginning of the forward step. However, the slopes of the plots for the reverse steps also remain larger than the (background level) slopes of the plots for the forward steps at potentials where the reduction of $Ni(cyclam)^{2+}$ to unadsorbed $Ni(cyclam)^{+}$ does not occur (i.e., -1.3 to -0.6 V). This is not the expected result. An explanation for this phenomenon is provided in the discussion section of this chapter.

The quantities of $Ni(cyclam)^{+}$ adsorbed at each potential as estimated from the single potential-step experiments are plotted vs. the electrode potential in Figure 2.6. The results confirm the adsorption of $Ni(cyclam)^{+}$ at potentials over 0.5 V more positive than the potential where $Ni(cyclam)^{+}$ is formed in solution. In addition, the adsorption appears to proceed in two potential-dependent stages with greater adsorption occurring at potentials more negative than -1.3 V. The dependence of the surface coverage of $Ni(cyclam)^{+}$ on the concentration of $Ni(cyclam)^{2+}$ in solution is shown for two potentials in Figure 2.7. Significant adsorption is measured at concentrations as low as 10^{-3} mM and the adsorption appears to be somewhat more dependent on the concentration of $Ni(cyclam)^{2+}$ at -1.6 V than at -1.0 V.

Figure 2.6 Potential dependence of the adsorption of $Ni(cyclam)^{+}$ at mercury in 0.1 M $KClO_4$ and 0.1 mM (open circles) and 1.0 mM (closed squares) $Ni(cyclam)^{2+}$. The bars indicate the range of values obtained in repetitive measurements.

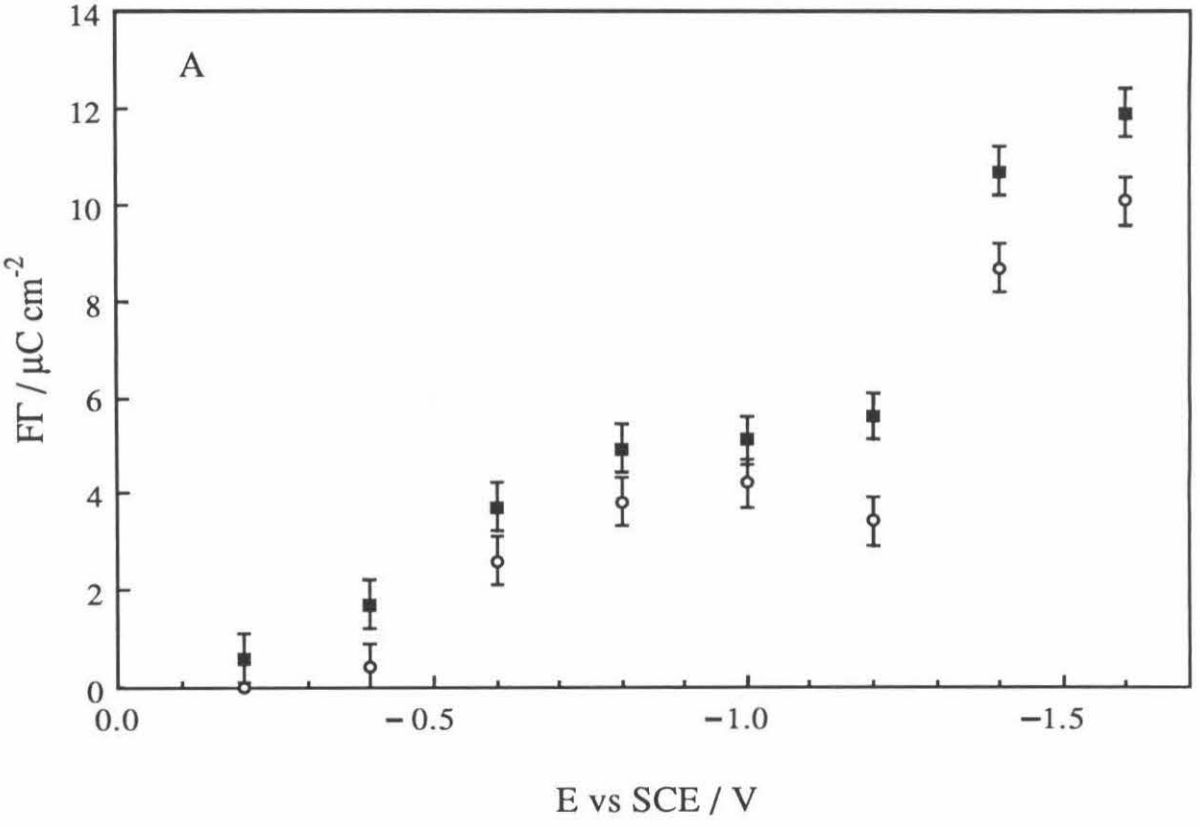

Figure 2.7 Concentration dependence of the adsorption of Ni(cyclam)$^{+}$ at mercury in 0.1 M $KClO_4$ and 0.1 mM (open circles) and 1.0 mM (closed squares) Ni(cyclam)$^{2+}$. The bars indicate the range of values obtained in repetitive measurements.

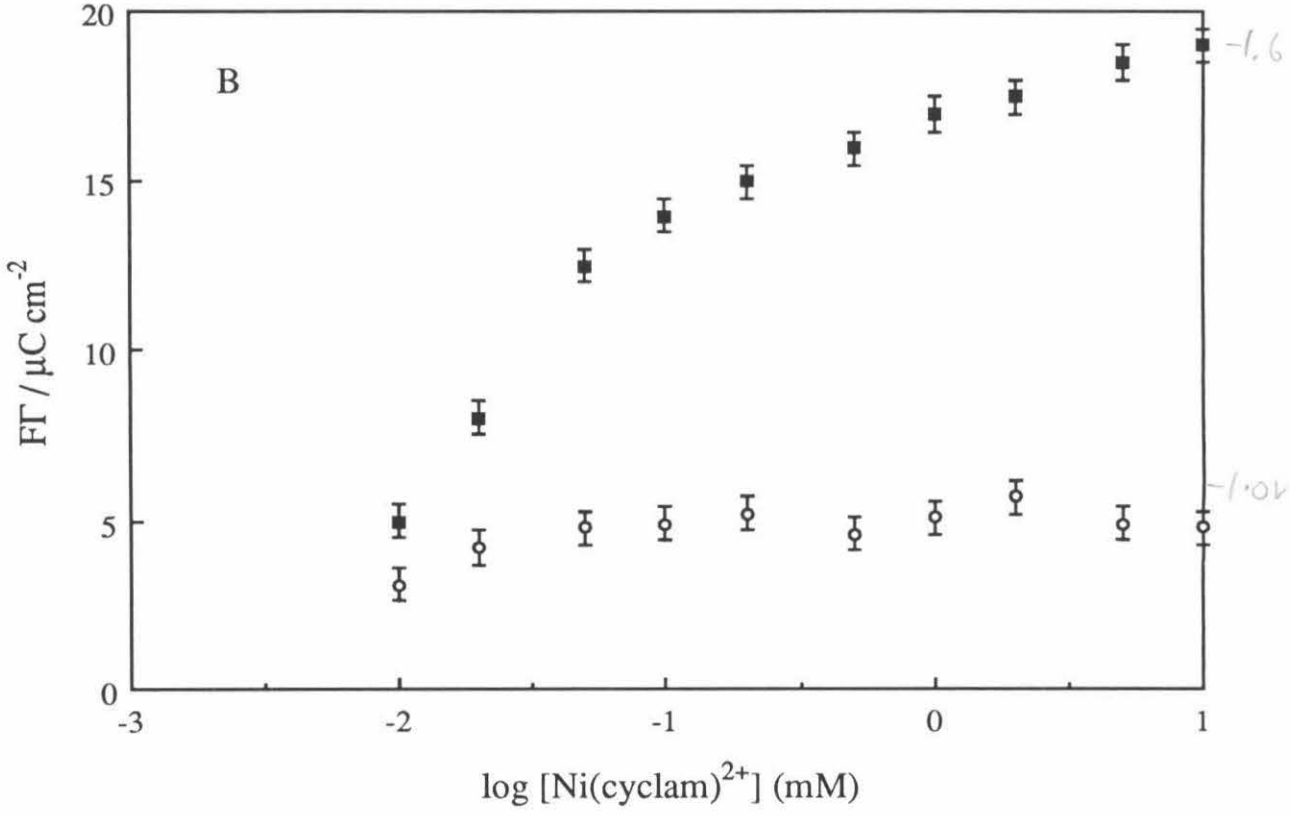

The rate at which the adsorbed Ni(cyclam)$^{+}$ complex accumulates on the mercury electrode surface at potentials ahead of the wave for the solution Ni(cyclam)$^{2+/+}$ couple was estimated from careful inspection of charge-time curves for potential steps from potentials where adsorption is absent, e.g., 0 V, to the potential of interest. Figure 2.8 shows a pair of curves corresponding to a step from 0 to -1.0 V in the absence and presence of Ni(cyclam)$^{2+}$. The small slope of the curve obtained in the background electrolyte reflects the reduction of residual impurities such as oxygen. The curve obtained in the presence of Ni(cyclam)$^{2+}$ has a higher slope for the first 40 msec as the Ni(cyclam)$^{2+}$ is reductively adsorbed. At longer times, when the electrode surface is saturated with Ni(cyclam)$^{+}_{ads}$, the two curves become parallel as the reduction of Ni(cyclam)$^{2+}$ ceases. The time that would be required for 4.9 μC cm^{-2} (the charge corresponding to the equilibrium value of Ni(cyclam)$^{+}_{ads}$ at -1.0V) to accumulate from the reduction of Ni(cyclam)$^{2+}$ at the diffusion-controlled rate in a 0.2 mM solution is only 8 msec. Thus, the much slower accumulation of Ni(cyclam)$^{+}_{ads}$ as revealed by the curve in Figure 2.8 suggests a kinetically controlled process in which the ordinary Ni(cyclam)$^{2+}$ present in the solution is converted to a form which is more reactive toward reductive adsorption on the mercury electrode.

2.3.7 Origin of Large Reverse-step Slopes in Double Potential-step Chronocoulometry

The large slopes obtained during the reverse potential steps of the experiments summarized in Table 2.4 reveal the presence in the solution near the electrode of a form of Ni(cyclam)$^{2+}$, generated by the oxidative desorption of Ni(cyclam)$^{+}_{ads}$, that is much more readily re-reduced to Ni(cyclam)$^{+}_{ads}$ than is the stable form of Ni(cyclam)$^{2+}$ obtained by dissolution of the salt. If the Ni(cyclam)$^{2+}$ generated by the oxidative desorption of Ni(cyclam)$^{+}_{ads}$ were the same complex obtained by dissolution of Ni(cyclam)$(ClO_4)_2$, its

Figure 2.8 Charge vs time curves for potential steps from 0 to -1.0 V in 0.1 M $KClO_4$ (open circles) and in 0.1 M $KClO_4$ and 0.2 mM $Ni(cyclam)^{2+}$ (closed squares).

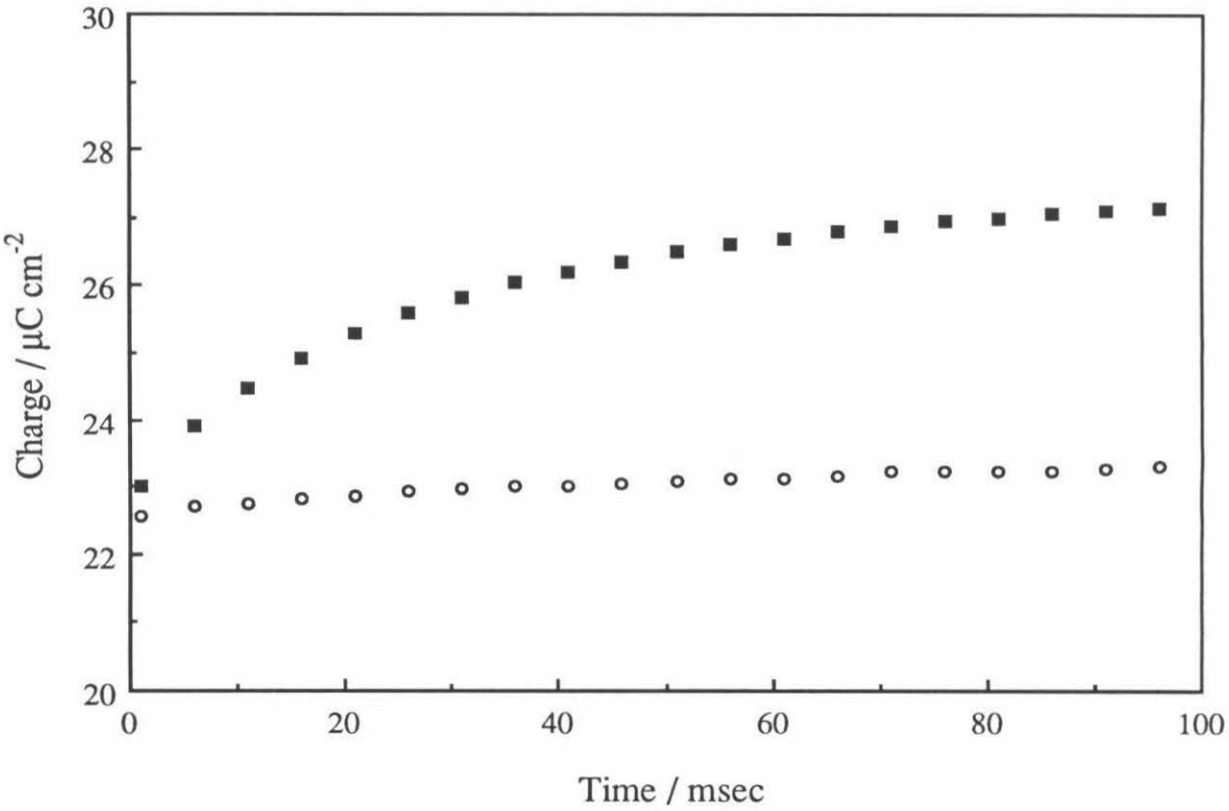

reduction to $Ni(cyclam)^{+}_{ads}$ would proceed at the slow rate measured by the slope of the cathodic charge-time curve shown in Figure 2.8. The much larger reverse slopes obtained in the double potential-step experiments of Table 2.4 are very close to the values expected if the form of $Ni(cyclam)^{2+}$ produced by oxidative desorption of $Ni(cyclam)^{+}_{ads}$ were reductively readsorbed at a diffusion-controlled rate. The charge-time behavior expected during the reverse step of double potential-step chronocoulometric experiments where a dissolved, one-electron reactant is present along with an adsorbed reactant which is instantaneously desorbed in the forward potential-step and readsorbed as fast as it diffuses back to the electrode surface during the reverse potential-step is give by Equation (2).[22]

$$Q_{rev} = Q_{d.l.} + \frac{2nFAD^{1/2}C^*}{\pi^{1/2}} (\tau^{1/2} + (t-\tau)^{1/2} - t^{1/2}) + nF\Gamma \left(1 - \frac{2}{\pi} \sin^{-1} \left(\frac{\tau}{t}\right)^{1/2}\right) \quad (2)$$

$Q_{d.l.}$, the charge required to charge the double layer, is consumed essentially instantaneously. The second term on the r.h.s. of Equation (2) represents the faradaic charge consumed by the product of the electrode reaction which was generated by the diffusion-limited reaction of the dissolved reactant during the forward step of duration τ. τ is the elapsed time since the forward potential step was applied. The other symbols have their usual significance. The third term on the r.h.s. of Equation (2) gives the faradaic charge consumed by the diffusion-limited reaction of the additional dissolved reaction product generated at the electrode surface by the instantaneous oxidative (or reductive) desorption of the reactant that was adsorbed on the electrode surface at the initial potential. It is this term which is responsible for the higher chronocoulometric slopes during the reverse potential steps in the experiments summarized in Table 2.4.

The $Ni(cyclam)^{2+}/Ni(cyclam)^{+}_{ads}$ system is different from those to which Equation (2) applies because only the Ni(II) complex produced by the oxidative desorption of $Ni(cyclam)^{+}_{ads}$ appears to be reducible at the diffusion-controlled rate at potentials more

positive than -1.3 V. For this situation, the charge-time behavior during the reverse potential step in a double potential-step chronocoulometric experiment should be given by Equation (3).

$$Q_{rev} = Q_{d.l.} + nF\Gamma\left(1-\frac{2}{\pi}\sin^{-1}\left(\frac{\tau}{t}\right)^{1/2}\right) \qquad (3)$$

Thus, plots of Q_{rev} vs $\sin^{-1}(\tau/t)^{1/2}$ should be linear with slopes determined by the quantity of Ni(cyclam)$^+$ that was adsorbed at the initial potential. A typical plot is shown in Figure 2.9. A straight line is obtained with a slope that corresponds to $F\Gamma = 5.5\ \mu C\ cm^{-2}$. This value compares favorably with the chronocoulometric estimate of $Ni(cyclam)^+_{ads}$ (4.9 μC cm^{-2} at -1.0 V). This result supports the suggestion that the Ni(cyclam)$^{2+}$ complex produced from the oxidative desorption of $Ni(cyclam)^+_{ads}$ differs from ordinary Ni(cyclam)$^{2+}$ in that it can be re-reduced to $Ni(cyclam)^+_{ads}$ at a diffusion-controlled rate at potentials where ordinary Ni(cyclam)$^{2+}$ is much less reactive.

2.3.8 Electrochemistry of Ni(cyclam)$^{2+}$ in Nonaqueous Solvents

Cyclic voltammograms for Ni(cyclam)$^{2+}$ in MeCN and DMF are shown in Figure 2.10. The magnitudes of the anodic and cathodic peak currents and their separation (60 mV) in these systems corresponded to the one-electron, diffusion-controlled reduction of Ni(cyclam)$^{2+}$ to Ni(cyclam)$^+$. Both cathodic and anodic peak currents varied linearly with the square root of the potential sweep rate and the ratio of these currents was one, indicating that the reductions are electrochemically reversible on the time scale of the experiment. For both solvents, a formal potential of -1.44 V for the Ni(cyclam)$^{2+/+}$ couple was derived from the average of the cathodic and anodic peak potentials.

In the MeCN system, a small anodic prepeak was noted at approximately -1.25 V; a cathodic counterpart was observed only sporadically and at potentials obscured by the main wave. Attempts to resolve this peak further were unsuccessful. It was noted that the age

Figure 2.9 Cathodic charge vs $\sin^{-1}(\tau/t)^{1/2}$ (Equation (3)) for the reverse step of a double potential-step chronocoulometric experiment with a 0.2 mM solution of $Ni(cyclam)^{2+}$ in 0.1 M $KClO_4$. Electrode potential held at -1.0 V, stepped to 0 V and the charge recorded for 5 msec, and then returned to -1.0 V.

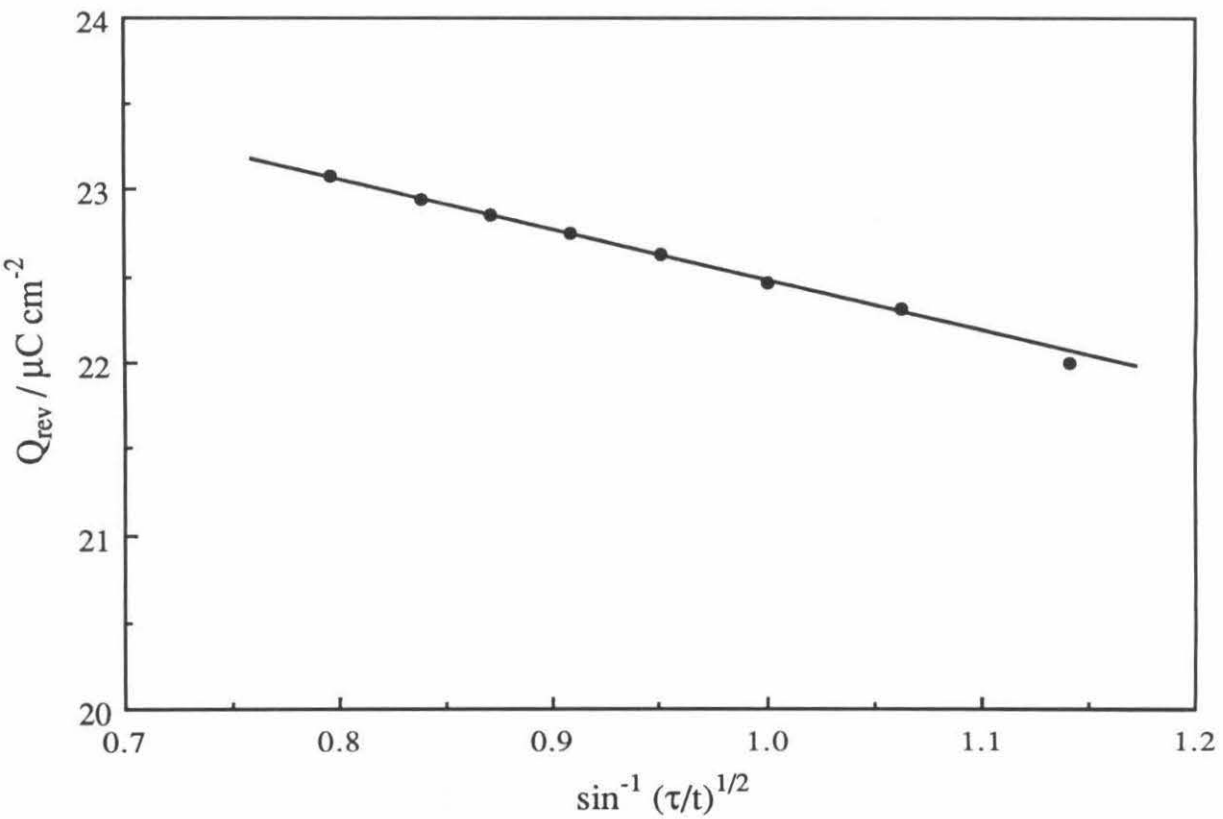

Figure 2.10 Cyclic Voltammograms of a 1.0 mM solution of Ni(cyclam)$(ClO_4)_2$ in 0.1 M TEAP in MeCN (dashed line) and DMF (solid line). Scan rate is 200 mV sec^{-1}. Hanging mercury drop working electrode.

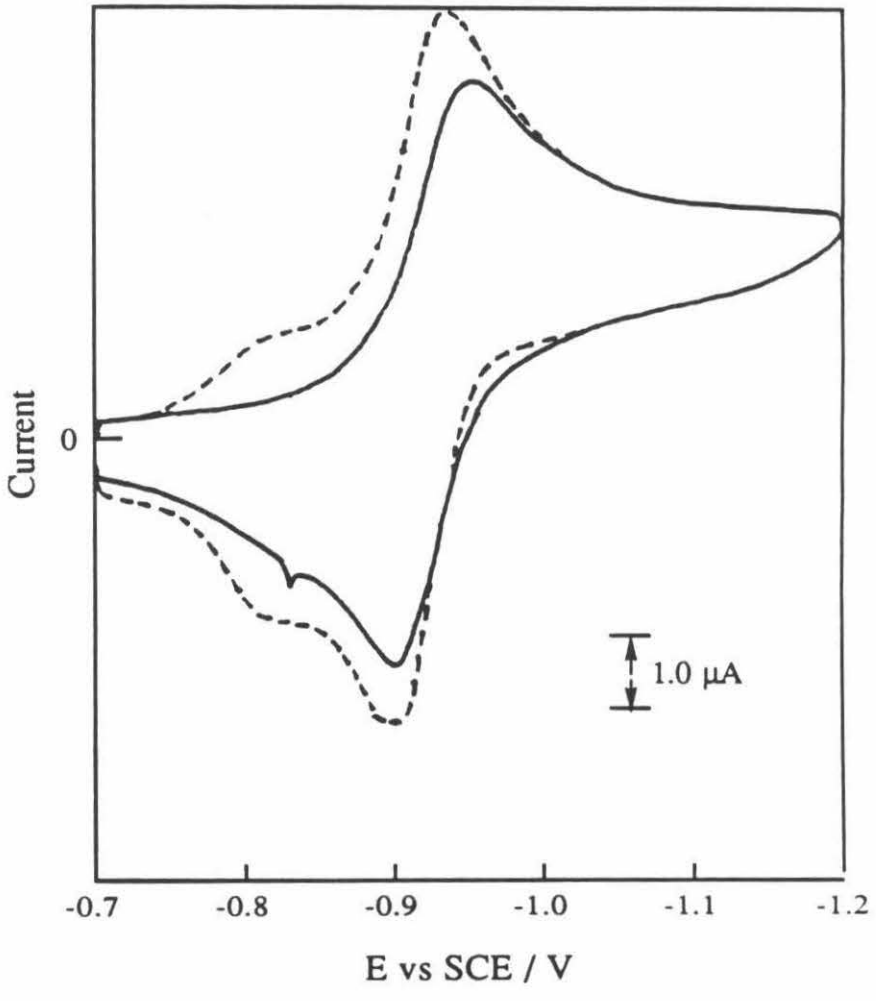

and purity of the electrolyte solution had a strong influence on the distinctness of the electrochemical response and therefore great pains were taken to avoid contamination. In the DMF system, the electrochemical responses were more consistent with well defined cathodic and anodic prepeaks were evident at -1.2 V. In contrast to the sharp (albeit small) peaks observed in both water and MeCN, the prepeaks in DMF were broad, spanning a potential range of 100 mV. However, the magnitudes of the prepeak currents in DMF varied linearly with the scan rate. This result, coupled with the fact that the integrated charge under the prepeaks was consistently comparable to that expected for the reduction or oxidation of a monolayer of adsorbed molecules on the surface, indicates that this prepeak arises as a result of the redox chemistry of $Ni(cyclam)^+$ on the electrode surface. It is not known at this time why the prepeak seen in MeCN is ill-defined; it may be that the adsorption process occurs more slowly than in other solvents. The sensitivity of the solvent purity on the adsorption bahavior may also affect the result.

In order to quantify the extent of adsorption of electroactive species on a mercury surface in nonaqueous solvents, chronocoulometric step experiments[19,20] were performed as previously described in Section 2.3.6. Experiments were done in the absence of $Ni(cyclam)^{2+}$ in order to determine the quantity of charge involved in double layer charging, and the results in the presence of $Ni(cyclam)^{2+}$ were corrected for these values. A summary of the results is presented in Table 2.5 and previous results in aqueous systems are provided for comparison.

Any adsorbed $Ni(cyclam)^{2+}$ at potentials of 0 to -1.0 V would be detected by a large difference in chronocoulometric intercepts for potentials steps from these potentials to a potential well into the main solution wave. As can be seen from the table, intercept differences of less than experimental error (with one exception, noted below) indicate that virtually no $Ni(cyclam)^{2+}$ is adsorbed between 0 and -1.0 V. Potential step experiments

with MeCN were erratic at potentials of 0 V; it is believed that the results for higher $Ni(cyclam)^{2+}$ concentrations are not reliable. Unknown electrochemical reactions, possibly related to solvent purity, appeared in the cyclic voltammograms at 0 V and are believed to be responsible for the anomolous results. Cathodic potential steps from potentials of -0.2 V did not show these anomolous results.

Potential steps of -1.0 and -1.6 to 0 V were employed to determine the extent of $Ni(cyclam)^{+}$ adsorption at these potentials, as was previously done in water. For initial potentials of -1.6 V, a large intercept difference indicated substantial adsorption of $Ni(cyclam)^{+}$ at this potential. This result was in agreement with the conclusions found in aqueous systems. In stark contrast to this latter behavior, there is a complete lack of intercept differences in the chronocoulometric results in DMF or MeCN at potentials positive of the prepeak seen in the cyclic voltammetry. Thus, no $Ni(cyclam)^{+}$ is adsorbed at these potentials.

Double potential-step chronocoulometry[20-22] was also used in an attempt to uncover the presence of $Ni(cyclam)^{+}$ at potentials positive of the prepeak seen in the cyclic voltammetry. The presence of high reverse slopes for an appropriate chronocoulometric plot such as that described in Section 2.3.7 is a good indicator of an adsorbed electroactive species. Potential steps with $Ni(cyclam)^{2+}$ in nonaqueous solvents showed almost no reverse slopes in contrast to the behavior observed in water (see Table 2.5). The slight variations observed with MeCN were attributed to the effects mentioned above.

The above evidence is very indicative of the absence of a nonaqueous two stage adsorption phenomena such as that seen in water. The only adsorptive process is that of $Ni(cyclam)^{2+}$ to $Ni(cyclam)^{+}_{ads}$ and this process occurs solely at the potentials of the prepeaks seen in the cyclic voltammetry.

2.3.9 Adsorption of Methylated Derivatives of Ni(cyclam)$^{2+/+}$ as Measured by Chronocoulometry

A similar analysis can be done for the amount of adsorbed electroactive species in systems of methylated derivatives of Ni(cyclam)$^{2+}$, hereafter referred to in general as NiL$^{2+/+}$. Chronocoulometric experiments[19,20] were done with Ni(TMC)$^{2+}$, Ni(DMC)$^{2+}$ and Ni(MMC)$^{2+}$.and were analyzed for the presence of any NiL^{+} or NiL^{2+} species at the electrode surface. This analysis was done less exhaustively than was the Ni(cyclam)$^{2+/+}$ system and is meant only to provide a basis of comparison between the two systems. For the methylated species, the system was cleaner due to the fact that the potentials of interest were well separated from the background, an advantage which was not available with Ni(cyclam)$^{2+/+}$. Because of the small potential window over which the electrochemistry of NiL$^{2+/+}$ occurred, single potential-step chronocoulometry was sufficiently accurate. A summary of the results is shown in Table 2.6; these values are representative of either *trans* I Ni(TMC)$^{2+}$ or *trans* III Ni(TMC)$^{2+}$ as no difference was noted in the chronocoulometric results between the two. Results for Ni(DMC)$^{2+}$ and Ni(MMC)$^{2+}$ were similar with the potential window shifted to more positive potentials. No evidence was seen for significant adsorption of Ni(TMC)$^{2+}$ as seen by the low intercept differences (intercepts in presence and absence of Ni(TMC)$^{2+}$) for cathodic potential steps positive of the potentials for the electrochemical reactions seen in the cyclic voltammograms, i.e., 0 to -0.7 V (Figure 2.4). The negative intercepts are most likely due to the effects of uncompensated IR drop. In addition, no evidence was seen for the adsorption of Ni(TMC)$^{+}$ at these potentials as evidenced by the lack of any significant intercept difference for similar anodic potential steps.

Chronocoulometric steps from potentials negative of -0.95 V (the potential of the prepeak seen in the cyclic voltammograms) to 0 V gave a large difference in intercepts. This result indicates that Ni(TMC)$^{+}$ is adsorbed at potentials negative of -0.95 V and that

the amount of adsorption (10 - 15 $\mu C\ cm^{-2}$) is roughly that of a monolayer of $Ni(TMC)^{+}_{ads}$ at the electrode surface. Because of the IR problems and the increased non-Faradaic to Faradaic charge ratio associated with large potential steps, the values obtained for the smallest potential steps (14 - 15 $\mu C\ cm^{-2}$) were assumed to be the actual electrode coverage. Concentration studies showed an almost total lack of dependence of surface coverage versus solution $Ni(TMC)^{2+}$ concentration for concentrations of up to 2 mM. Solutions of $Ni(TMC)^{2+}$ as dilute as 20 μM exhibited almost a full monolayer of coverage.

In all respects, the adsorption of methylated derivatives of cyclam complexes followed a diffusion-controlled, reductive adsorption process. This process occurred solely at the potential of the prewave observed in the cyclic voltammograms and no evidence was seen for the unusual adsorptive behavior that was observed with $Ni(cyclam)^{2+/+}$. However, this is not surprising since, a) prepeaks of this nature are indicative of the reductive adsorption process at the electrode surface[23] and b) the integrated area under the prepeak seen in the cyclic voltammograms of the methylated cyclams (10 - 15 $\mu C\ cm^{-2}$) is very close to the amount of charge measured by chronocoulometry (14 - 16 $\mu C\ cm^{-2}$).

2.4 *Discussion*

2.4.1 Adsorption of Ni(cyclam)$^+$ on Mercury

The electrochemical behavior of Ni(cyclam)$^{2+}$ at mercury electrodes is unusual in several respects. The reductive adsorption proceeds at potentials where Ni(cyclam)$^{2+}$ is thermodynamically prohibited from being reduced to Ni(cyclam)$^+$ in solution. Strong stabilizing interactions between electrode surfaces and the products of electrode reactions are well-known to produce prewaves at potentials ahead of the main reduction (or oxidation) wave with magnitudes which are limited by the surface area of the electrode.[23] However, it is rare for prewaves to appear at potentials as far ahead of the main wave as does the adsorptive reduction of Ni(cyclam)$^{2+}$. The production of $\text{Ni(cyclam)}^{+}_{ads}$ at potentials almost one volt less negative that the formal potential Ni(cyclam)$^{2+/+}$ couple in solution bespeaks a very strong chemical interaction between the adsorbed complex and the mercury surface. The evidence given in Table 2.2 for possible weak adsorption of Ni(cyclam)$^{2+}$ between -1.0 and -1.3 V from 0.2 mM but not from 1 mM solutions may be a further indication of the strength of the interaction between $\text{Ni(cyclam)}^{+}_{ads}$ and the mercury surface: A weaker dependence on concentration of the adsorption of Ni(cyclam)$^{2+}$ than of Ni(cyclam)$^+$ would lead to the behavior shown in Table 2.2.

Solutions of Ni(cyclam)$^{2+}$ are known to contain several configurational isomers of the complex[24,25] and it is conceivable that the presence of one of these isomers in minor amounts might be responsible for the reductive adsorption. The dominant isomers present in solution at equilibrium are the *trans* III (85%) and *trans* I (~ 15%) (Figure 2.11) with the other forms present in amounts below one percent.[24,25] In crystalline samples of Ni(cyclam)$(ClO_4)_2$ the complex is present entire in the *trans* III form[26] and the attainment of isomerization equilibrium after dissolution of the salt can be monitored by proton NMR. NMR spectra of freshly prepared and aged solutions indicate that the isomerization requires

Figure 2.11 Configurational isomers of square planar $Ni(cyclam)^{2+}$ in solution and the percentages of each isomer present at equilibrium.

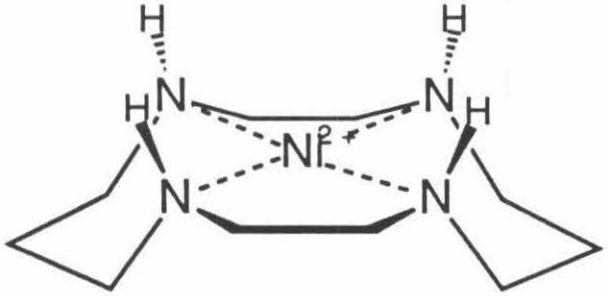

Trans I
15%

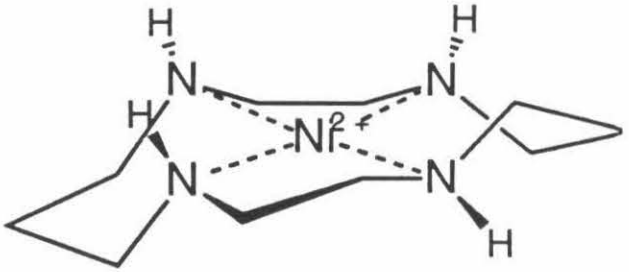

Trans II
< 1%

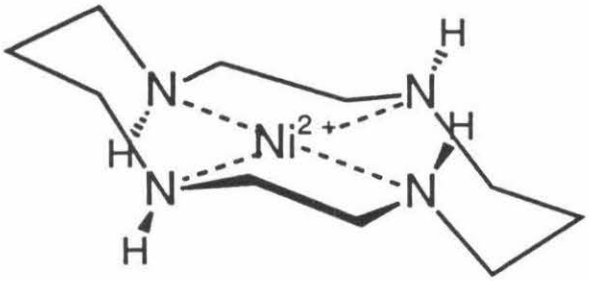

Trans III
85%

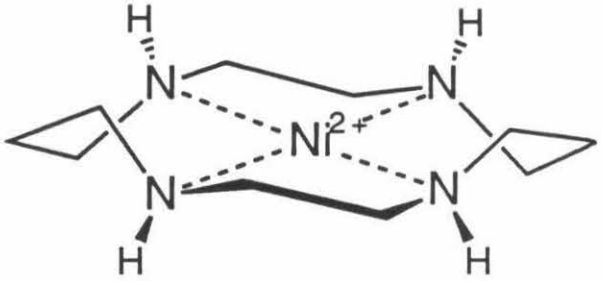

Trans IV
< 1%

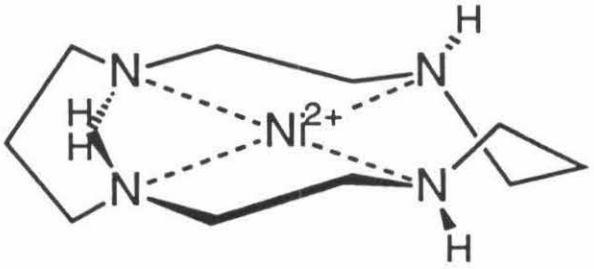

Trans V
< 1%

several hours to reach equilibrium.[24] This previous result was confirmed in this study and representative spectra are shown in Figure 2.12. The appearance of the second isomer in solution can be monitored by the growth of several peaks between 1.0 and 3.5 ppm. The rate of the reductive adsorption from $Ni(cyclam)^{2+}$ solutions as measured by chronocoulometry was no different in freshly prepared and aged solutions so that the less dominant *trans* I isomer is not the complex which is responsible for the unusual reductive adsorption of $Ni(cyclam)^{+}$.

If another isomer, present at a low equilibrium concentration, were the species that was reductively adsorbed at a rate limited by its diffusion to the electrode surface, the current-time curves obtained in normal pulse polarography should adhere to the Cottrell equation. Plots of current vs $t^{-1/2}$ should be linear if the rate of attainment of isomerization equilibria were slow. If the isomerization equilibria were more rapid the currents should show increasingly positive deviations from the Cottrell line at large measurement times. The data in the insert in Figure 2.2 do not match either expectation. Thus, the species which undergoes the reductive adsorption is probably produced in a slow structural transformation of the $Ni(cyclam)^{2+}$ complex at or on the electrode surface followed by rapid electron transfer to yield the reduced, adsorbed product, $Ni(cyclam)^{+}_{ads}$.

Despite the lack of complete identification of the structural rearrangements, several conclusions can be drawn regarding the process. The structural rearrangements in the coordinated cyclam ligand that led to the production of $Ni(cyclam)^{+}_{ads}$ are apparently retained when the adsorbed complex is oxidatively desorbed, because the $Ni(cyclam)^{2+}$ that is desorbed can be re-reduced to $Ni(cyclam)^{+}_{ads}$ at a diffusion-controlled rate at potentials as positive as -0.6 V. This is a property not exhibited by the $Ni(cyclam)^{2+}$ complex obtained by dissolution of $Ni(cyclam)(ClO_4)_2$. The abbreviation cyclam* designates the form of the coordinated ligand that produces the more easily reduced Ni(II) complex, $Ni(cyclam\ *)^{2+}$.

Figure 2.12 Proton NMR of 5 mM solutions of Ni(cyclam)Cl_2 in D_2O. Top spectra is 10 minutes after dissolution of salt and lower spectra is 1 hour later.

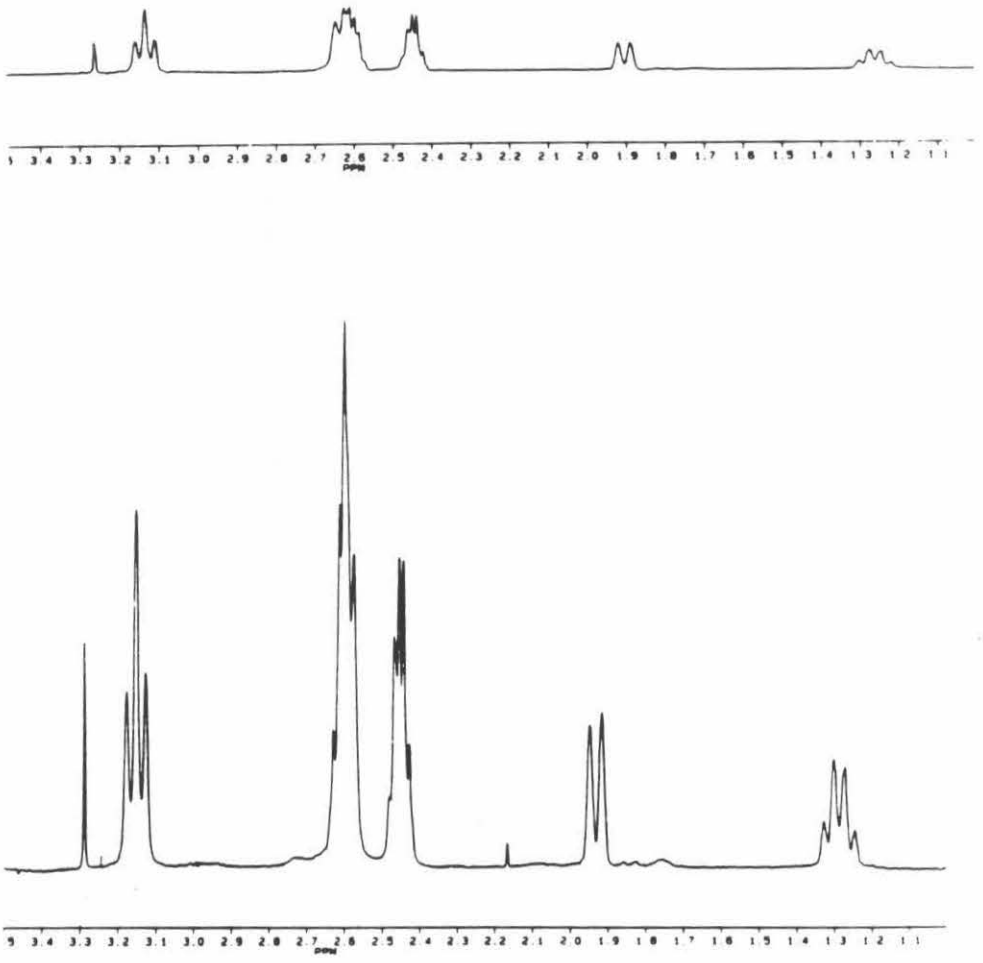

The Ni(cyclam*)$^{2+}$ complex that is readily reductively adsorbed is not long-lived: Attempts to generate measurable quantities of it by carrying out successive reductive adsorption-oxidative desorption cycles for many hours at a large mercury pool electrode in a solution of Ni(cyclam)$^{2+}$ produced a solution with electrochemical properties indistinguishable from those of the original solution. Extending the duration, τ, of the oxidative desorption step in double potential-step chronocoulometric experiments produced linear plots of Q_{rev} vs $\sin^{-1}(\tau/t)^{1/2}$ (e.g., Figure 2.9), a result which requires that the Ni(cyclam*)$^{2+}$ complex persist during the largest value of τ employed, 2 sec. These data bracket the lifetime of the complex to be between several seconds and several minutes.

To examine the possibility of generating Ni(cyclam*)$^{2+}$ from unadsorbed Ni(cyclam)$^{+}$, an asymmetric double potential-step experiment was conducted. The electrode was held at -1.6 V for 30 seconds to cover the electrode surface fully with $Ni(cyclam)^{+}_{ads}$. The potential was then stepped to 0 V to oxidatively desorb the $Ni(cyclam)^{+}_{ads}$ and to oxidize the solution phase Ni(cyclam)$^{+}$ to Ni(cyclam)$^{2+}$. Finally, the potential was stepped to -1.0 V where the anodic oxidation of the Ni(cyclam)$^{+}$ in solution continued while the Ni(cyclam*)$^{2+}$ produced in the oxidative desorption was reductively re-adsorbed at a diffusion-controlled rate along with the original Ni(cyclam)$^{2+}$ complex which was reductively adsorbed at the lower rate evident in Figure 2.8. If the Ni(cyclam)$^{2+}$ that was electrogenerated from the unadsorbed Ni(cyclam)$^{+}$ had the same ligand configuration as the Ni(cyclam)$^{2+}$ complex generated from $Ni(cyclam)^{+}_{ads}$, the values of Q_{rev} obtained during the final step would increase more rapidly (until the electrode surface became saturated with $Ni(cyclam)^{+}_{ads}$.

The measured values of Q_{rev} were corrected for the anodic contribution from the continued oxidation of Ni(cyclam)$^{+}$ and the cathodic contribution from the slow reductive adsorption of the original Ni(cyclam)$^{2+}$. The resulting charge, Q_{corr}, was plotted against

$\sin^{-1}(\tau/t)^{1/2}$ for values of Q_{corr} less than that required to saturate the electrode surface with $Ni(cyclam)^{+}_{ads}$ at -1.0 V. The $F\Gamma$ value calculated from the slope of the resulting plot (Figure 2.13) was 11 $\mu C\ cm^{-2}$. This value was close to the value calculated on the basis of Equation (2), 12 $\mu C\ cm^{-2}$, in which the only faradaic contribution to Q_{corr} is assumed to result from the reduction of the $Ni(cyclam^*)^{2+}$ produced by the oxidative desorption of the $Ni(cyclam)^{+}_{ads}$. This agreement shows that only $Ni(cyclam)^{+}_{ads}$ is the precursor to the $Ni(cyclam^*)^{2+}$ which is rapidly re-reduced to $Ni(cyclam)^{+}_{ads}$ at - 1.0 V. Thus, the strong interactions between the mercury surface and the $Ni(cyclam)^{+}$ complex that are responsible for its adsorption are apparently also involved in the changes in ligand configuration leading to the production of $Ni(cyclam)^{2+}$ when the adsorbed complex is oxidatively desorbed.

All the experiments described thus far employed the $Ni(cyclam)^{2+}$ complex in which the two open coordination sites of the Ni(II) center were in the *trans* configuration. An interesting question is whether the more reactive $Ni(cyclam^*)^{2+}$ is also accessible from *cis*-Ni(cyclam($(OH_2)^{2+}$ (Figure 2.14). The rate of isomerization of *cis*-Ni(cyclam)$(OH_2)^{2+}$ to the thermodynamically favored mixture of *trans*-Ni(cyclam)$(OH_2)^{2+}$ and square planar $Ni(cyclam)^{2+}$ is known[15] to proceed too slowly for $Ni(cyclam^*)^{2+}$ and *cis*-Ni(cyclam)$(OH_2)^{2+}$ to be the same complex. Experiments with solutions of *cis*-Ni(cyclam)$(OH_2)^{2+}$ showed that its reductive adsorption on mercury at - 1.0 V was less extensive (see Table 2.7) than that exhibited from a solution containing the original $Ni(cyclam)^{2+}$ complex. In addition, the rate of attainment of adsorption equilibrium from a solution of the dissolved salt proceeded at an even slower rate than that of $Ni(cyclam)^{2+}$. Thus, *cis*-Ni(cyclam)$(OH_2)^{2+}$ does not appear to be an intermediate in the formation of $Ni(cyclam^*)^{2+}$.

The *cis*-Ni(cyclam)$(OH_2)^{2+}$ in solution is reversibly converted to the *trans* V isomer (Figure 2.14) by increasing the concentration of ClO_4^- anions in the supporting electro-

Figure 2.13 Corrected cathodic charge (see text) vs $\sin^{-1}(\tau/t)^{1/2}$ (Equation (2)) for the reverse step of an asymmetric double potential-step chronocoulometric experiment with a 0.2 mM solution of $Ni(cyclam)^{2+}$. Electrode potential held at -1.6 V, the potential stepped to 0 V for 10 msec and then returned to -1.0 V.

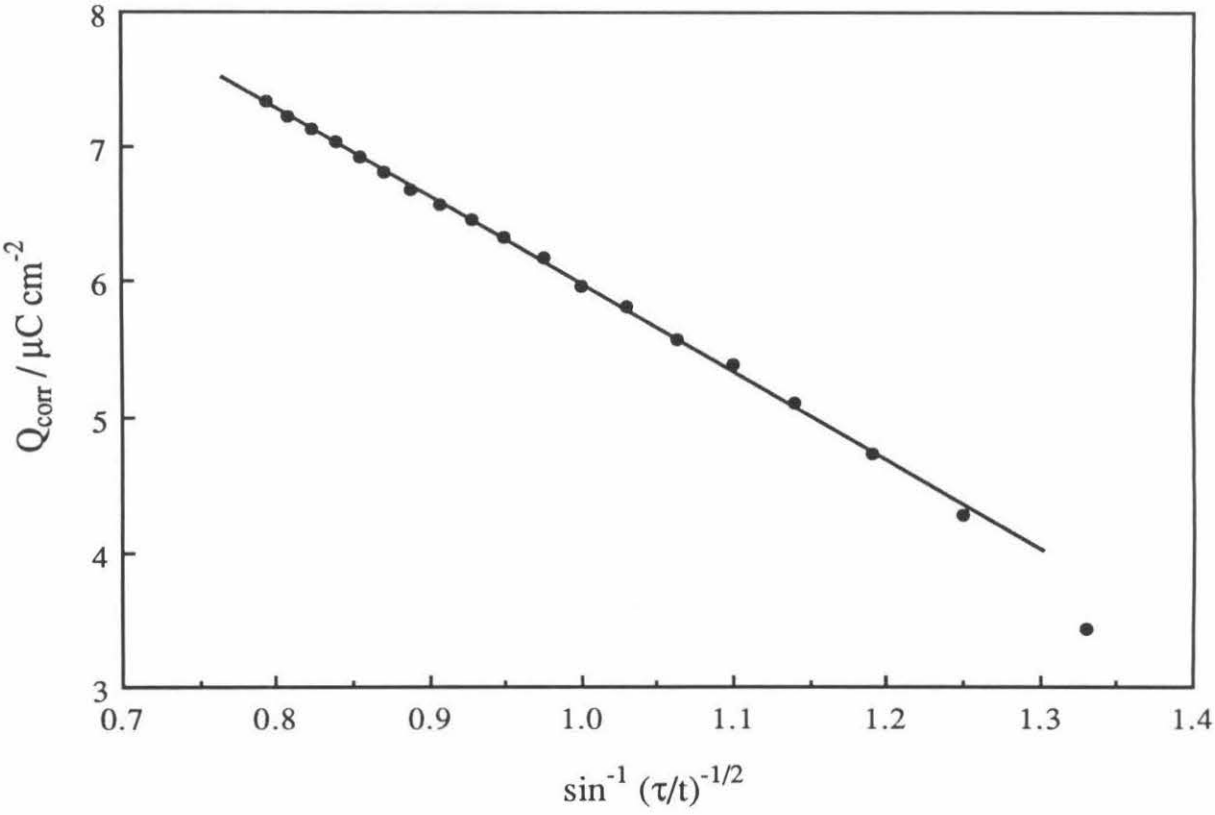

Figure 2.14 *Cis* -Ni(cyclam)$^{2+}$ (top figure) and α-(Trans V) Ni(cyclam)$(ClO_4)_2$ (lower figure).

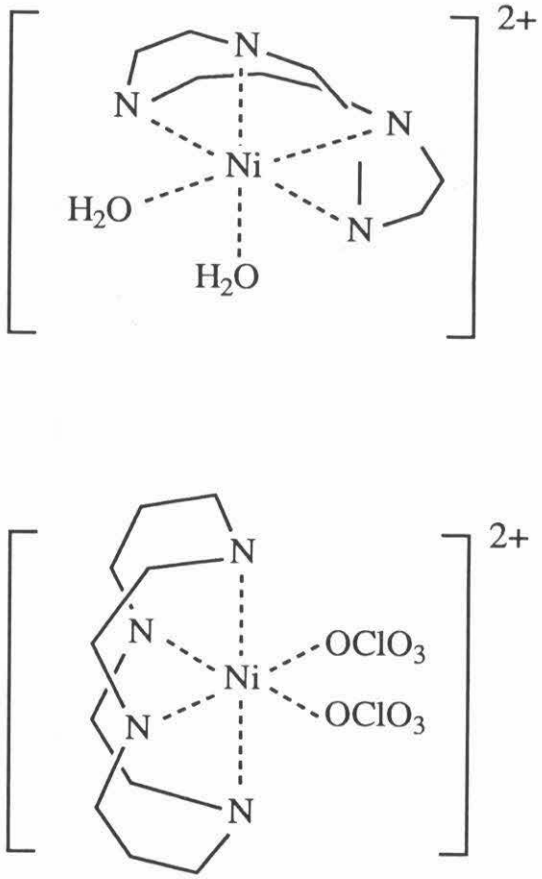

lyte.[15] The rate at which the reductive adsorption on mercury proceeded in 4 M $NaClO_4$ solutions was no different than that in 0.1 M $KClO_4$ so that the *trans* V isomer is also not a likely candidate for the Ni(cyclam*)$^{2+}$ complex.

2.4.2 Adsorption of Methylated Derivatives of Ni(cyclam)$^{+}$ on Mercury

There are several important characteristics which separate Ni(cyclam)$^{+}$ and Ni(TMC)$^{+}$ and influence their adsorptive behavior. First, the presence of methyl groups on the ligand acts to stabilize the Ni(I) oxidation state[27] by altering the orbital environment around the metal center, resulting in an anodic shift of the formal potential of the $NiL^{2+/+}$ couple[16] (see Table 2.1). Second, the increased steric bulk of the methylated ligands might result in different adsorption behavior if the ligand structure has intimate contact with the mercury surface. Third, the coordination of the ligand to the metal would be expected to be different. Finally, interconversion of the configurational isomers of the cyclam ligand requires deprotonation of the nitrogens of the ring, a situation which has been shown by Barefield *et al.*[28,29] not to occur with the tetramethyl cyclam. All of these factors may be present in varying degrees, which makes a comparison of the experimental results between the various ligands worthwhile.

Since the first publication of the synthesis of Ni(I) complexes of tetramethylcyclam,[7] many other studies have appeared on the coordination of this complex.[28-31] Ni(II) complexes of this ligand exhibit extreme propensity towards pentacoordination, rather than the predominantly square planar coordination exhibited by Ni(cyclam)$^{2+}$. In solution, this fifth coordination site is occupied by a solvent molecule, and the Ni(II) center lies outside of the plane of the ligand. Presumably, the larger Ni(I) center would lie even farther from the plane of the ligand, allowing a stronger interaction to occur between the metal center and the mercury surface. Or, if the complex were situated such that the ligand was between the electrode surface and the nickel center, the asymmetry

of the Ni(II) or Ni(I) center might reduce the interaction with the surface. As seen in Table 2.6, very strong adsorption of this complex does occur, and there is no evidence for the "two stage" adsorption seen with the non-methylated complex. The most likely explanation is that the inability of the tetramethylated cyclam to interconvert between different configurational isomers prevents the analogous TMC* complex from ever being formed. The other possible explanations-solvation, steric bulk, and coordination are deemed to influence this aspect of the adsorption to a lesser degree.

The result that there is only one configuration of the $Ni(TMC)^+$ which is adsorbed and the fact that the reductive adsorption process appears to proceed at a rate controlled only by the diffusion of molecules to the electrode surface leads to one of two conclusions. Either the $Ni(TMC)^+$ adsorption process does not involve a ligand rearrangement, or the ligand rearrangement occurs much faster than the mass transfer of molecules to the surface. There is some evidence[32] that the presence of strongly coordinating solvents, especially amines, can rapidly increase an otherwise slow isomerization reaction. An intriguing possibility is that the mercury could also effect such an interaction, a possibility which fits well with the central focus of the unusual adsorption behavior of $Ni(cyclam)^+$: The mercury is necessary to stabilize the Ni(I) center. Unfortunately, a further investigation of this possibility is beyond the scope of this thesis.

2.4.3 Adsorption of $Ni(cyclam)^+$ in Nonaqueous Solvents

Although the subject of this thesis is limited to aqueous CO_2 electroreduction, a comparison of the electrochemical behavior of the catalyst in nonaqueous systems is worthwhile. In aqueous solutions of $Ni(cyclam)^{2+}$ the equilibrium[33] between the square planar and octahedral complexes is described by Equation (4).

$$Ni(cyclam)^{2+} + 2\,H_2O \rightleftharpoons Ni(cyclam)(OH_2)_2^{2+} \qquad (4)$$

The value of K for this equilibria (0.38) indicates that most $Ni(cyclam)^{2+}$ molecules exist in the square planar, low spin form. An increase in the temperature or in the ionic strength of the solution shifts the equilibrium to the right.

The presence of a strongly coordinating solvent has been shown to shift the solvation equilibrium.[34,35] Studies of $Ni(TMC)^{2+}$ and of $Ni(cyclam)^{2+}$ have shown that non-aqueous solvent molecules or unidentate ligands can strongly bind to these complexes. An interesting question at this point is whether the presence of a strongly coordinating solvent has an effect on the adsorption behavior of $Ni(cyclam)^{+}$. A caveat is that solvent and ligand binding studies have only been done on $Ni(cyclam)^{2+}$, the precursor to $Ni(cyclam)^{+}_{ads}$. Although $Ni(cyclam)^{+}$ has been isolated in nonaqueous solvents, no ligand binding studies have been done.

The solvents chosen for this study include DMF and MeCN as these were shown[35] to have a much larger K value (27.15 and 8.85, respectively) for the solvation equilibria such as that of Equation (4). Chronocoulometric results for experiments in these solvents show a total lack of adsorption at potentials positive of the prewave at -1.3 V. The presence of the strongly coordinating species apparently renders impossible the slow isomerization of $Ni(cyclam)^{2+}$ to $Ni(cyclam)^{+}_{ads}$ at these potentials. At potentials negative of the prepeak, the quantity of adsorption is the same as that seen in the aqueous system.

In all of these solvents (H_2O, MeCN, DMF), the prepeak occurs at approximately the same potential. It is surprising that solvent interactions with the adsorbate would have no effect on the adsorptive process, given the variations in the degree of solvation for these systems. The solvent molecule coordination to the $Ni(cyclam)^{2+}$ has no effect on the extent of adsorption of $Ni(cyclam)^{+}$ on mercury for the main stage of adsorption, i.e., adsorption at potentials negative of -1.3 V. However, the peculiar "pre-adsorption" of $Ni(cyclam)^{+}$ at potentials of -0.6 to -1.2 V is blocked by the presence of strongly coordinating solvent

molecules. Only in the case of aqueous systems is $Ni(cyclam)^{2+}$ unhindered enough so that reductive adsorption to $Ni(cyclam)^{+}_{ads}$ can occur. Measurements of the quantity of adsorbed species at -1.0 V with various ionic strengths showed no differences from 0.05 M to 4 M. It is reasonable to conclude that either the effect of a shift in the equilibrium of Equation (4) is too small to be noticed, or water molecules are readily displaced anyway.

It is not believed that the presence of a strongly coordinating solvent physically blocks the $Ni(cyclam)^{2+}$ from ever reaching the electrode surface close enough for the necessary metal center/electrode interactions to occur. Rather, it is more likely that the ligand coordination is affected in such a way as to prevent the intimate interaction of the nickel center with the mercury surface. This behavior was also proposed to occur in the case of $Ni(TMC)^{+}$, a species which has also been shown to exhibit no adsorption at potentials positive of the prepeak seen in the cyclic voltammetry. Classical adsorptive behavior of all three systems, $Ni(TMC)^{2+}$, $Ni(cyclam)^{2+}$ in aqueous and in nonaqueous solvents, occurs at potentials negative of this prepeak. Steric or solvent effects play a much less significant role. In these cases, the close access of the metal center to the electrode is not as essential as is the case with the "preadsorption" of $Ni(cyclam)^{+}$.

2.4.4 Nature of the Oxidatively Desorbed $Ni(cyclam^*)^{2+}$ Complex

The unusual electrochemical reactivity of the $Ni(cyclam^*)^{2+}$ complex is most simply explained as the result of an unusual, metastable configuration adopted by the cyclam ligand when the $Ni(cyclam)^{+}$ complex is adsorbed on the mercury surface. If we assume that the complex of Ni(II) and cyclam produced by the oxidative desorption retains the unusual ligand configuration for at least a few seconds, its more facile reductive re-adsorption can be understood because no arrangements of the ligand would be required before the adsorption could proceed at the diffusion-controlled rate revealed by the large slopes observed during the reserve potential steps in Table 2.4. The strong interaction

between the nickel-cyclam complex and the mercury electrode surface that is required in order for the reductive adsorption to proceed at the observed potentials presumably requires a ligand configuration which facilitates binding between the metal center and the mercury surface. The reduction of the complex from Ni(II) to Ni(I) may facilitate the binding by forcing the larger Ni(I) center somewhat out of the macrocyclic plane.[25,36] The resulting adsorbed complex, which is evidently able to bind CO_2 and function as a CO_2 reduction catalyst, would have a coordination geometry closer to octahedral and thus would not resemble any of the configurations shown in Figure 2.11 for unadsorbed cyclam complexes of Ni(II).

$Ni(cyclam)^{2+}$ is highly resistant to dissociation into its components, even in concentrated acid solutions[16,37] (where the dissociation is thermodynamically favored[38]). Therefore, it would not be surprising if major alterations in the configuration of the cyclam ligand were required for the nickel center to interact strongly with the mercury surface. However, the altered ligand configuration (cyclam*) can not cause the oxidatively desorbed $Ni(cyclam^*)^{2+}$ complex to dissociate rapidly in acidic media because the large chronocoulometric reverse slopes, which are the best evidence for the existence of a more electrochemically reactive complex, persist when the supporting electrolyte is changed from neutral 0.1 M $KClO_4$ to 0.1 M HCl. The possibility that a hydride complex of Ni(cyclam) is involved is unlikely, due to the lack of dependence of the chronocoulometric results on the pH of the supporting electrolyte between pH 1 and 10. The electrochemistry of the $Ni(cyclam)^{2+/+}$ couple in solution is completely independent of the pH, as evidenced by the cyclic voltammograms of $Ni(cyclam)^{2+}$ in solutions of pH 1 to 13. The pK_a of the proton of a coordinated water molecule of the complex $Ni(cyclam)(OH_2)_2^{2+}$ has been determined[34] to be 13.67.

An alternative for the more reactive complex involving mercuration of the $Ni(cyclam)^{+}$ complex when it is oxidized at 0 V was considered. However, all attempts to

detect mercury in the complex by experiments with a rotating mercury disk-platinum ring electrode were negative. Similarly, exposure of solutions of $Ni(cyclam)^{+}$ (generated electrochemically at pH 12 where the lifetime of the reduced complex is adequate) to Hg(I) or Hg (II) salts produced no evidence of the formation of mercurated products: Either no reaction occurred or mercury metal was deposited.

The results presented in this chapter are best explained in terms of a form of $Ni(cyclam)^{+}_{ads}$ with an unusual ligand configuration which is produced as a result of its adsorption on mercury. The unusual configuration is retained temporarily when the complex is oxidatively desorbed to yield the metastable $Ni(cyclam^{*})^{2+}$ complex. It should be noted that isomerization of an extensively methylated cyclam complex of Ni(II) by interaction with mercury surfaces was proposed in a previous study[27] although the evidence presented would be equally compatible with an isomerization accompanying the type of reductive adsorption that is exhibited by the $Ni(cyclam)^{2+}$ complex. A contrast can be drawn from the chronocoulometric results of Ni(TMC) given in Table 2.6 and Section 2.3.8. The total lack of dependence of the adsorption behavior of $Ni(TMC)^{+}$ on the ligand configuration suggests that the ligand configuration itself plays a minor role in the adsorptive behavior of $Ni(cyclam)^{+}$. Instead, the major factor is the ability of the preferred ligand to allow the strong interaction between the Ni(I) center and the mercury electrode. As mentioned, this intimate interaction is necessary to account for the stabilization of the Ni(I) complex at the potentials observed (Figure 2.6).

2.4.5 Comparison with Previous Results

To date, no detailed studies have been done on the adsorption of methylated complexes of cyclam at mercury. In those areas where electrochemical experiments have been done[1-4,13] with Ni(cyclam)$^{2+/+}$, the results are in general agreement with those presented in this thesis although the report[27] that Ni(cyclam)$^{2+}$ is not reduced at dropping or hanging mercury drop electrodes was clearly erroneous. No strong evidence was obtained to support the proposal that the limited lifetime of Ni(cyclam)$^{+}$ in aqueous solutions might result from the expulsion of the Ni(I) center from the ring.[3] A reconciliation of the differences in the observed results is offered in chapter three. The reduction of the Hg(cyclam)$^{2+}$ complex and the oxidation of Hg electrodes in the presence of cyclam produced electrochemical responses that have no resemblance to those obtained with the Ni(cyclam)$^{2+/+}$ system. A complete discussion of the electrochemistry of Hg(cyclam)2+ and of the ligand cyclam at a mercury electrode is addressed in chapter four.

Both Sauvage and co-workers[1] and Fujihara and co-workers[3] cited the approximate coincidence of the peak potentials of the small prewave obtained in Ni(cyclam)$^{2+}$ solutions under argon and that of the catalytic wave for the reduction of CO_2 in concluding that the catalysis commences at the potential where Ni(cyclam)$^{2+}$ is reduced to Ni(cyclam)$^{+}_{ads}$. The results of this study point to a somewhat different conclusion. The prewave obtained in solutions of Ni(cyclam)$^{2+}$ represents only about 0.3 $\mu C\ cm^{-2}$ of charge, much less than the 14 $\mu C\ cm^{-2}$ that would correspond to a monolayer of Ni(cyclam)$^{+}_{ads}$. Moreover, the chronocoulometric results show that the reductive adsorption commences at potentials well ahead of the prewave (Table 2.1, 2.3, 2.4). The potential dependence of the adsorption of Ni(cyclam)$^{+}$ (Figure 2.6) shows that the prewave marks the potential where the extent of adsorption increases abruptly, probably because of a rearrangement of the adsorbed complex to allow a denser packing on the mercury surface. An accompanying small

change in the double layer capacitance of the electrode would provide a reasonable explanation for both the presence and the magnitude of the prewave. This is in sharp contrast to the results observed for the methylated cyclam complexes discussed in Section 2.4.3.

The electrocapillary curves obtained in this study and by Fujihira and co-workers,[3] are in moderate agreement but the interpretations offered for the depression in surface tension produced by the presence of $Ni(cyclam)^{2+}$ in solution are different. Without the benefit of independent chronocoulometric estimates of the adsorbed species, Fujihira and co-workers proposed substantial adsorption of both $Ni(cyclam)^{2+}$ and $Ni(cyclam)^{+}$. The results detailed in this thesis indicate only weak adsorption of $Ni(cyclam)^{2+}$ and only within a narrow potential range in dilute solutions of $Ni(cyclam)^{2+}$ (Table 2.2).

2.5 *Conclusions*

The results presented in this chapter have provided a comprehensive summary of the adsorption of nickel complexes of cyclam and of its derivatives. In addition, this study has provided additional information concerning the ability of adsorbed $Ni(cyclam)^{+}$ to serve as an electrocatalyst for the reduction of CO_2 at mercury electrodes. This topic is discussed further in chapter five. The new results demonstrate that the adsorption of $Ni(cyclam)^{+}$ on mercury stabilizes the complex so that it can be generated at potentials almost 1.0 V positive of the formal potential of the $Ni(cyclam)^{2+/+}$ couple in solution. The sharp cathodic prewaves observed at mercury electrodes in solutions of $Ni(cyclam)^{2+}$ appear to be associated with a structural rearrangement of the $Ni(cyclam)^{+}_{ads}$ layer on the electrode surface rather than a reductive adsorption process.

The reductive adsorption of $Ni(cyclam)^{+}$ is apparently accompanied by a reconfiguration of the cyclam ligand in the adsorbed complex which persists when it is oxidatively desorbed. The $Ni(cyclam^{*})^{2+}$ complex can then be re-reduced to

$Ni(cyclam)^{+}_{ads}$ at a diffusion-controlled rate. The ligand reconfiguration required before the original $Ni(cyclam)^{2+}$ complex can be reduced to $Ni(cyclam)^{+}_{ads}$ proceeds at at much slower rate.

Chapter 2 References

1. Beley, M.; Collin, J.-P.; Ruppert, R.; Sauvage, J.-P. *J. Am. Chem. Soc.* **1986**, *108*, 7461.
2. Beley, M.; Collin, J.-P.; Ruppert, R.; Sauvage, J.-P. *J. Chem. Soc., Chem. Commun.* **1984**, 1315.
3. Fujihira, M.; Hirata, Y.; Suga, K. *J. Electroanal. Chem.* **1990**, *292*, 199.
4. Fujihira, M.; Nakamura, Y.; Hirata, Y.; Akiba, U.; Suga, K. *Denki Kagaku*, **1991**, *59*, 532.
5. Balazs, G.B.; Anson, F. C. *J. Electroanal. Chem.* **1992**, *322*, 325.
6. Bosnich, B.; Tobe, M.L.; Webb, G.A. *Inorg. Chem.* **1965**, *8*, 1102,1109.
7. Barefield, E.K.; Wagner, F. *Inorg. Chem.* **1973**, *12*, 2435.
8. Wagner, F.; Barefield, E.K. *Inorg. Chem.* **1976**, *15*, 408.
9 Ciampolini, M.; Fabbrizzi, L.; Licchelli, M.; Perotti, A.; Pezzini, F.; Poggi, A. *Inorg. Chem.* **1986**, *25*, 4131.
10. Billo, E.J. *Inorg. Chem.* **1981**, *20*, 4019.
11. Lauer, G.; Abel, R.; Anson, F.C. *Anal. Chem.* **1967**, *39*, 765.
12. Collin, J.-P.; Jouaiti, A.; Sauvage, J.-P. *Inorg. Chem.* **1988**, *27*, 1986.
13. Taniguchi, I.; Nakashima, N.; Matsushita, K.; Yasukouchi, K. *J. Electroanal. Chem.* **1987**, *224*, 199.
    Taniguchi, I.; Shimpuku, T.; Yamashita, K.; Ohtaki, H. *J. Chem. Soc., Chem. Commun.* **1990**, 915.
14. Bard, A.J.; Faulkner, L.R.; Electrochemical Methods; Wiley and Sons: New York, 1980, p. 186.
15. Billo, E.J. *Inorg. Chem.* **1984**, *23*, 236.
16. Barefield, E.K.; Freeman, G.M.; Van Derveer, D.G. *Inorg. Chem.* **1986**, *25*, 552.
17. Madeyski, C.M.; Michael, J.P.; Hancock, R.D. *Inorg. Chem.* **1984**, *23*, 1487.

18. Milner, G.W.C.; The Principles and Applications of Polarography; Longmans, Green and Co.: London, 1957, p. 70.

19. Christie, J.H.; Anson, F.C.; Lauer, G.; Osteryoung, R.A. *Anal. Chem.* **1963**, *35*, 1979.

20. Anson, F.C.; Osteryoung, R.A. *J. Chem. Ed.* **1983**, *60*, 293.

21. Anson, F.C. *Anal. Chem.* **1967**, *39*, 1514.

22. Christie, J.H.; Osteryoung, R.A.; Anson, F.C. *J. Electroanal. Chem.* **1967**, *13*, 236.

23. Wopschall, R.; Shain, I. *Anal. Chem.* **1967**, *39*, 1514.

24. Connolly, P.J.; Billo, E.J. *Inorg. Chem.* **1987**, *26*, 3224.

25. Adam, K.R.; Antolovich, M.; Brigden, L.G.; Lindoy, L.F. *J. Am. Chem. Soc.* **1991**, *113*, 3346.

26. Bosnich, B.; Mason, R.; Pauling, P.J.; Robertson, G.B.; Tobe, M.L. *Chem. Commun.* **1965**, *6*, 97.

27. Jubran, N.; Ginzburg, G.; Cohen, H.; Koresh, Y.; Meyerstein, D. *Inorg. Chem.* **1985**, *24*, 251.

28. D'Aniello, M.J.; Mocella, M.T.; Wagner, F.; Barefield, E.K.; Paul, I.C. *J. Am. Chem. Soc.* **1975**, *97*, 192.

29. Wagner, F.; Mocella, M.T.; D'Aniello, M.J.; Wang, A.H.J.; Barefield, E.K. *J. Am. Chem. Soc.* **1974**, *96*, 2625.

30. Micheloni, M.; Paoletti, P.; Bürke, S.; Kaden, T.A. *Helv. Chim. Acta* **1982**, *65*, 587.

31. Buxtorf, R.; Kaden, T.A. *Helv. Chim. Acta* **1974**, *57*, 1035.

32. Moore, P.; Sachinidis, J.; Willey, G.R. *J. Chem. Soc., Chem. Commun.* **1983**, 522.

33. Anichini, A.; Fabbrizzi, L.; Paoletti, P.; Clay, R.M. *Inorg. Chim. Acta Lett.* **1977**, *24*, 21.

34. Herron, N.; Moore, P. *Inorg. Chim. Acta* **1979**, *36*, 89.

35. Vigee, G.S.; Watkins, C.L.; Bowen, H.F. *Inorg. Chim. Acta* **1979**, *35*, 255.

36. Thöm, V.J.; Fox, C.C.; Boeyenes, J.C.A.; Hancock, R.D. *J. Am. Chem. Soc.* **1984**, *106*, 5947.

37. Busch, D.H. *Acc. Chem. Res.* **1978**, *11*, 392.

38. Hinz, F.P.; Margerum, D.W. *Inorg. Chem.* **1974**, *13*, 2941.

Table 2.1 Summary of electrochemical potentials for Ni(II) complexes of tetraaza macrocyclic ligands. All are 0.2 mM NiL^{2+} in 0.1 M $KClO_4$; scan rate is 100 mV sec^{-1}.

Complex	Reduction potential[a]	
	prewave	main wave
$Ni(cyclam)^{2+}$	-1.35	-1.56
cis-$Ni(cyclam)^{2+}$	-1.15	-1.54
α-$Ni(cyclam)^{2+}$	---	-1.64[b]
$Ni(MMC)^{2+}$	-1.26	-1.48
$Ni(DMC)^{2+}$	-1.20	-1.39
trans I $Ni(TMC)^{2+}$	-0.86	-1.02
trans III $Ni(TMC)^{2+}$	-0.90	-1.07

a. Obtained from an average of the cathodic and anodic peak potentials in V vs SCE. See Results section.

b. Cathodic peak potential only.

Table 2.2 Assays for Ni(cyclam)$^{2+}$ adsorbed on mercury electrodes in 0.1 M $KClO_4$ as measured by single potential-step chronocoulometry.

	ΔQ, $\mu C\ cm^{-2}$ [b]	
E_i [a]	0.2 mM Ni(cyclam)$^{2+}$	1.0 mM Ni(cyclam)$^{2+}$
0.0	0.1	-3.5
-0.1	0.0	-4.1
-0.2	0.3	-4.3
-0.3	0.1	-3.4
-0.4	-0.1	-1.4
-0.5	0.0	-0.6
-0.6	-0.3	-0.5
-0.7	-0.7	-0.7
-0.8	0.1	-0.1
-0.9	1.1	0.0
-1.0	1.5	0.2
-1.1	2.7	1.4
-1.2	3.1	0.9
-1.3	3.1	-0.6
-1.4	1.0	-3.0
-1.5	0.1	-2.9

a. The potential was stepped from E_i to -1.6 V and the resulting charge flow measured for 10 msec.

b. Difference between the intercepts of plots of charge vs (time)$^{1/2}$ in the presence and absence of Ni(cyclam)$^{2+}$

Table 2.3 Assays for $Ni(cyclam)^{+}$ adsorbed on mercury electrodes in 0.1 M $KClO_4$ as measured by single potential-step chronocoulometry.

	ΔQ, $\mu C\ cm^{-2}$ [b]	
E_i [a]	0.2 mM $Ni(cyclam)^{2+}$	1.0 mM $Ni(cyclam)^{2+}$
-1.6	12.3	13.0
-1.5	13.1	13.8
-1.4	10.8	11.2
-1.3	5.0	6.1
-1.2	3.8	4.2
-1.1	3.9	4.2
-1.0	4.9	5.0
-0.9	4.3	4.7
-0.8	4.8	4.7
-0.7	4.3	4.3
-0.6	3.4	3.8
-0.5	2.3	3.1
-0.4	1.0	1.8
-0.3	0.4	1.0
-0.2	0.1	0.3
-0.1	0.0	0.1

a. The potential was stepped from E_i to 0 V and the resulting charge flow measured for 10 msec.

b. Differences between the intercepts of plots of charge vs $(time)^{1/2}$ in the presence and absence of $Ni(cyclam)^{2+}$.

Table 2.4 Double potential-step chronocoulometric assays for Ni(cyclam)$^{+}$ adsorbed on mercury electrodes from a 0.2 mM Ni(cyclam)$^{2+}$ solution.

Ei [a]	Forward step [b]		Reverse step [c]		
	Intercept, $\mu C\ cm^{-2}$	Slope, $\mu C\ cm^{-2}\ s^{-1/2}$	Intercept, $\mu C\ cm^{-2}$	Slope, $\mu C\ cm^{-2}\ s^{-1/2}$	$F\Gamma$,[d] $\mu C\ cm^{-2}$
-1.6	4.19	63.3	26.7	201	13.9
-1.5	40.6	20.7	24.3	192	14.9
-1.4	36.8	7.7	24.8	132	11.0
-1.3	31.1	4.1	25.0	75.9	5.6
-1.2	28.3	1.9	24.0	64.7	3.9
-1.1	27.0	1.9	22.7	64.4	3.9
-1.0	25.8	2.0	21.5	64.4	3.9
-0.9	24.2	1.5	20.2	61.6	3.7
-0.8	22.1	1.5	18.6	55.2	3.2
-0.7	20.0	1.7	17.2	45.7	2.6
-0.6	17.4	1.2	15.3	32.6	1.9
-0.5	14.1	1.0	13.0	17.3	1.0
-0.4	10.5	1.0	10.2	5.2	0.3
-0.3	7.6	0.8	7.5	1.5	0.1
-0.2	5.0	0.6	5.0	0.3	0.0
-0.1	2.6	0.5	2.6	0.2	0.0

a. The potential of the electrode was held at E_i volts for 30 seconds to reduce all of the Ni(cyclam)$^{2+}$ in the vicinity of the electrode to Ni(cyclam)$^{+}$. The electrode potential was then stepped from E_i to 0 V for 10 msec and back to E_i and the charge recorded during this time. Data points for the first 2 msec were discarded.

b. The intercept and slope were obtained from least-squares fitting of plots of anodic charge vs $(\text{time})^{1/2}$.

c. The intercept and slope were obtained from least-squares fitting of plots of cathodic charge vs $(\tau^{1/2} + (t-\tau)^{1/2} - t^{1/2})$, where τ is the duration of the forward step.

d. Quantity of Ni(cyclam)$^{+}$ adsorbed at E_i expressed in $\mu C\ cm^{-2}$. Calculated from the difference of the intercepts of the forward and reverse steps after applying the small correction specified in reference 22.

Table 2.5 Assays for $Ni(cyclam)^{+}$ adsorbed on mercury electrodes in various solvents as measured by single potential-step chronocoulometry. Supporting electrolyte was 0.1 M; see Experimental section for details.

	ΔQ, $\mu C\ cm^{-2}$ [b]					
	0.2 mM $Ni(cyclam)^{2+}$			1.0 mM $Ni(cyclam)^{2+}$		
Potential steps, V [a]	H_2O [c]	MeCN	DMF	H_2O [c]	MeCN	DMF
Cathodic						
0.0 to -1.6	0.1	1.2	1.1	-3.5	8.6	0.4
-1.0 to -1.6	1.5	1.0	-0.1	0.2	-3.0	-0.3
Anodic						
-1.0 to 0	4.9	1.2	0.5	5.0	2.5	0.8
-1.6 to 0	12.3	16.0	16.3	13.0	19.1	18.3
DPSCC reverse slopes [d]						
-1.0 to 0 to -1.0	64.4	9.5	6.2	---	18.7	6.2

a. The electrode potential was held at the initial value for 30 seconds, stepped to the final value and the resulting charge flow was measured for 10 msec.

b. Difference in the intercepts of plots of charge vs $(time)^{1/2}$ in the presence and absence of $Ni(cyclam)^{2+}$.

c. Data for aqueous system taken from Tables 2.2 and 2.3.

d. Double Potential-Step Chronocoulometry. Reverse slopes (in $\mu C\ cm^{-2}\ s^{-1/2}$) for a plot of cathodic charge vs $(\tau^{1/2} + (t-\tau)^{1/2} - t^{1/2})$ for the given potential step. See Results section for details.

Table 2.6 Assays for $Ni(TMC)^{2+}$ and $Ni(TMC)^{+}$ adsorbed on mercury in 0.1 M $KClO_4$ as measured by single potential-step chronocoulometry.

	ΔQ, $\mu C\ cm^{-2}$ [b]	
Cathodic potential steps [a]	0.2 mM $Ni(TMC)^{2+}$	1.0 mM $Ni(TMC)^{2+}$
0 to 1.5	-1.6	-2.8
-0.7 to 1.5	1.3	2.7
Anodic potential steps		
-0.7 to 0	0.4	1.0
-0.95 to 0	15.7	15.2
-1.5 to 0	11.3	11.0
-0.95 to 0	15.3	14.3

a. The electrode was held at the first potential for 30 seconds, stepped to the final potential and the resulting charge measured for 10 msec.

b. Difference between the intercepts of plots of charge vs $(time)^{1/2}$ in the presence and absence of $Ni(TMC)^{2+}$.

Table 2.7 Assays for *cis*-Ni(cyclam)$^{2+}$ adsorbed on mercury in 0.1 M $KClO_4$ (buffered at pH 3) as measured by single potential-step chronocoulometry.

	ΔQ, $\mu C\ cm^{-2}$ [b]	
E_i, V [a]	0.2 mM NiL^{2+}	1.0 mM NiL^{2+}
cis-Ni(cyclam)$^{2+}$		
-1.0	1.0	1.0
-1.6	11.6	11.8
Ni(cyclam)$^{2+}$ [c]		
-1.0	4.9	5.0
-1.6	12.3	13.0

a. The electrode potential was stepped from E_i to 0 V and the resulting charge flow measured for 10 msec.

b. Difference between the intercepts of plots of charge vs (time)$^{1/2}$ in the presence and absence of NiL^{2+}

c. Results for Ni(cyclam)$^{2+}$ taken from Table 2.3.

Chapter 3

Electrochemistry of Ni(cyclam)$^{2+}$ under CO and CO_2 at a Mercury Electrode

3.1 *Introduction*

An investigation of the mechanism and kinetics of the catalytic electroreduction of carbon dioxide must address not only the chemistry of the catalyst, such as described in chapter two, but also the electrochemistry of the catalyst and its precursors to the substrate, CO_2. The extent of binding of the catalyst with the product, in this case CO, is also important. In the original report of the electrochemical reduction of CO_2 using $Ni(cyclam)^+_{ads}$ as a catalyst,[1] Sauvage and co-workers proposed an overall catalytic cycle (Figure 1.2), but only briefly mentioned it in the discussion section. The aqueous electrochemistry of the catalyst in the presence of CO was not addressed, nor was the unexpected, sharp decrease in catalytic current at more negative potentials explained. The former issue has been addressed in work by Fujihira and co-workers[2] and they proposed that in the presence of CO or CO_2, $Ni(cyclam)^+_{ads}$ desorbs completely at potentials negative of -1.7 V due to the formation of an unadsorbable Ni(I)cyclam-CO species. Also proposed was the idea that the reduction of the $Ni(cyclam)^{2+}$ complex led to the ligand loss reaction (1),

$$Ni(cyclam)^+ + 2H_2O \longrightarrow Ni^+_{aq} + H_2cyclam^{2+} + 2OH^- \qquad (1)$$

and the presence of CO accelerated this reaction. The presence of several features in the voltammetry of $Ni(cyclam)^{2+}$ at mercury was attributed to the demetalation of this complex. The objective of the research described in this chapter is to examine some of the questions concerning the electrochemistry of $Ni(cyclam)^{2+}$ under CO and CO_2 atmospheres with the goal of understanding further the mechanism of the electrocatalytic reduction of CO_2.

3.2 *Experimental*

3.2.1 Materials

Cyclam (Aldrich) was recrystallized from *p*-dioxane. Tetramethylcyclam (TMC, Aldrich) was used as received. Ni(cyclam)$(ClO_4)_2$ was prepared according to the method of Bosnich *et al.*[3], recrystallized twice from methanol/diethyl ether and dried *in vacuo* at 60°C for 24 hours. The synthesis of *trans* I Ni(TMC)$(ClO_4)_2$ was performed following literature procedures[4]. $KClO_4$ was prepared by the addition of $HClO_4$ to a solution of KOH. The product was recrystallized twice from water and dried *in vacuo* at 80°C for 24 hours. All solutions were prepared from analytical grade reagents; distilled water was further purified by passage through a Barnstead Organopure contaminant removal system. Buffered solutions were either acetate, borate or an appropriate concentration of HCl or KOH; $KClO_4$ was added if necessary to provide a total ionic strength of 0.1 M. Prepurified argon was bubbled through a solution of V(II) to remove residual oxygen. Carbon monoxide (Matheson) of 99.9% purity and used as received. Solutions of carbon dioxide were prepared by bubbling with CO_2 (Matheson, 99.9%) or by the addition of aliquots of a standardized Na_2CO_3 solution to a solution buffered at pH 4 to 6.

3.2.2 Electrochemical Measurements

Triply distilled mercury (Bethlehem Instrument Co.) was used in a Brinkman model #410 Hanging Mercury Drop Electrode (HMDE). The surface area of this electrode was 0.027 cm^2 as determined by weight, averaging a large number of drops. Controlled potential reductions were performed with a mercury pool electrode (surface area of 4 cm^2) instead of the HMDE. Rotating disc electrode (RDE) experiments were performed with a Hg/Au RDE which was prepared by dipping an Au electrode (area = 0.44 cm^2) into

mercury to form a thin layer of mercury on the surface. Most experiments were done in 0.1 M $KClO_4$ as supporting electrolyte utilizing a conventional two compartment electrochemical cell. Solutions were deaerated by bubbling with argon for at least 15 minutes prior to each experiment and a blanket of argon was kept over the solution during the course of the experiments.

Cyclic voltammograms were obtained with a Princeton Applied Research (PAR) Model 173 Potentiostat and a PAR Model 175 programmer. RDE voltammetry was done with a Pine Instruments Model RDE 3 potentiostat. For normal pulse polarography a dropping mercury electrode (DME) was employed with a PAR Model 174 potentiostat. The flow rate of the DME was typically 1 mg/sec which provided a drop area of 0.0085 cm^2 for drop times of 1 second. Chronocoulometric and chronoamperometric experiments were done with a previously described computer-controlled instrument.[5]

All experiments were carried out at ambient laboratory temperature, 22 ±2 °C. All potentials were measured with respect to a saturated calomel reference electrode (SCE).

3.3 *Results*

3.3.1 Electrochemistry of $Ni(cyclam)^{2+}$ in the Presence of CO

Cyclic voltammetry

The cyclic voltammetry of $Ni(cyclam)^{2+}$ in a solution saturated with CO exhibits several features which are not present in the absence of CO. Two slightly different results are possible, depending on whether the concentration of CO is greater or less than that of $Ni(cyclam)^{2+}$. Figures 3.1 and 3.2, respectively, illustrate this point. As $Ni(cyclam)^{2+}$ is titrated into a solution saturated with CO (solubility of CO is 0.96 mM in 0.1 M $KClO_4$),

Figure 3.1 Cyclic voltammogram of $Ni(cyclam)^{2+}$ at a HMDE in presence (solid line) and absence (dashed line) of CO. $[Ni(cyclam)^{2+}]$ is 0.5 mM; [CO] is 1mM. Initial potential is -1.0 V; scan rate is 100 mV sec^{-1}.

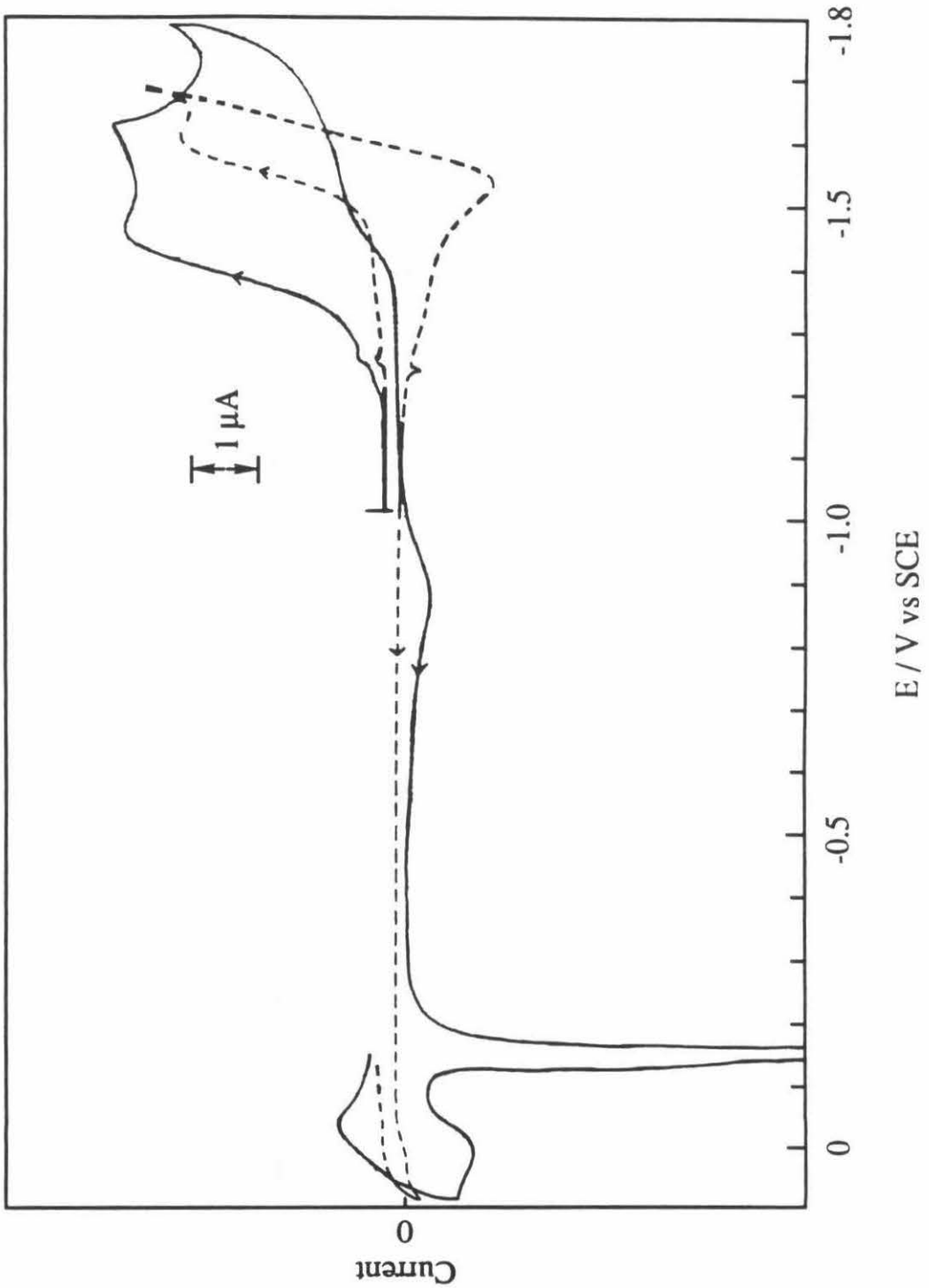
1 µA
Current
0
0
-0.5
-1.0
-1.5
-1.8
E / V vs SCE

Figure 3.2 Cyclic voltammogram of Ni(cyclam)$^{2+}$ at a HMDE in presence (solid line) and absence (dashed line) of CO. [Ni(cyclam)$^{2+}$] is 2.0 mM; [CO] is 1mM. Initial potential is -1.0 V; scan rate is 100 mV sec^{-1}.

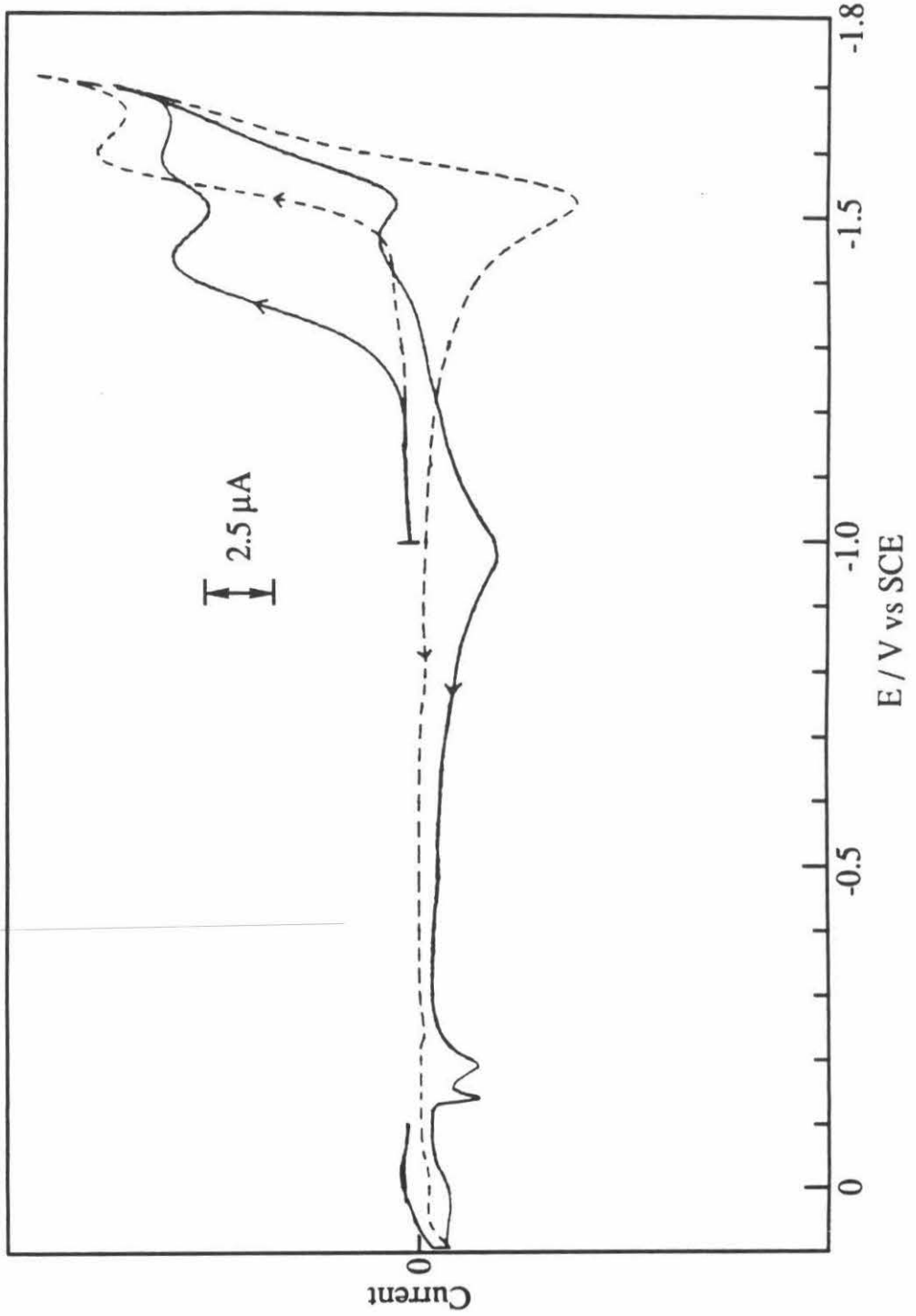
2.5 µA
Current
0
0
-0.5
-1.0
-1.5
-1.8
E / V vs SCE

an irreversible reduction appears at approximately -1.5 V and is composed of a diffusional peak at -1.45 V followed by a sharp spike at -1.54 V. The exact number of electrons (n) associated with this reduction is difficult to ascertain due to the irreversibility and unusual shape of the peaks, but the magnitude of the total peak current is comparable to that which is expected for a two-electron process. As the concentration of $Ni(cyclam)^{2+}$ exceeds the concentration of CO in the solution, the cathodic spike disappears and a reversible wave is noted at a potential of -1.56 V (average of cathodic and anodic peak potentials). This reversible wave is representative of the electrochemistry of the $Ni(cyclam)^{2+/+}$ couple as described in section 2.3.1. The irreversible peak and spike are associated with the reduction of $Ni(cyclam)^{2+}$ in the presence of CO as shown by Equation (2).

$$Ni(cyclam)^{2+} + CO \xrightarrow{e^-} Ni(cyclam)^{+}\text{-}CO \xrightarrow{e^-} Ni(cyclam)^{0}\text{-}CO \quad (2)$$

Since Ni(I) carbonyl complexes of tetraazamacrocycles (NiL^{+}-CO) have been formed by the reduction of NiL^{2+} with solvated electrons to Ni(II)L· and the subsequent reaction of this radical with CO,[6] their formation by electrochemical means is not surprising. The exact structure of the Ni(0) carbonyl complex is not known, but it is hereafter referred to as $Ni(cyclam)^{0}$-CO. Although an electrochemical binding study could not be done with $Ni(cyclam)^{2+}$ and CO due to the irreversibility of reaction (2), there is evidence that Equation (2) is representative of the stoichiometry, i.e., only one CO molecule is coordinated to the complex during the reduction. $Ni(TMC)^{+}$ complexes show coordination to a single carbonyl ligand (Section 3.3.2) and an octahedrally coordinated Ni(I) or Ni(0) species is rare and is therefore considered unlikely.

Chronocoulometry

As noted above, the exact value of n for Equation (2) is difficult to measure with cyclic voltammetry and thus potential step experiments were done to determine this value. Chronocoulometric slopes[7] (see Section 2.3.5) for a potential step across the entire cathodic feature were analyzed to determine the value of n. For two solutions of $Ni(cyclam)^{2+}$, identical except that one was saturated with CO and one with argon, the chronocoulometric slopes for the CO saturated solution (80 $\mu C\ cm^{-2}\ s^{-1/2}$) displayed an almost twofold increase over that of the argon saturated solution (47 $\mu C\ cm^{-2}\ s^{-1/2}$) for potential steps from -1.0 to -1.6 V. The value for the slope representing $Ni(cyclam)^{2+}$ reduction in the absence of CO is equal to the value expected based on the concentration of $Ni(cyclam)^{2+}$ used in the experiment. The lack of an exact doubling of the slopes is attributed to the fact that the hydrogen evolution background is more prominent for the argon saturated solution at -1.6 V.

Normal pulse polarography

Normal pulse polarograms[8] of $Ni(cyclam)^{2+}$ solutions saturated with CO and with argon are shown in Figure 3.3. For the solution containing no CO, the magnitude of the current on the plateau corresponds to that which is expected for the one-electron reduction of $Ni(cyclam)^{2+}$ to $Ni(cyclam)^{+}$. With the addition of an excess of CO, the reduction process shifts to more positive potentials and is separated into two waves. The more positive wave has a half-wave potential of -1.43 while the second has a potential of -1.56 V. Rather than exhibiting a current plateau, the second feature is peaked in shape and the current decreases sharply at potentials negative of -1.72 V. After correction for the background response in the absence of $Ni(cyclam)^{2+}$, the magnitude of the currents is approximately equal to that expected for two, one-electron processes as described in

Figure 3.3 Normal pulse polarogram of 0.5 mM $Ni(cyclam)^{2+}$ in 0.1 M $KClO_4$. Lower trace is under argon, upper trace is under CO. Initial potential is -1.2 V.

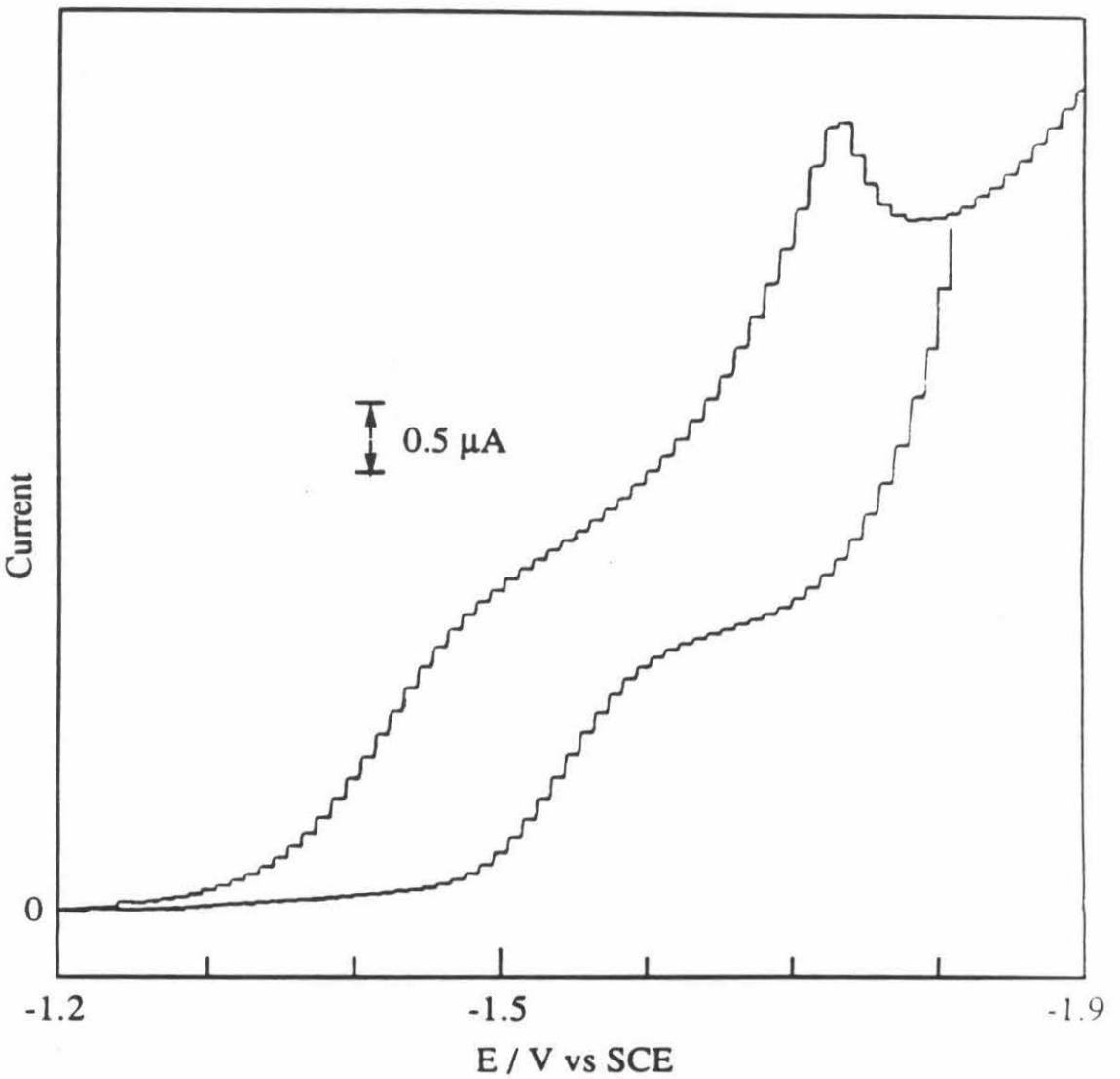

Equation (2). On the basis of the chronocoulometric and polarographic results, it can be concluded that Equation (2) is a two-electron reduction overall.

The reason for the differing electrochemical responses of $Ni(cyclam)^{2+}$ in the presence of CO as a function of the relative concentrations of these species is best explained by a consideration of the physical situation at the surface of the electrode with varying concentration ratios. When CO is in excess, reaction (2) occurs for all $Ni(cyclam)^{2+}$ molecules arriving at the surface of the electrode. When the concentration of $Ni(cyclam)^{2+}$ in solution exceeds that of CO, $Ni(cyclam)^{2+}$ is reduced at the potential of the first peak until the concentration of CO at the electrode surface is zero. After this point is reached, all additional $Ni(cyclam)^{2+}$ molecules arriving at the electrode surface are reduced at the normal potential associated with this complex (-1.56 V).

Several other features were noted in the cyclic voltammetry of $Ni(cyclam)^{2+}$ in the presence of CO. A broad anodic feature was observed at a potential of -0.9 V. The distinctness of this feature varied with the concentration of $Ni(cyclam)^{2+}$ and the potential at which the sweep was reversed. Since the appearance of this feature coincided with the passage of faradaic current associated with reaction (2), it is likely that it corresponds to the reoxidation of $Ni(cyclam)^{+}$-CO. Another much larger anodic feature occurred at -0.15 V. The magnitude of the current of this spike increased as the length of time the electrode was poised negative of -1.3 V was increased. Neither of these anodic features was observed if the electrode potential was not swept negative enough to cause the flow of cathodic current.

The sharp nature and huge charge associated with the feature at -0.15 V indicate that the current is representative of the oxidation of a species confined to the surface of the electrode. Since the amount of charge represented by this anodic spike was dependent on the duration of the prior cathodic electrochemistry, no attempts were made to quantify the charge represented by the peak. This charge was substantially greater than that which

would be expected for the oxidation of a monolayer of electroactive species and thus was not easily ascribable to any simple adsorbed Ni(cyclam) species. Rather, it is the oxidation of a precipitate on the electrode which is responsible for the anodic response at -0.15 V. The reduction of $Ni(cyclam)^{2+}$ under CO has been proposed herein to result in the formation of $Ni(cyclam)^{0}$-CO; it is therefore likely that this precipitate is $Ni(cyclam)^{0}$-CO. Since the anodic spike appears whenever the electrode is scanned to any potential negative of the onset of the reduction of $Ni(cyclam)^{2+}$ in the presence of CO, this reduction must in part result in the formation of $Ni(cyclam)^{0}$-CO. The formation of a precipitate could physically block any diffusing electroactive species from reaching the electrode surface, a situation which would produce the peaked response seen in the second cathodic feature of the cyclic voltammetry in Figure 3.1.

An interesting effect was noted as the ratio of the concentrations of $Ni(cyclam)^{2+}$ and CO in solution were varied: The ratio of the current magnitudes of the features at -0.9 and -0.15 changed as the reactant concentration varied. With CO present in excess, the feature at -0.15 V was quite prominent while the feature at -0.9 V was barely detectable. As the concentration of $Ni(cyclam)^{2+}$ was increased over that of CO, the reverse was true. Since the reduction of $Ni(cyclam)^{2+}$ under CO to $Ni(cyclam)^{+}$-CO and $Ni(cyclam)^{0}$-CO occurs irregardless of the concentration of $Ni(cyclam)^{2+}$ in solution, the following discussion is the only reasonable explanation for the relative magnitude of these two anodic features. The presence of both $Ni(cyclam)^{0}$-CO and an excess of $Ni(cyclam)^{2+}$ at the surface of the electrode causes the redox reaction shown in Equation (3).

$$Ni(cyclam)^{0}\text{-}CO + Ni(cyclam)^{2+} \longrightarrow Ni(cyclam)^{+}\text{-}CO + Ni(cyclam)^{+} \qquad (3)$$

Reaction (3) is thermodynamically feasible since the formal potential of the $Ni(cyclam)^{+/0}$-CO couple (estimated to be -1.57 V in pulse polarography) is more negative

than that for the $Ni(cyclam)^{2+/+}$ couple (measured as -1.56 V). The actual potential for the $Ni(cyclam)^{+/0}$-CO couple may be even more negative due to the inaccuracies encountered in estimating a half-wave potential in the absence of a well defined plateau. At potentials where $Ni(cyclam)^{2+}$ is reduced to $Ni(cyclam)^{+}$ at the electrode, the following reaction may also cause the annihilation of $Ni(cyclam)^{0}$-CO.

$$Ni(cyclam)^{0}\text{-}CO + Ni(cyclam)^{+} \longrightarrow Ni(cyclam)^{0} + Ni(cyclam)^{+}\text{-}CO \qquad (4)$$

Stated another way, the affinity of $Ni(cyclam)^{+}$ for CO is greater than that of $Ni(cyclam)^{0}$ and a ligand exchange occurs. At all potentials, an excess of $Ni(cyclam)^{2+}$ renders $Ni(cyclam)^{0}$-CO unstable and $Ni(cyclam)^{+}$-CO is produced at the expense of $Ni(cyclam)^{0}$-CO. The observable result in the cyclic voltammetry is that the spike at -0.15 V decreases in magnitude while the anodic feature at -0.9 increases.

Origin of the reversible wave at 0 V

Depending on the experimental conditions, a reversible wave at approximately 0 V was noted in the cyclic voltammetry of $Ni(cyclam)^{2+}$ in the presence of CO. Under conditions which led to the formation of $Ni(cyclam)^{0}$-CO at the electrode surface, this reversible wave was present. If the $Ni(cyclam)^{0}$-CO were allowed to decompose on the electrode surface by potentiostating the electrode positive of -1.2 V, resulting in a reduction of the anodic spike at -0.15 V, the wave at 0 V increased in magnitude. This wave was also seen in the absence of CO when the electrode was scanned into the cathodic background, resulting in the evolution of hydrogen through the reduction of water by $Ni(cyclam)^{+}$. In fact, this wave was seen quite clearly in the absence of any electroactive species, if the electrode potential was scanned into the hydrogen evolution background (see Figure 3.4). The reversible wave is easily explained by the oxidation of the mercury electrode in the presence of OH^{-} (see also chapter four). Any reaction that

Figure 3.4 Cyclic voltammetry of 0.1 M $KClO_4$. Initial potential is -0.5 V; scan rate is 100 mV sec^{-1}. One minute pause at -1.8 V before continuting scan.

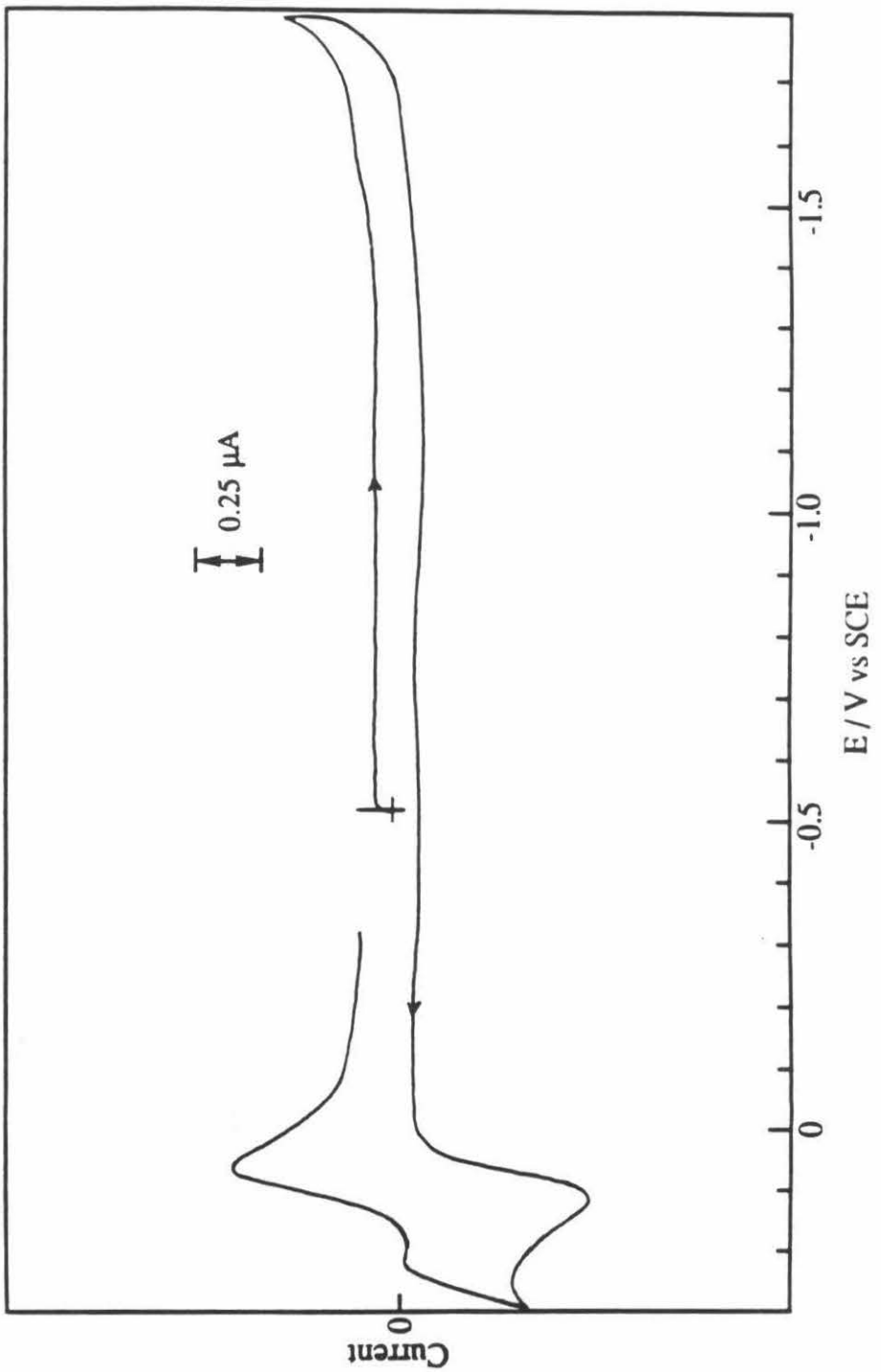

leads to the formation of hydrogen, such as the reduction of water by $Ni(cyclam)^{+}$ or $Ni(cyclam)^{0}$-CO, will produce a wave for the oxidation of mercury at 0 V.

Controlled potential electrolysis of $Ni(cyclam)^{2+}$ under CO

Controlled potential electrolysis experiments were done with a stirred solution of $Ni(cyclam)^{2+}$ saturated with CO by potentiostating the mercury pool working electrode at -1.4 V. The current did not decrease to zero with time as expected, but reached a steady-state value which was significantly greater than the background response with no $Ni(cyclam)^{2+}$ present. Even after one hour, the charge passed was far in excess of that which would have been expected for the one- or two-electron reduction of $Ni(cyclam)^{2+}$ under CO. In addition, the pH of the solution rose considerably during the course of the electrolysis. The obvious conclusion is that the decomposition of $Ni(cyclam)^{0}$-CO or $Ni(cyclam)^{+}$-CO with the evolution of hydrogen prevented a definite coulometric endpoint from being reached. The increase in pH was approximately equal to that calculated for the reduction of water by the charge passed in excess of that which was required for the complete reduction of $Ni(cyclam)^{2+}$ to $Ni(cyclam)^{0}$-CO.

During the course of the experiment, the color of the solution changed from light yellow to lime-green and a metallic grey precipitate formed on the mercury pool working electrode. The green color is presumably due to the formation of $Ni(cyclam)^{+}$-CO in solution and the precipitate is $Ni(cyclam)^{0}$-CO. All attempts to characterize these complexes were unsuccessful as both are quite unstable in water. If the working electrode was unpotentiostated or held at potentials positive of -1.2 V, or if the solution was bubbled with argon to remove all CO in solution, both the precipitate and the green color of the solution disappeared.

An experiment was done to discover any connection between the anodic features seen in the cyclic voltammetry and the disappearance of the precipitate. A mercury pool

electrode was scanned to -1.5 V and held there, resulting in the production of Ni(cyclam)$^{+}$-CO in solution around the electrode and the precipitation of Ni(cyclam)^{0}-CO on the surface. If the electrode were then stopped for a brief time (30 sec) at -1.0 V during the scan to 0 V, the precipitate on the mercury pool slowly disappeared and it was found that both anodic features had diminished considerably as seen after the resumption of the scan. If the electrode potential was not paused at -1.0 V, the precipitate disappeared at the exact moment that the potential was scanned positive of the feature at -0.15 V. An analogous result was seen with the HMDE, although no precipitate was observable on the electrode surface.

All of the above evidence leads to the following conclusions. Ni(cyclam)$^{2+}$ is reduced under CO to Ni(cyclam)$^{+}$-CO and Ni(cyclam)^{0}-CO at potentials negative of -1.3 V. Ni(cyclam)$^{+}$-CO is reoxidized electrochemically to Ni(cyclam)$^{2+}$ and CO at -0.9 V and Ni(cyclam)^{0}-CO (which is insoluble and precipitates on the electrode surface) is reoxidized electrochemically at -0.15 V. Both Ni(cyclam)$^{+}$-CO and Ni(cyclam)^{0}-CO are unstable in water and are oxidized back to Ni(cyclam)$^{2+}$ and CO, resulting in the evolution of hydrogen. A summary of these conclusions is shown in Figure 3.5.

Figure 3.5 Electrochemistry of $Ni(cyclam)^{2+}$ under CO.

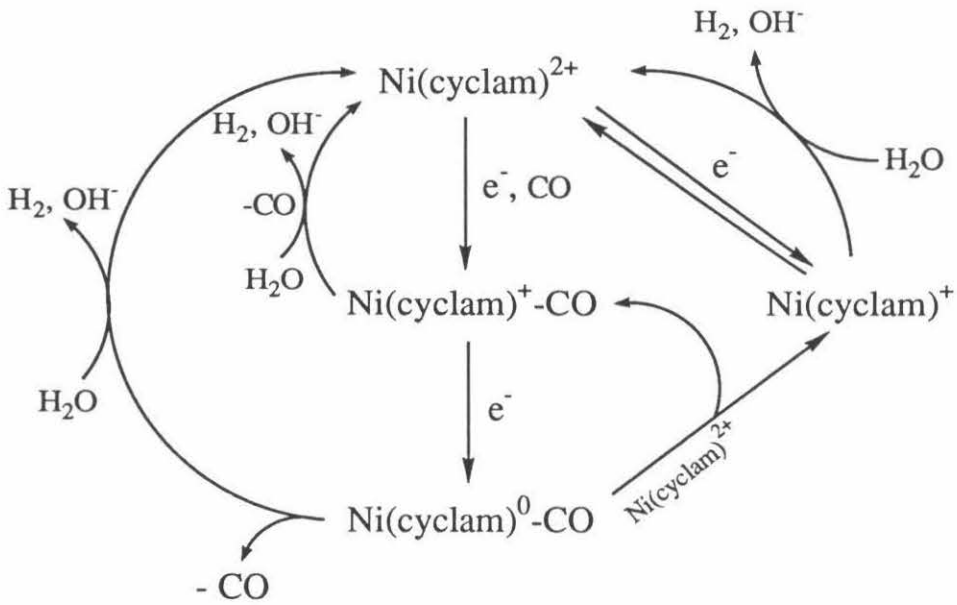

Adsorption of Ni(cyclam)$^{2+}$ under CO as measured by chronocoulometry

Single step chronocoulometric experiments[7] were done with Ni(cyclam)$^{2+}$ solutions saturated with CO in order to determine the effect that CO has on the adsorption of Ni(cyclam)$^{+}$. These experiments and the data analysis were performed in an analogous fashion to the chronocoulometric experiments done in the absence of CO (Section 2.3.6).[9] The initial potentials of the step experiments ranged from -0.1 to -1.3 V. Unfortunately, it was not possible to fix the initial potential at values more negative than this due to interference from the formation of the Ni(cyclam)^{0}-CO precipitate on the electrode surface. Therefore, all potential steps were at potentials positive of the solution electrochemistry for Ni(cyclam)$^{2+}$ in the presence of CO. The results of these experiments showed no difference in the quantity of Ni(cyclam)$^{+}$ adsorbed at potentials of -0.6 and -1.3 V in the presence and absence of CO. In addition, comparison of the charge vs time curves for the initial adsorption of Ni(cyclam)$^{+}$ (see section 2.3.6) also showed no difference between experiments done in the presence and absence of CO. The results of these experiments demonstrate that CO has no effect on the quantity of Ni(cyclam)$^{+}$ adsorbed at potentials between -0.6 and -1.3 V, but it does not answer the question of whether or not CO binds to $\text{Ni(cyclam)}^{+}_{ads}$ at these potentials.

3.3.2 Electrochemistry of $Ni(TMC)^{2+}$ in the presence of CO

The cyclic voltammetry of $Ni(TMC)^{2+}$ in a solution saturated with CO is shown in Figure 3.6. As was observed with $Ni(cyclam)^{2+}$, several new features are noted with the methylated complex under a CO atmosphere. The wave for the reduction of $Ni(TMC)^{2+}$ to $Ni(TMC)^{+}$ and the peak for the reduction of $Ni(TMC)^{2+}$ to $Ni(TMC)^{+}_{ads}$ are both shifted positive by approximately 150 mV. The $Ni(TMC)^{2+/+}$ couple in the presence of CO retains its reversibility (peak to peak separation is 60 mV, i_{pa}/i_{pc} is unity), in contrast to the results observed with the unmethylated cyclam. At a potential of -1.45 V, a second, irreversible reduction peak is seen. Equations (5) and (6) are proposed to account for these observations.

$$Ni(TMC)^{2+} + CO + e^- \rightleftharpoons Ni(TMC)^{+}\text{-}CO \quad E^0 = -0.84\ V \quad \left(\frac{E_{pa}+E_{pc}}{2}\right) \qquad (5)$$

$$Ni(TMC)^{+}\text{-}CO + e^- \longrightarrow Ni(TMC)^{0}\text{-}CO \quad E_{pc} = -1.45\ V \qquad (6)$$

The reversibility of reaction (5) allows the determination of the exact stoichiometry of the reaction by measuring the shift of the reduction potential for the reaction as a function of the concentration of CO.[10] A high ratio of the concentration of CO to that of $Ni(TMC)^{2+}$ was used so that the concentration of CO remained essentially constant during the reduction. For the reversible reduction of $Ni(TMC)^{2+}$ under CO, the shift in the redox potential is related to the standard potential by Equation (7),

$$E = E^{0'} + \frac{RT}{nF} \ln (K_{co}) + q \frac{RT}{nF} \ln [CO] \qquad (7)$$

where q is the number of CO molecules binding to the Ni(I) metal center and K_{co} is the equilibrium constant for the binding of CO to the metal center. Implicit in this equation is

Figure 3.6 Cyclic Voltammogram of $Ni(TMC)^{2+}$ under CO at a HMDE. $[Ni(TMC)^{2+}]$ is 0.2 mM; scan rate is 100 mV sec^{-1}. Initial potential is -0.5 V. Dashed line is scan reverse at -1.0 V.

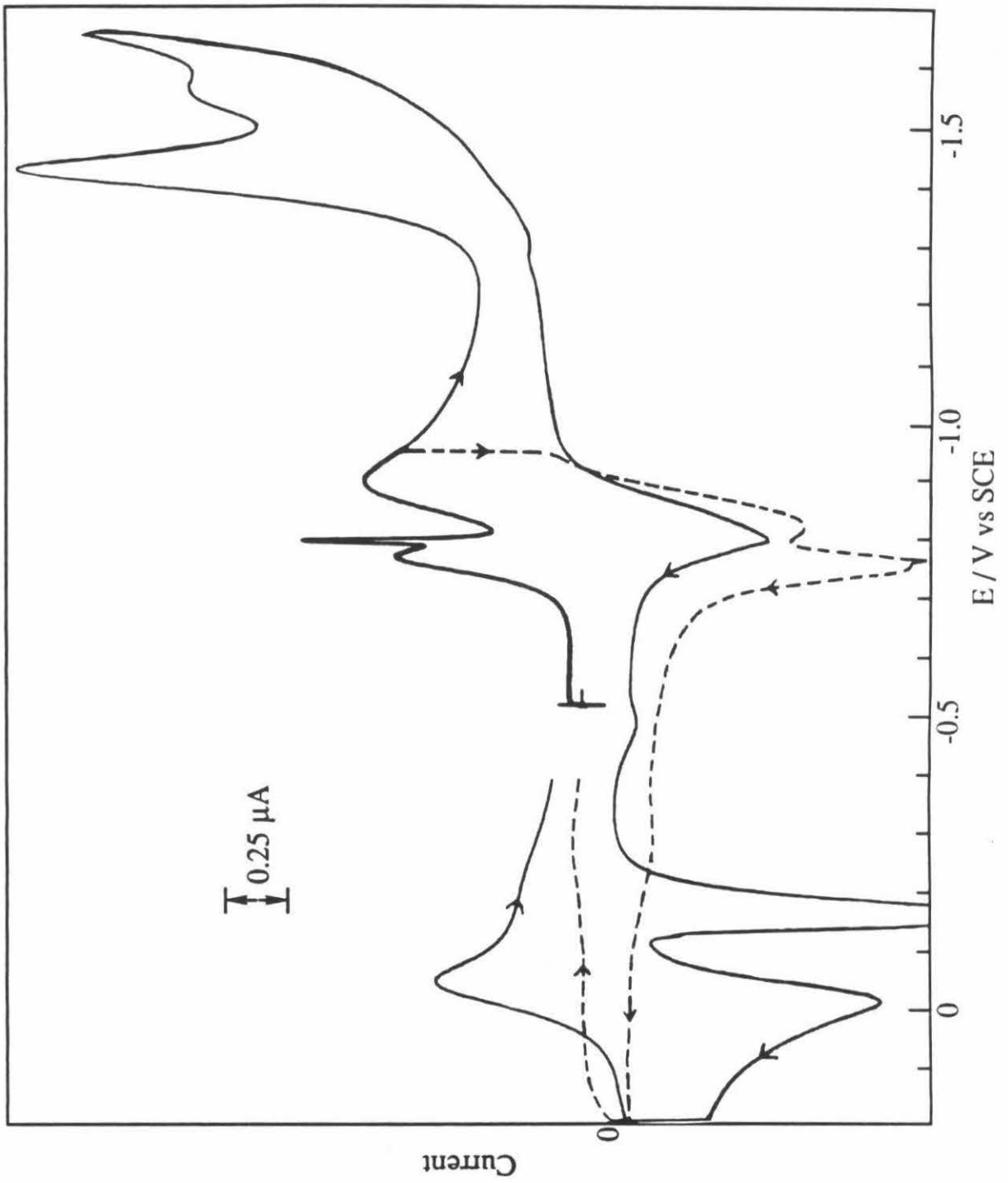
0.25 µA
Current
0
0
-0.5
-1.0
-1.5
E / V vs SCE

the assumption that the binding of CO to $Ni(TMC)^{2+}$ is insignificant compared to the binding of CO to $Ni(TMC)^{+}$. Since no evidence was seen for significant binding of CO to $Ni(TMC)^{2+}$, this simplification in Equation (7) is valid. A plot of E vs ln [CO] should be linear, with a slope of $q\frac{RT}{nF}$. Such a plot is shown in Figure 3.7. The slope of the least-squares line through the points (62 mV) indicates that one CO molecule binds to the $Ni(TMC)^{+}$ complex.

A sharp anodic feature was observed at -0.15 V in the cyclic voltammogram and was attributed to the reoxidation of a $Ni(TMC)^{0}$-CO species following the analogous reasoning given in section 3.3.1 for $Ni(cyclam)^{0}$-CO. This anodic feature was not observed if the electrode potential was not scanned over the second cathodic feature at -1.45 V (Figure 3.6, dashed line). In contrast to the behavior observed with $Ni(cyclam)^{+}$, the reduction of $Ni(TMC)^{2+}$ under CO occurs in two distinct one-electron steps. The precipitate $Ni(TMC)^{0}$-CO is formed only by way of the further electrochemical reduction of the stable $Ni(TMC)^{+}$-CO species.

The reversible wave at 0 V has been previously described as resulting from the oxidation of mercury in the presence of hydroxide ion (see section 3.3.1). It is interesting to note, however, that the one-electron reduction of $Ni(TMC)^{2+}$ under CO to $Ni(TMC)^{+}$-CO does not result in the evolution of hydrogen and subsequent rise in pH (Figure 3.6, dashed line). Only the further reduction to $Ni(TMC)^{0}$-CO , resulting in the evolution of hydrogen, leads to the presence of hydroxide ions as evidenced by the reversible wave at 0 V (Figure 3.6, solid line).

Figure 3.7 Plot of the shift in formal potential of $Ni(TMC)^{2+}$ versus the log of the concentration of CO. 0.05 mM $Ni(TMC)^{2+}$ in 0.1 M $KClO_4$. The concentration of CO in the solution was varied by injecting aliquots of the appropriate amount of a 0.1 M $KClO_4$ solution saturated with CO (the solubility of CO under these experimental conditions is 0.96 mM).

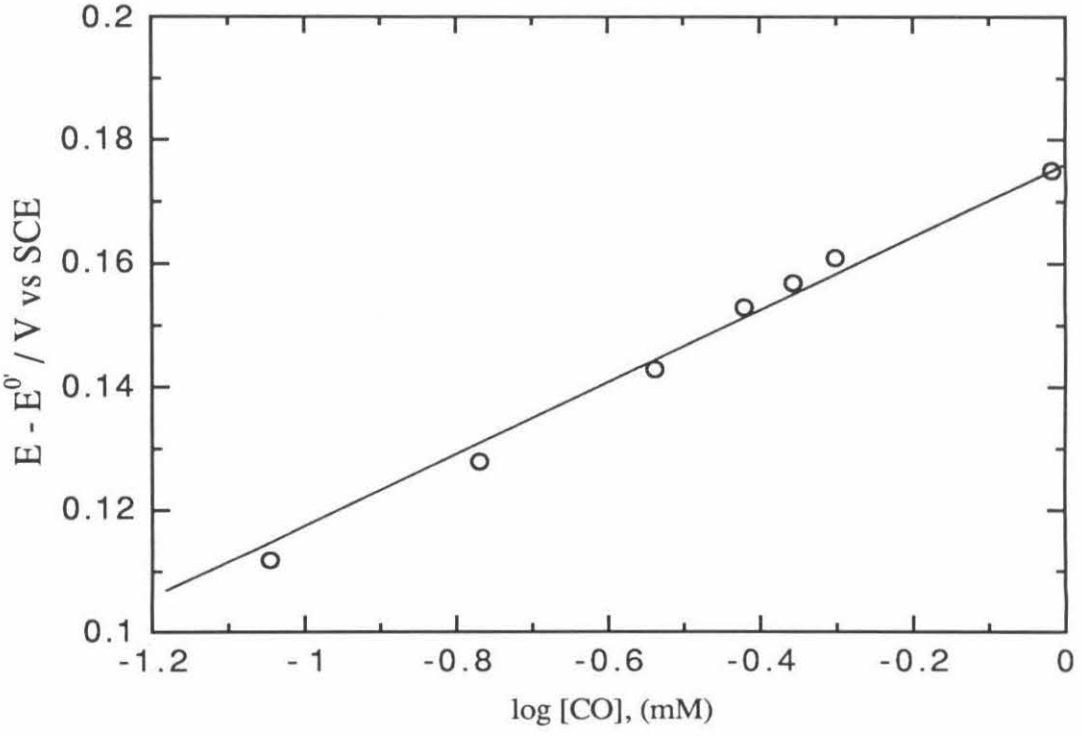

3.3.3 *Electrochemistry of Ni(cyclam)$^{2+}$ under CO_2*

The cyclic voltammogram of Ni(cyclam)$^{2+}$ in a 0.1 M $KClO_4$ solution saturated with CO_2 is shown in Figure 3.8. As described in previous publications,[1,2] the irreversible cathodic peak at -1.40 is representative of the reduction of CO_2 as catalyzed by $Ni(cyclam)^{+}_{ads}$. The overall reaction is shown in Equation (8).

$$CO_2 + 2\,e^- + H^+ \longrightarrow CO + OH^- \qquad (8)$$

In the absence of Ni(cyclam)$^{2+}$, virtually no CO_2 reduction current is seen at these potentials. The magnitude of the catalytic peak current is substantially less than that which would be expected if the diffusion of CO_2 molecules to the electrode surface were the only factor limiting the current. In addition, the current decreases rapidly after the peak, and remains at almost zero for the remainder of the scan. The lack of any substantial current at potentials negative of -1.7 V is also indicative of the suppression of hydrogen evolution by the presence of CO_2.

A small prepeak is visible at the foot of the CO_2 reduction wave. This feature is due to the direct reduction of protons at catalyzed by Ni(cyclam)$^{2+}$; proton reduction in the absence of Ni(cyclam)$^{2+}$ occurs at much more negative potentials. Addition of HCl to the CO_2 saturated solutions increased the height of this prepeak by an amount corresponding to the quantity of protons added but resulted in no change in the CO_2 reduction current. Although CO_2 (H_2CO_3) is a weak acid and therefore the concentration of protons is relatively low in saturated CO_2 solutions, the diffusion coefficient of protons is large enough so that their reduction is an observable fraction of the CO_2 reduction current.

Figure 3.8 Cyclic voltammogram of 2.0 mM $Ni(cyclam)^{2+}$ at a HMDE in 0.1 M $KClO_4$ solution saturated with CO_2. Scan rate is 100 mV sec^{-1}. Initial potential is -1.0 V.

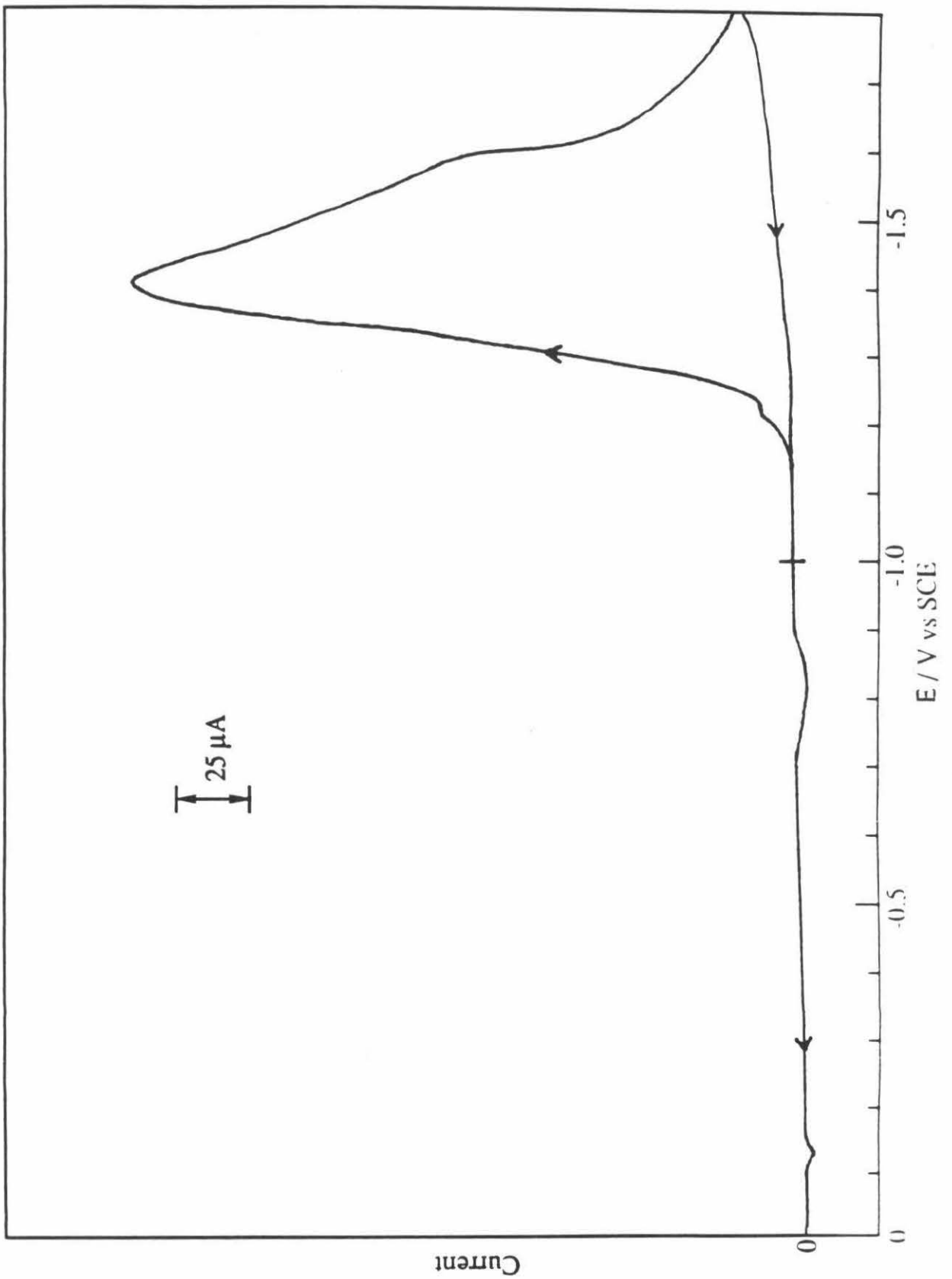
25 µA
Current
0
0
-0.5
-1.0
-1.5
E / V vs SCE

Using solutions which contained much smaller concentrations of CO_2, many other features can be seen in the cyclic voltammetry of $Ni(cyclam)^{2+}$ (Figure 3.9). The catalytic CO_2 reduction peak is still present, although its peak potential is shifted slightly positive. By utilizing carefully standardized CO_2 solutions, it was found that the catalytic current represented by the peak is equal to that which would be expected for the diffusion-controlled, two-electron reduction of CO_2. However, at CO_2 concentrations of greater than approximately 1 mM, the ratio of experimental to theoretical current decreased. At potentials negative of the CO_2 reduction peak, an irreversible peak (E_{pc} = -1.46 V) and a reversible wave ($\frac{E_{pa} + E_{pc}}{2}$ = -1.56 V) are seen in the cyclic voltammetry. These two features correspond to the reduction of $Ni(cyclam)^{2+}$ in the presence of CO, when the concentration of $Ni(cyclam)^{2+}$ is greater than that of CO (Section 3.3.1). The concentration of CO_2 used in this experiment (0.5 mM) was low enough so that the concentration of CO at the electrode surface would always be less than that of $Ni(cyclam)^{2+}$.

Regardless of the concentration of CO_2 present, the anodic sweep of the cyclic voltammogram revealed the presence of an anodic spike at -0.15 V. The presence of this feature has been attributed to the reoxidation of insoluble $Ni(cyclam)^{0}$-CO on the electrode surface (Section 3.3.1). This feature appeared even if the electrode potential was only briefly scanned into the onset of the CO_2 reduction wave.

By considering the electrochemistry of $Ni(cyclam)^{2+}$ under both CO_2 and CO, all of the voltammetric features in Figure 3.9 are easily explained. The presence of CO at the electrode surface (from the reduction of CO_2) causes a shift in the reduction peak of $Ni(cyclam)^{2+}$ and results in the formation of $Ni(cyclam)^{+}$-CO and $Ni(cyclam)^{0}$-CO. The potentials of the peak for the catalytic reduction of CO_2 and of the reduction of $Ni(cyclam)^{2+}$ under CO are sufficiently close so that $Ni(cyclam)^{+}$-CO and $Ni(cyclam)^{0}$-CO are formed whenever CO_2 is reduced at the electrode. Although the reduction of CO_2 will

Figure 3.9 Cyclic voltammogram of 0.5 mM Ni(cyclam)$^{2+}$ at a HMDE in 0.1 M $KClO_4$ solution containing 0.5 mM CO_2 (solid line) and no CO_2 (dashed line). Scan rate is 100 mV sec^{-1}. Initial potential is -1.0 V.

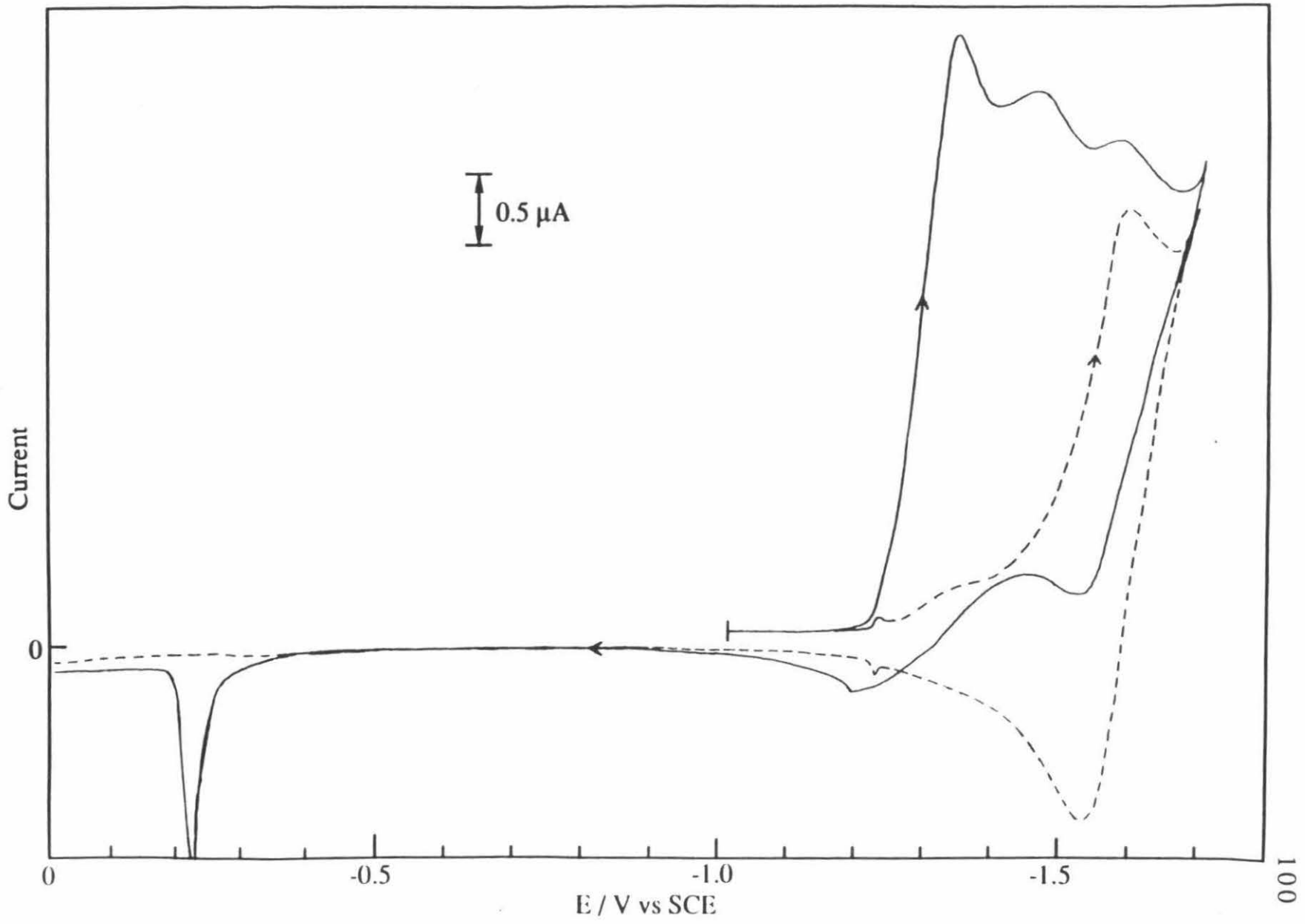
0.5 µA
Current
0
0
-0.5
-1.0
-1.5
E / V vs SCE
100

result in an increase in the pH at the electrode surface (Equation 8), the electrochemistry of Ni(cyclam)$^{2+}$ under CO showed no dependency on pH and thus it is unlikely that the Ni(cyclam)$^{2+}$/CO chemistry is affected by the presence of CO_2. In effect, the observable electrochemistry of Ni(cyclam)$^{2+}$ under CO_2 is that of Ni(cyclam)$^{2+}$ under CO with a large cathodic peak for the reduction of CO_2 superimposed on top.

The sharp drop in the CO_2 reduction current at potentials negative of -1.7 V (Figure 3.8) merits concern regarding the feasibility of the electrocatalytic reduction of CO_2. In order to investigate this characteristic further, a series of rotating disc electrode experiments were done. The use of a RDE provides a steady flux of reactant to the electrode surface so that concentration depletion effects, such as those which occur with stationary electrodes, are not present. A series of RDE experiments are shown in Figure 3.10. The rotating electrode was scanned from -1.0 V to increasingly negative potentials in the CO_2 reduction peak. After a 30 second pause during which time the magnitude of the current was carefully observed, the scan was reversed and the potential scanned to 0 V. It was noted that when the electrode was held at the lower potential, the current decreased drastically with time. At potentials near the top of the reduction peak seen in the cyclic voltammetry, the reduction current at the RDE decreased to almost zero after 30 seconds. These results are contrary to the expected behavior since the constant flux of CO_2 molecules to the electrode surface should result in a constant current at any potential sufficiently negative to cause the reduction of CO_2 to occur. The decrease in current with time observed in Figure 3.10 has two possible causes. Either the flux of CO_2 to the surface of the electrode has decreased, or the electrode has been deactivated towards the reduction of CO_2. The former possibility will be addressed in chapter five; a discussion of the latter possibility is given here.

Figure 3.10 Voltammogram of 0.2 mM Ni(cyclam)$^{2+}$ in 0.1 M $KClO_4$ saturated with CO_2 at a RDE. Rotation rate is 200 rpm, scan rate 0.1 V sec^{-1}, initial potential is -1.0 V.

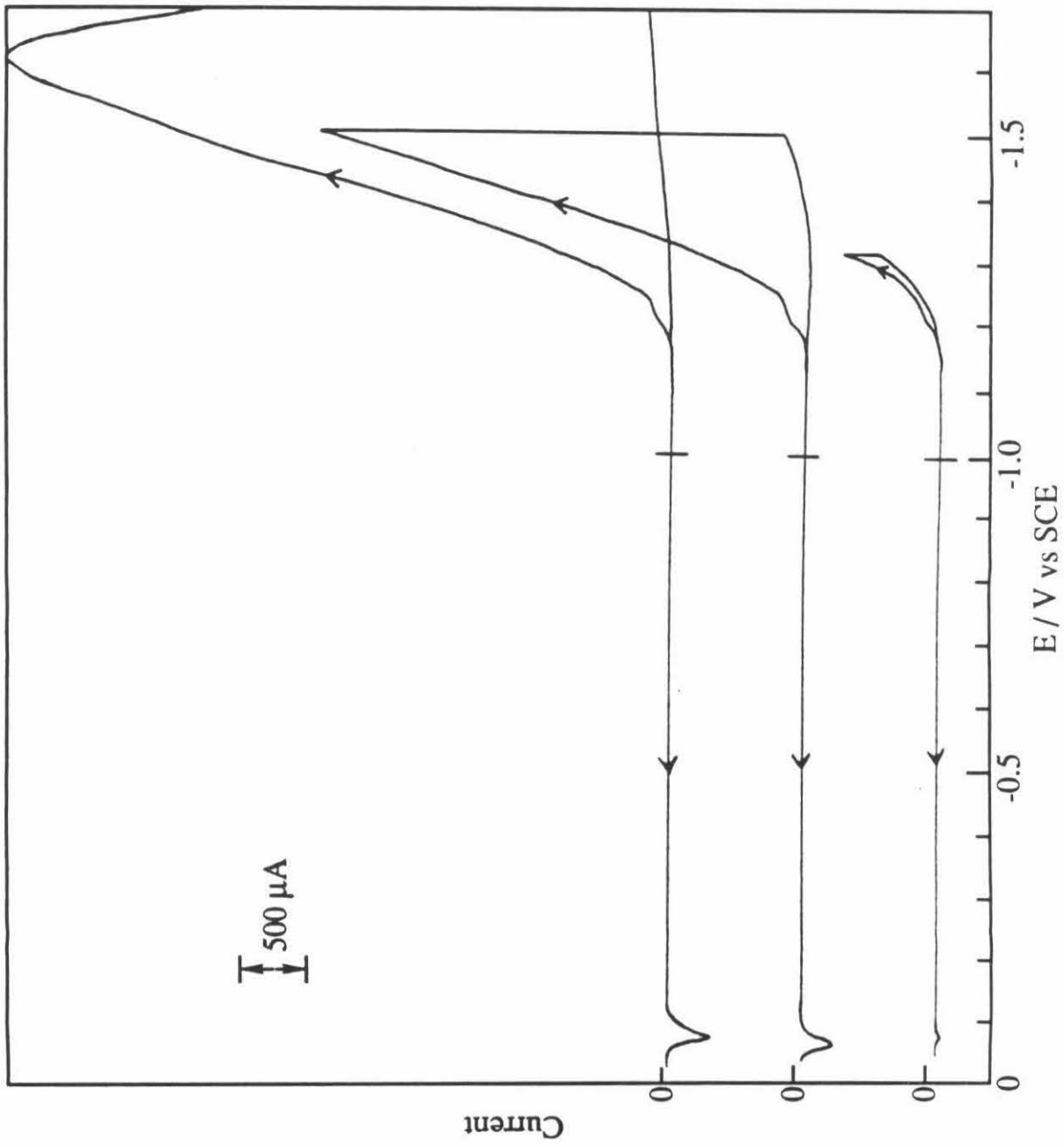

During the reverse scan at the RDE, an anodic peak was also seen at - 0.1 V; this peak has been attributed to the oxidation of a Ni(cyclam)^0-CO precipitate on the electrode surface. As was seen with a stationary mercury electrode, the magnitude of this anodic spike increased as the length of time that the electrode potential was negative enough to cause reduction of CO_2 was increased. Since the reduction of CO_2 results in the precipitation of Ni(cyclam)^0-CO at the electrode surface, it is reasonable to assume that this precipitate blocks, or deactivates, the catalytic electrode surface. In all of the RDE experiments, the unexpected decrease in catalytic current was linked to the appearance of the anodic feature at -0.1 V, and vice versa. The obvious conclusion is that the precipitate hinders the adsorption of Ni(cyclam)$^+$, thus slowing the rate of CO_2 reduction. At potentials where the rate of production of Ni(cyclam)^0-CO is greater than the rate of the decomposition (either through hydrogen evolution or oxidation by Ni(cyclam)$^{2+}$), the blocking of the electrode is complete and the CO_2 reduction current is reduced to zero. Based on the above RDE experiments, complete passivation occurred at all potentials negative of -1.4 V.

Since the passivation of the electrode surface is indirectly linked to the solubility of Ni(cyclam)^0-CO, the presence of a higher solution concentration of Ni(cyclam)$^{2+}$ should result in a greater amount of precipitate. This was observed experimentally; as the concentration of Ni(cyclam)$^{2+}$ in solution was increased, the decrease in catalytic current at the RDE occurred more rapidly, and the extent of passivation was greater (i.e., the current after a given time was closer to zero).

Several experiments were done to determine if the electrode could be "reactivated" towards CO_2 reduction after complete passivation had occurred. Since the electrode passivation agent, Ni(cyclam)^0-CO, is unstable in water and decomposes with time, the electrode should be slowly restored to its original condition when held under conditions where Ni(cyclam)^0-CO is not stable on the electrode surface. Both hanging mercury drop

and rotating disc electrodes were used for these experiments; representative results for the HMDE are shown in Figure 3.11. In these experiments, the electrode potential was scanned negative in the presence of $Ni(cyclam)^{2+}$ and CO_2 until the CO_2 reduction current peaked and had decreased to almost zero. The scan was reversed and the electrode was held at a potential of -1.0 V for varying amounts of time. The electrode potential was again scanned in the negative direction and the resultant current for the "second pass" of the CO_2 reduction peak was recorded. As can be seen in Figure 3.8, the longer the potential was held at -1.0 V, the greater the current of the second pass. With a pause in the potential scan of one minute at -1.0 V, the current was almost restored to its original value. These results indicate that the passivation of the electrode is reversible, and that the electrode surface can be restored to its original catalytic condition.

The explanation for these results is as follows. $Ni(cyclam)^{0}$-CO is not stable in the presence of oxidizing species such as $Ni(cyclam)^{2+}$ or water. When the electrode is held at potentials where the reduction of $Ni(cyclam)^{2+}$ to $Ni(cyclam)^{0}$-CO cannot occur (i.e., at potentials positive of the CO_2 reduction wave), the slow decomposition of $Ni(cyclam)^{0}$-CO occurs. The disappearance of the precipitate allows $Ni(cyclam)^{2+}$ to be reductively adsorbed at the electrode surface again and the catalyst is reestablished. During the decomposition of the $Ni(cyclam)^{0}$-CO species, CO and H_2 are released. As shown in Section 3.3.1, the presence of CO has no effect on the quantity or rate of adsorption of $Ni(cyclam)^{+}$ at potentials positive of -1.3 V. In addition, the adsorption of $Ni(cyclam)^{+}$ is independent of pH (Section 2.4.4) and thus the rise in pH associated with the evolution of hydrogen also has no effect on the $Ni(cyclam)^{+}$ adsorption process. As soon as the electrode surface is cleared of $Ni(cyclam)^{0}$-CO, reestablishment of the active catalytic species and resumption of CO_2 reduction can occur.

Figure 3.11 Consecutive cyclic voltammetry scans of 0.5 mM $Ni(cyclam)^{2+}$ in 0.1 M $KClO_4$ saturated with CO_2 at a HMDE. The first cycle (solid line) is from -1.0 to -2.0 V and back; the elapsed time before the start of the second cycle (dashed line, same potential range) is shown in seconds. Scan rate is 100 mV sec^{-1}.

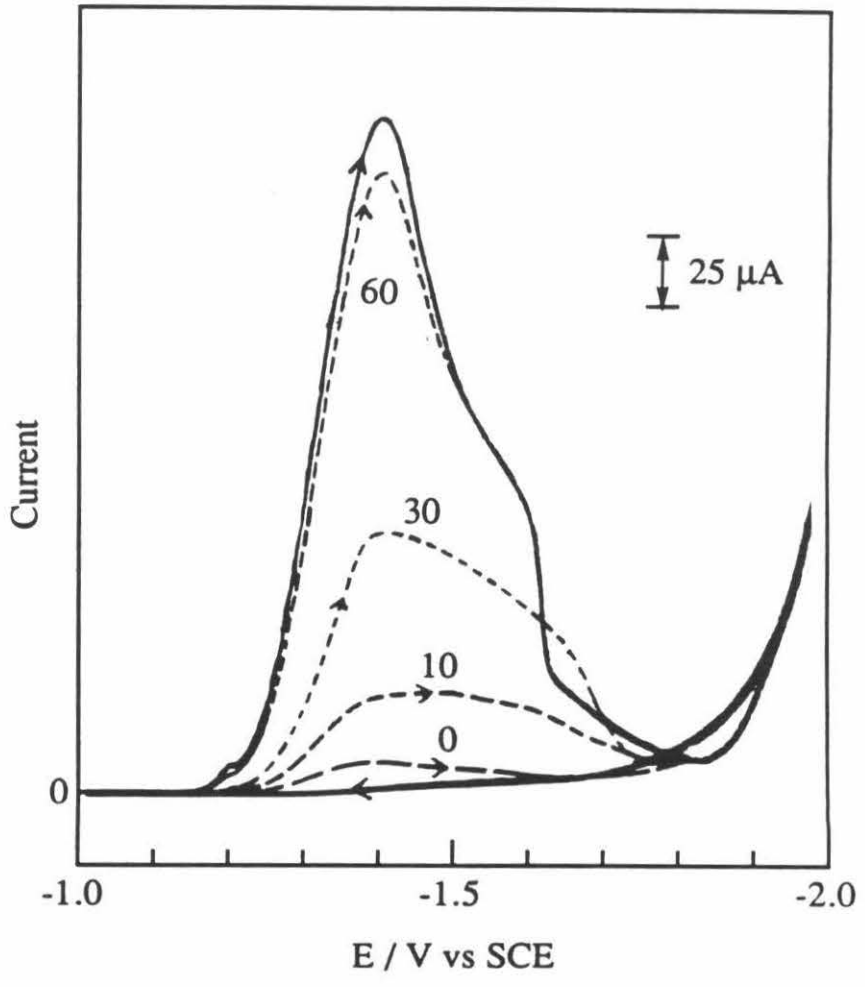

3.4 *Discussion*

Nature of the Ni(cyclam)^0-CO Species

The exact structure of the Ni(cyclam)^0-CO precipitate is as yet unresolved. Ni(0) complexes are known,[11] and a large percentage of these have one or more carbonyl ligands. The Ni(0) cyclam carbonyl complex is likely to be pentacoordinate since an analogous compound, Ni(TMC)$^{2+}$, was found to bind only one CO upon reduction. Carbonyl Ni(I) complexes of tetraaza macrocycles are also known, and their chemistry has been studied.[6,12] In these compounds, the metal d orbitals play a minor role in CO binding and the predominant interaction is through σ interactions with the metal 4s and 4p orbitals. In addition, all of the carbonyl Ni(I) complexes of tetraazamacrocycles studied exhibited pentacoordination. In the complex Ni(cyclam)$^+$, the Ni(I) center is too large to lie in the plane of the ligand;[13] the even larger Ni(0) would lie even farther outside of the cyclam plane, thereby lessening the chance for coordination numbers higher than five.

Additional possibilities for the insoluble species produced as a result of the two-electron reduction of Ni(cyclam)$^{2+}$ under CO were investigated. $Ni(CO)_4$ showed no electrochemistry in the potential range from 0 to -1.8 V and it is therefore unlikely that this species is responsible for the observed results. The free ligand cyclam (chapter four) demonstrated none of the features observed, even in the presence of CO. Although the oxidation of Ni(0) on mercury does occur at approximately 0 V, it is a slow, drawn out process, even in the presence of CO. The conclusion is that Ni(0), cyclam, and CO together are necessary to produce the precipitate.

An interesting result is that the precipitate formed by the reduction of Ni(TMC)$^{2+}$ under CO, presumably Ni(TMC)^0-CO, is reoxidized at the same potential as

$Ni(cyclam)^0$-CO. Since the electrochemical potentials of these two Ni complexes are otherwise well separated, it is surprising that the reoxidation peaks of the Ni(0) carbonyl complexes would be so similar. The only explanation at this point is that the Ni(0) is pushed so far out of the plane of the ligand that the substantial metal/ligand orbital overlap which occurs with the Ni(II) and, to a lesser extent, Ni(I) centers, no longer exists.

The insoluble $Ni(cyclam)^0$-CO (or $Ni(TMC)^0$-CO) species is unstable in the presence of water or excess $Ni(cyclam)^{2+}$. The presence of water limits the stability of the precipitate to potentials negative of -1.2 V. With a large mercury pool electrode, bubbles form on the surface if the potential is moved positive of this value. These bubbles are either H_2 or CO, produced by the decomposition of $Ni(cyclam)^0$-CO. Evidence for the production of hydrogen is the presence of a hydroxide wave at approximately 0 V (see Figure 3.1 and 3.4). In addition, measurements of the charge show that the charge used in the reduction of $Ni(cyclam)^{2+}$ under CO to $Ni(cyclam)^0$-CO is not all retrieved when this latter species is reoxidized. Presumably, this lost charge is due to the irreversible hydrogen evolution reaction. At potentials negative of -1.2 V, $Ni(cyclam)^0$-CO is continuously being formed by the reduction of $Ni(cyclam)^{2+}$ under CO or CO_2, but in the presence of $Ni(cyclam)^{2+}$ or $Ni(cyclam)^+$, it is unstable. This decomposition process must be slower than the rate of formation of $Ni(cyclam)^0$-CO since the latter is observed as a precipitate on a mercury pool electrode. In effect, a steady-state situation is reached where the rate of the decomposition of $Ni(cyclam)^0$-CO is equal to the rate of its formation.

3.4.2 Comparison with Previous Results

The general findings of this research agree with the results previously published by Sauvage and co-workers.[1] The catalyzed reduction of CO_2 proceeds at a remarkably fast rate at potentials considerably more positive than those previously reported. In addition,

the results of this current study have elucidated the electrochemical mechanisms behind CO_2 reduction to a much greater extent.

The results of this study show that several of the conclusions made by Fujihira *et al.*[2] are in error. No evidence was obtained to support the conclusion that Ni(cyclam)$^+$ is involved in a demetalation reaction (Equation 1). Rather, the sharp anodic spike is due to the reoxidation of Ni(cyclam)^0-CO which had precipitated on the electrode surface. The reversible wave at approximately 0 V is also not due to a byproduct of a ligand loss reaction, but rather is a result of the evolution of hydrogen caused by the reduction of water by Ni(cyclam)^0-CO. The evolution of hydrogen causes a rise in the pH of the solution in the vicinity of the electrode and thus results in the presence of a wave at 0 V due to the reversible oxidation of mercury in the presence of hydroxide ion. Both of these features, the anodic spike at -0.15 V and the wave at 0 V, are present in the electrochemistry of Ni(cyclam)$^{2+}$ in the presence of CO was well as CO_2.

Another assertion by Fujihira and co-workers was that the adsorbed catalyst, $Ni(cyclam)^+_{ads}$, is desorbed completely at potentials more negative than -1.7 V under CO or CO_2. Presumably, it is not the CO_2 itself which causes the desorption, but the CO produced by the reduction of CO_2 at these potentials. The evidence for this claim was based on the electrocapillary data which showed no drop in the surface tension of mercury in the presence of CO (or CO_2) and Ni(cyclam)$^{2+}$ at potentials negative of -1.7 V. These data may be flawed if the precipitation of Ni(cyclam)^0-CO on the electrode surface affects the electrocapillary data. The possibility of a precipitate was not considered in this previous study. Although the results discussed in this present study cannot state conclusively that $Ni(cyclam)^+_{ads}$ desorbs at potentials negative of -1.7 V in the presence of CO, the chronocoulometric experiments (Section 3.3.1) provide conclusive evidence that CO does not cause the desorption of $Ni(cyclam)^+_{ads}$ at potentials positive of -1.3 V. The prepeak which was ascribed in previous studies[1,2] to the reduction of Ni(cyclam)$^{2+}$ to

$Ni(cyclam)^{+}_{ads}$, shows no shift in potential in the presence of CO. This is not unexpected, as this prepeak has been shown in chapter two of this thesis to result not from a reductive adsorption process, but from a shift in the double layer charging due to a rearrangement of the $Ni(cyclam)^{+}_{ads}$. Since chronocoulometric experiments show no effect in the adsorption of $Ni(cyclam)^{+}$ under CO at potentials at least as negative as the potential of the prepeak, it is not surprising that the presence of CO has no effect on the rearrangement of $Ni(cyclam)^{+}_{ads}$. In contrast to this behavior, the prepeak representing the reduction of $Ni(TMC)^{2+}$ to $Ni(TMC)^{+}_{ads}$ exhibits a pronounced potential shift as the concentration of CO in solution is increased. This is also the expected result because this prepeak results from a true reductive adsorption process as described in Equation (9).

$$Ni(TMC)^{2+} + CO + e^{-} \rightleftharpoons Ni(TMC)^{+}_{ads}\text{-}CO \qquad (9)$$

Fujihira and co-workers explained the decrease in the CO_2 electrocatalytic reduction current negative of -1.5 V as a result of desorption of the catalyst. The decrease in the adsorption of $Ni(cyclam)^{+}_{ads}$ was attributed to the perturbation of the equilibria between the surface and adsorbed $Ni(cyclam)^{2+}$ and $Ni(cyclam)^{+}$ species by CO. Evidently, the concentration of CO is not great enough at the electrode surface at potentials positive of -1.5 V to cause this desorption to occur. This explanation cannot account for the slow reduction in catalytic current with time as seen in this chapter, at potentials more positive than -1.5 V (Figure 3.10).

The presence of a precipitate on the electrode surface and the lack of any chronocoulometric evidence in this study for the desorption of $Ni(cyclam)^{+}_{ads}$ point to a much different conclusion than that reached by Fujihira *et al.*[2] CO does not affect the adsorption of $Ni(cyclam)^{+}$ at potentials where the catalytic reduction of CO_2 occurs and the drop in this reduction current is caused by the precipitation of $Ni(cyclam)^{0}$-CO on the electrode surface. While it is still possible that $Ni(cyclam)^{+}_{ads}$ desorbs at potentials negative

of -1.7 V in the presence of CO, this would not affect the electrocatalytic reduction of CO_2 as this reaction proceeds at potentials far positive of -1.7 V. An interesting aspect of this mechanism is that at low concentrations of $Ni(cyclam)^{2+}$ in solution, the current for the catalytic reduction of CO_2 decreases less rapidly than for higher concentrations of $Ni(cyclam)^{2+}$. A substantial fraction of a monolayer of $Ni(cyclam)^{+}_{ads}$ is still present even at $Ni(cyclam)^{2+}$ concentrations as low as 10 μM (Figure 2.7). Since the rate of formation of the precipitate $Ni(cyclam)^{0}$-CO is much slower at lower solution concentrations of $Ni(cyclam)^{2+}$, it is not surprising that the catalytic CO_2 reduction passivation by $Ni(cyclam)^{0}$-CO is not as severe. This effect was also noted in the RDE experiments (Figure 3.10) where the decrease of the CO_2 reduction current with time occurred at a slower rate. Unfortunately, the results of the work by Fujihira and co-workers and of this present study cannot establish the quantity of the catalyst $Ni(cyclam)^{+}$ adsorbed at the potentials where the reduction of CO_2 proceeds at the maximum rate.

3.4.3 Summary

The results of these experiments indicate that the electrochemistry of the catalytic reduction of CO_2 by $Ni(cyclam)^{+}_{ads}$ is closely linked to the electrochemistry of the product, CO. The cyclic voltammetry of $Ni(cyclam)^{2+}$ in the presence of CO_2 exhibits not only those features associated with the reduction of CO_2, but also responses due to the interaction of $Ni(cyclam)^{+}$ with CO. These two processes are not separable, and the degree of the electrochemical interaction of the product of the catalytic CO_2 reduction with the catalyst has a strong influence on the overall scheme. The presence of CO shifts the potential for the reduction of $Ni(cyclam)^{2+}$ to more positive values and renders it irreversible. The reduction proceeds all the way to $Ni(cyclam)^{0}$-CO, which precipitates on the electrode surface. The presence of CO, either originally in the solution or formed as a product of the reduction of CO_2, results in a passivation of the electrode surface. In this manner, the product of the electrocatalytic reaction is a poison for the catalyst. Fortunately,

at appropriate potentials, the poisoning of the catalyst is not complete. At potentials of -1.3 V or positive, the catalyst is still functional, although the reduction of CO_2 is slowed to a rate which is much less than the diffusion-controlled rate which is obtainable in the first few moments after the beginning of the reaction. The poisoning of the catalyst is not irreversible, and appropriate treatment of the electrode can restore its functionality. In the original study by Sauvage *et al.*[1], no mention was made of this decrease in catalytic activity and all measurements were made at potentials where this effect was least noticeable. However, even at potentials where the effects of the poisoning are least noticeable, the effectiveness of the catalyst is diminished considerably.

Chapter 3 References

1. Beley, M.; Collin, J.-P.; Ruppert, R.; Sauvage, J.-P. *J. Am. Chem. Soc.* **1986**, *108*, 7461.

   Beley, M.; Collin, J.-P.; Ruppert, R.; Sauvage, J.-P. *J. Chem. Soc., Chem. Commun.* **1984**, 1315.

2. Fujihira, M.; Hirata, Y.; Suga, K. *J. Electroanal. Chem.* **1990**, *292*, 199.

3. Bosnich, B.; Tobe, M.L.; Webb, G.A. *Inorg. Chem.* **1965**, *8*, 1102,1109.

4. Barefield, E.K.; Wagner, F. *Inorg. Chem.* **1973**, *12*, 2435.

5. Lauer, G.; Abel, R.; Anson, F.C. *Anal. Chem.* **1967**, *39*, 765.

6. Gagné, R.R.; Ingle, D.M. *Inorg. Chem.* **1981**, *20*, 420.

7. Christie, J.H.; Anson, F.C.; Lauer, G.; Osteryoung, R.A. *Anal. Chem.* **1963**, *35*, 1979.

   Anson, F.C.; Osteryoung, R.A. *J. Chem. Ed.* **1983**, *60*, 293.

8. Bard, A.J.; Faulkner, L.R., Electrochemical Methods; Wiley and Sons: New York, 1980, p. 186.

9. Balazs, G.B.; Anson, F.C. *J. Electroanal. Chem.* **1992**, *322*, 325.

10. Bard, A.J.; Faulkner, L.R. Electrochemical Methods; Wiley and Sons: New York, 1980, p. 163.

11. Cotton, F.A.; Wilkinson, G., Advanced Inorganic Chemistry; Wiley and Sons: New York, 1988, p. 754.

12. Furenlid, L.R.; Renner, M.W.; Szalda, D.J.; Fujita, E. *J. Am. Chem. Soc.* **1991**, *113*, 883.

13. Jubran, N.; Cohen, H.; Meyerstein, D. *Israel J. Chem.* **1985**, *25*, 118.

Adam, K.; Antlovich, M.; Brigden, L.G.; Lindoy, L.F. *J. Am. Chem. Soc.* **1991**, *113*, 3346.

Thöm, V.; Fox, C.C.; Boeyens, J.C.A.; Hancock, R.D. *J. Am. Chem. Soc.* **1984**, *106*, 5947.

Chapter 4

Electrochemistry of Cyclam at a Mercury Electrode

4.1 *Introduction*

The continuing interest in the electrocatalytic reduction of CO_2 by $Ni(cyclam)^+_{ads}$ has led to many investigations of the electrochemistry of this complex at a mercury electrode.[1-6] In one such study,[6] it was proposed that the reduction of the Ni(II) center can lead to its expulsion from the cavity in the macrocyclic ligand and that the electrochemistry of the free ligand cyclam was responsible for several of the features observed in the voltammetry of $Ni(cyclam)^{2+}$. The one previous report[7] on the anodic oxidation of mercury electrodes in the presence of the cyclam ligand (Figure 4.1) involved only buffered solutions and no study has appeared to date on the electrochemistry of cyclam at mercury under conditions which would be present during the electrocatalytic reduction of CO_2. In this present study, the oxidation of mercury electrodes in unbuffered solutions of the free cyclam ligand was investigated and compared to the response obtained for the reduction of the separately prepared $Hg(cyclam)^{2+}$ complex. The two processes gave rise to voltammetric responses which were far from the simple inverses of each other. An account of the observed behavior and its rationalization are the subject of this chapter; the research is based on a recent publication by this author.[8]

4.2 *Experimental*

4.2.1 Materials

Cyclam (1,4,8,11-tetraazacyclotetradecane) (Aldrich) was recrystallized from *p*-dioxane. $Hg(cyclam)(ClO_4)_2$ was prepared and purified as described,[9] and was stored in the dark. Evidence of decomposition was noted after long exposure to light.

Figure 4.1 Structure of 1,4,8,11-tetraazacyclotetradecane (cyclam).

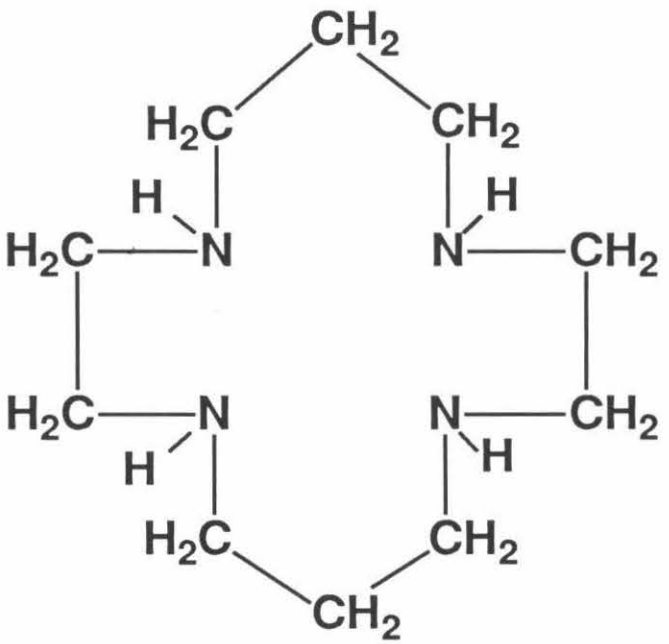

$KClO_4$ was prepared by adding $HClO_4$ to a solution of KOH. The product was recrystallized twice from water and dried at 80 °C in vacuo for 24 hours. Solutions were prepared from laboratory distilled water which was further purified by passage through a contaminant removal system (Barnstead Nanopure). Solutions were deaerated with prepurified argon which was passed through a solution of V(II) to remove any reisdual oxygen. Mercury for the electrodes was triply distilled (Bethlehem Instrument Co.).

4.2.2 Apparatus and Procedures

Conventional two compartment cells were used for all electochemical measurements. For the measurement of cyclic voltammograms, a Princeton Applied Research (PAR) Model 173 Potentiostat and a PAR Model 175 Programmer were used with a hanging mercury drop electrode (HMDE). The drop area of this electrode was 0.027 cm^2 as calculated from the weight, averaging over a large number of drops. Polarograms were obtained with a PAR Model 174 Potentiostat and a dropping mercury electrode (DME). The flow rate of this electrode was 0.69 mg/sec, which yielded an electrode surface area of 0.66 mm^2 for a drop time of 1 second. The supporting electrolyte for most experiments was dearated 0.1 M $KClO_4$. Buffered solutions were either acetate, borate, or an appropriate concentration of either HCl or KOH. The ionic strength was maintained at 0.1 M by the addition of $KClO_4$ if necessary. All potentials were measured with respect to a saturated calomel reference electrode (SCE). All experiments were conducted at the ambient laboratory temperature, 22 ±2 °C.

4.3 *Results*

4.3.1 Cyclic Voltammetry of $Hg(cyclam)^{2+}$

An unusual feature in the cyclic voltammetry of the ligand cyclam at mercury electrodes is the large difference in the responses for the oxidation of mercury in the presence of cyclam and for the reduction of the $Hg(cyclam)^{2+}$ complex. In buffered solutions no difference in the responses is obtained; they are simply inverses of each other. In Figure 4.2 is shown a cyclic voltammogram for the reduction of $Hg(cyclam)^{2+}$. The cathodic and anodic waves are broad but the peak currents are approximately equal. The cathodic peak corresponds to a two electron reduction of the $Hg(cyclam)^{2+}$ complex. The diffusion coefficient of the complex was assumed to be approximately 6.5×10^{-6}, which is a typical value for complexes of this size and structure. The anodic peak corresponds to the oxidation of the mercury electrode in the presence of the cyclam ligand released during the reduction of $Hg(cyclam)^{2+}$. The half-reaction responsible for the voltammetric response is given in equation (1).

$$Hg(cyclam)^{2+} + 2\,e^- \rightleftharpoons Hg^0 + Cyclam \qquad (1)$$

Note that although the ligand cyclam is a weak base, the degree of protonation of the free ligand released during the reduction is left unspecified. This topic will be addressed at a later point (Section 4.4).

4.3.2 Cyclic Voltammetry of the Ligand Cyclam

In Figure 4.3 is shown the cyclic voltammogram which results when a mercury electode is scanned toward more postive potentials in an unbuffered solution containing only the cyclam ligand. Two anodic peaks appear with two cathodic counterparts. The first anodic peak corresponds to the two electron oxidation of each molecule of cyclam

Figure 4.2 Cyclic voltammogram of 0.2 mM $Hg(cyclam)^{2+}$ at a HMDE in 0.1 M $KClO_4$. Initial potential is 0.3 V. Scan rate is 200 mV sec^{-1}.

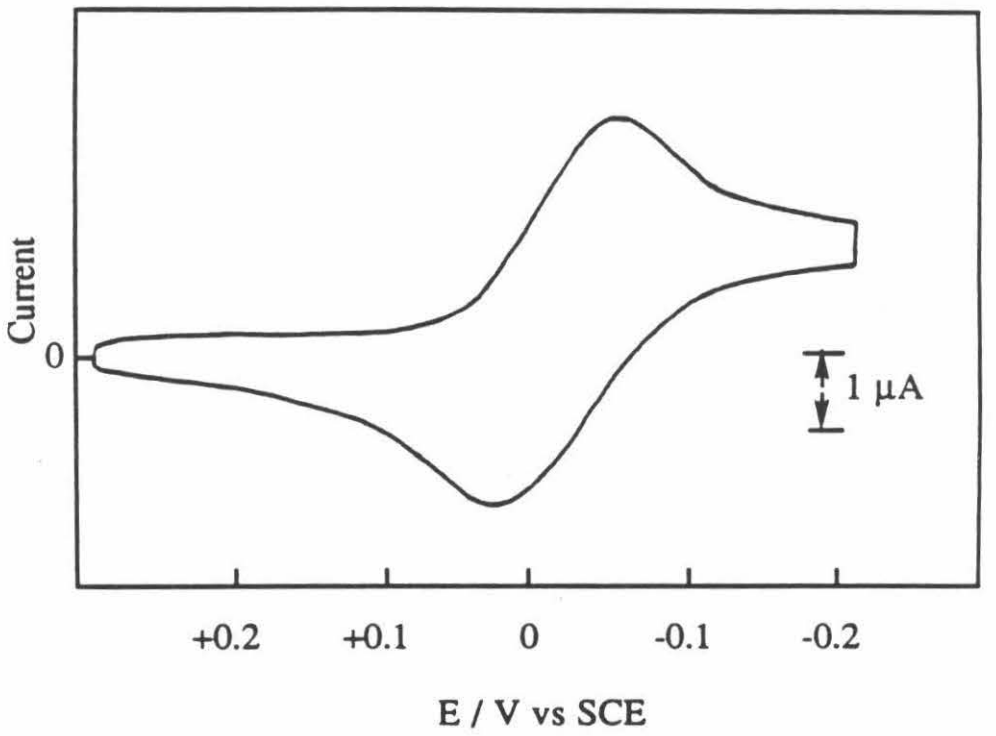

Figure 4.3 Cyclic voltammogram of 0.2 mM cyclam at a HMDE in 0.1 M $KClO_4$ (solid line). Initial potential is -0.3 V. Scan rate is 200 mV sec^{-1}. Dashed line is after addition of 0.2 mmole NaOH per liter.

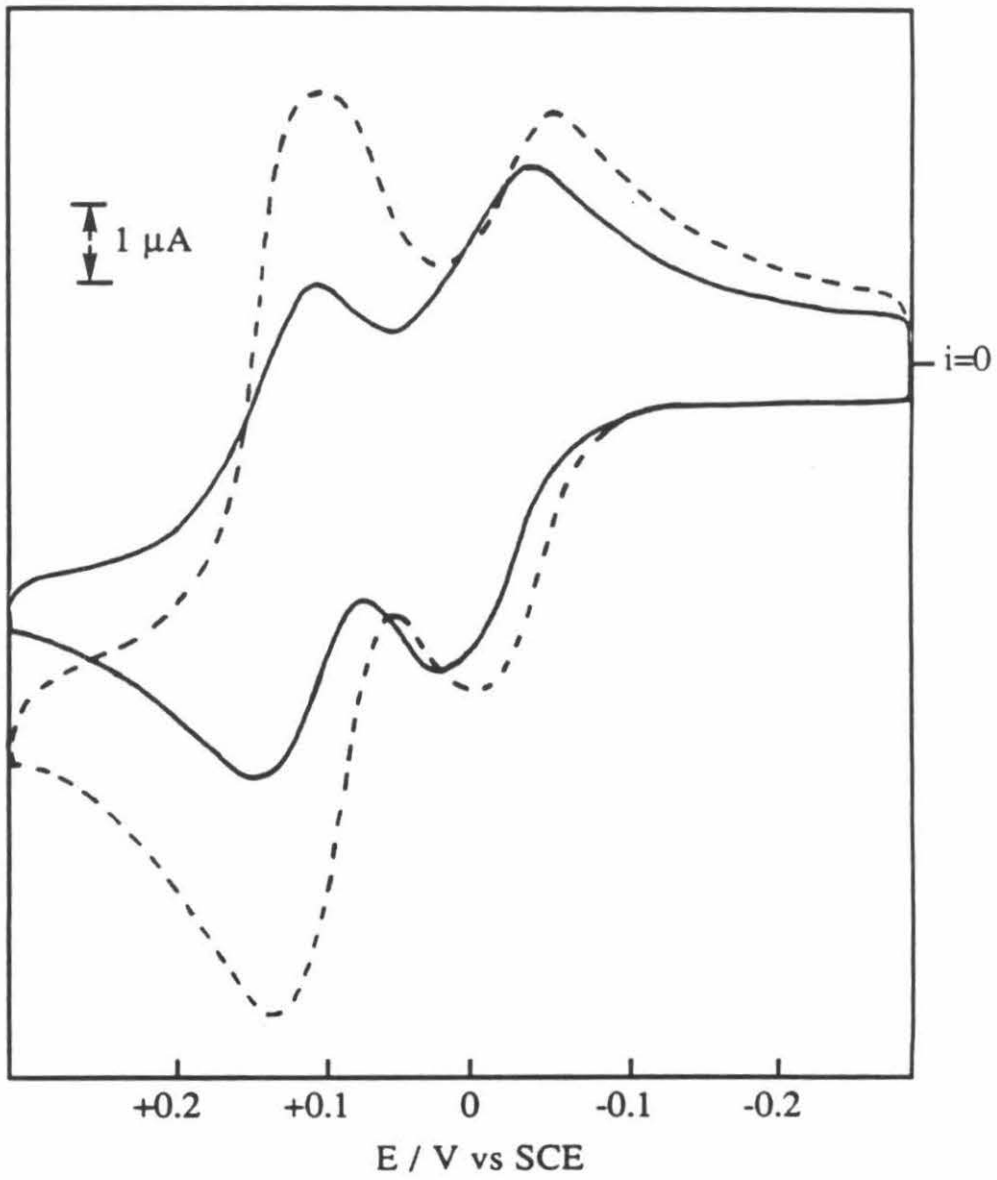

reaching the electrode surface as would be expected for the inverse of half-reaction (1). However, the positon of the anodic peak is slightly different from that of the anodic peak shown in Figure 4.2. The second anodic peak in Figure 4.3 arises from the oxidation of the mercury electrode in the presence of hydroxide ions as shown in Equation (2).

$$2\,OH^- + Hg \rightleftharpoons Hg(OH)_2 + 2e^- \qquad (2)$$

This process has been well characterized by Kirowa-Eisner and Osteryoung in an earlier study.[10] The origin of this peak was verified by the addition of hydroxide to the solution, which caused the magnitude of the second anodic peak current to increase without affecting the magnitude of the first peak current (see Figure 4.3, dashed curve). As expected, the peak potentials of both peaks were shifted to less positive values by the addition of hydroxide ion.

4.3.3 Normal Pulse Polarography of Cyclam and Hg(cyclam)$^{2+}$

Normal Pulse polarograms[11] of Hg(cyclam)$^{2+}$ contain a single cathodic wave as expected from Figure 4.2, while two anodic waves appear in normal pulse polarograms for solutions of the cyclam ligand. Typical polarograms are shown in Figure 4.4. As was observed with cyclic voltammetry, the magnitude of the current observed in Figure 4.4A corresponds to the two electron reduction of Hg(cyclam)$^{2+}$ (Equation 1), and the magnitude of the currents observed in Figure 4.4B correspond to two, two-electron oxidations (Equations 1 and 2). The feature near 0.4 V in curve 4.4B was also observed in a previous study[11] and was ascribed to the effects resulting from the deposition of coatings of insoluble $Hg(OH)_2$ on the electrode surface.

Figure 4.4 Normal pulse polarograms at a DME in 0.1 M $KClO_4$ for (A) 0.5 mM $Hg(cyclam)^{2+}$; initial potential is 0.3 V and (B) 0.5 mM cyclam; initial potential is -0.3 V. Electrode area is 0.66 mm^2. Pulse width is 2 mV.

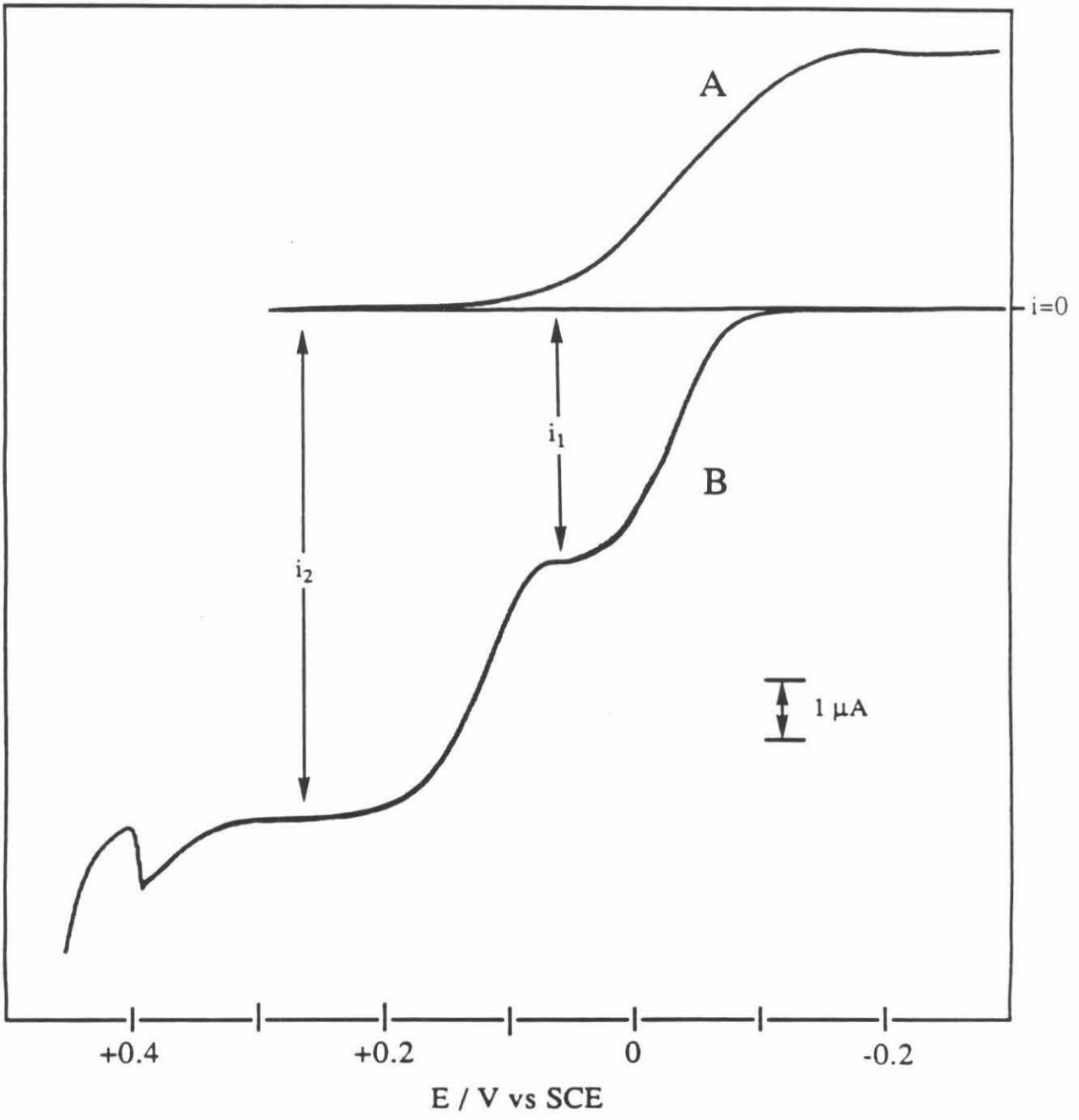

4.4 *Discussion*

The superficially puzzling differences between Figure 4.2 and 4.3 can be understood by recognizing that cyclam is a reasonably strong base which spontaneously protonates when added to aqueous solutions, producing hydroxide ions. The four pK_a values for the tetraprotonated cyclam are 11.4, 10.3, 1.6, and 0.9.[12,13] From these values a speciation diagram can be constructed; such a diagram is shown in Figure 4.5. In an unbuffered 1 mM solution of cyclam a mixture consisting primarily of $(cyclamH)^+$, $(cyclam)H_2)^{2+}$ and OH^- is present. Thus, a more accurate description of the processes occurring at the mercury electrode surface at the first anodic peak in Figures 4.3 and 4.4B is that given in half-reaction (3).

$$Hg + (cyclamH_x)^{x+} \rightleftharpoons Hg(cyclam)^{2+} + 2e^- + xH^+ \qquad (3)$$

The value of x indicates the average number of protons bound to the cyclam in solution. The solution also contains x moles of hydroxide ions per mole of cyclam. These OH^- ions are available to react with the H^+ ions generated by half-reaction (3). The rate of generation of H^+ ions at the electrode surface is governed by the rate of diffusion of the protonated cyclam molecules to the electrode surface. In contrast, the hydroxide ions arrive at the surface at the higher rate corresponding to their higher diffusion coefficient. As a result, the supply of OH^- ions at the electrode surface exceeds that of H^+ ions. The second anodic peak in Figures 4.3 and 4.4B corresponds to the consumption of the excess of OH^- anions by half reaction (2) above.

A logical question at this point would be why does the reoxidation of the mercury electrode in the presence of the cyclam liberated by the reduction of $Hg(cyclam)^{2+}$ give rise to only one peak (Figure 4.2)? When the cyclam ligand is produced at the electrode surface by reduction of $Hg(cyclam)^{2+}$, rather than by the dissolution of the free ligand cyclam, the unequal diffusion coefficients of OH^- and the protonated cyclam molecules produce

Figure 4.5 Distribution of protonated forms of cyclam as a function of pH.

o = $(cyclamH_4)^{4+}$, Δ = $(cyclamH_3)^{3+}$, ■ = $(cyclamH_2)^{2+}$, o = $(cyclamH)^{+}$ ♦ = cyclam

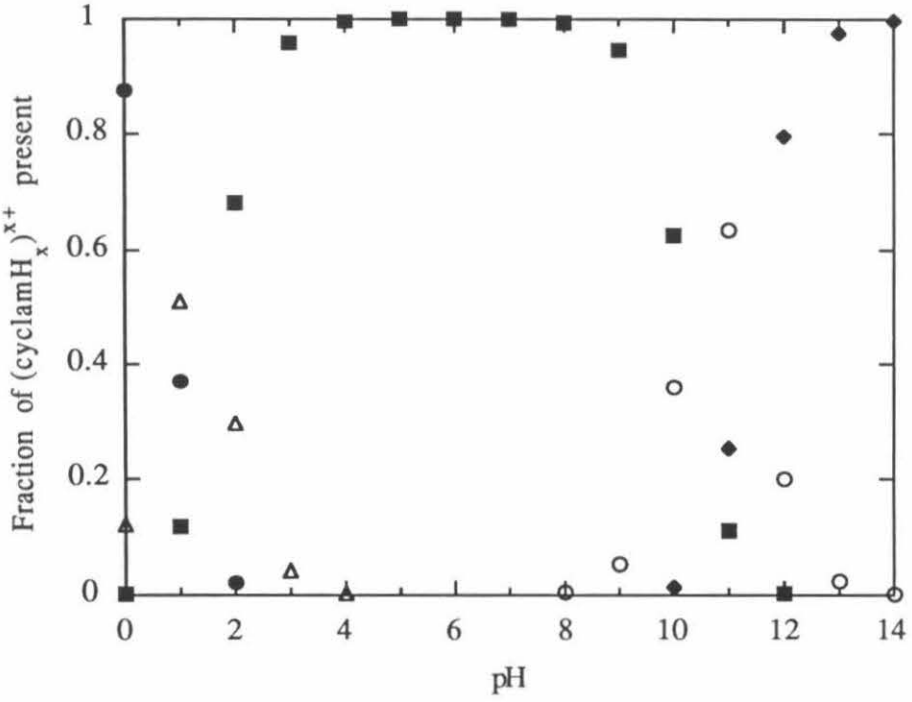

unequal concentration gradients of the reactants at the electrode surface. The gradients are just those required for all of the OH^- ions that diffuse back towards the electrode surface during the reverse scan to be exactly neutralized by the H^+ ions released by the reaction of the anodically generated Hg^{2+} ions with the protonated cyclam molecules which also diffuse back to the electrode surface. The more rapidly diffusing OH^- ions diffuse farther from the electrode surface during the reductive half of the voltammetric scan than do the more slowly diffusing $(cyclamH)^+$ and $(cyclamH_2)^{2+}$ cations, but the fluxes of the anions and cations match perfectly at the electtode during the reverse scan. No OH^- ions remain to allow the oxidation of mercury to continue further, and no second anodic peak is seen in Figure 4.2.

Because of a steady-state situation at the electrode surface, pulse polarography is better suited than cyclic voltammetry for the measurement of currents at potentials where the rate of the reaction is diffusion limited. The magnitudes of the two plateau currents to be expected in pulse polarograms such as the one in Figure 4.4B can be predicted from a knowledge of the diffusion coefficients of cyclam and OH^- and the pK_a values of protonated cyclam. The current on the plateau of the first wave in Figure 4.4B, i_1, can be calculated from the Cottrell equation

$$i_1 = FAnC_c(D_c)^{1/2}(\pi t)^{-1/2} \qquad (4)$$

where F is Faraday's constant, A is the electrode area, n is the number of electrons involved in the reaction, (two in the case of cyclam), C_c is the total concentration of cyclam present, D_c is the common diffusion coefficient of all forms of the protonated cyclam molecules, and t is the measurement time. The total current on the second plateau, i_2, is the sum of i_1 and the Cottrell current for the diffusion of OH^- ions to the electrode surface. The latter quantity is diminished by the fraction of OH^- ions which are removed in the

diffusion layer by reacting with H^+ ions generated according to half-reaction (3) during the flow of i_1 on the first plateau. The Cottrell current for OH^- is given by equation (5)

$$i_{OH} = FAnC_{OH}(D_{OH})^{1/2} (\pi t)^{-1/2} \quad (5)$$

where n = 1 and C_{OH} and D_{OH} are the concentration and diffusion coefficient of OH^- ions, respectively, in the bulk of the solution. The average degree of protonation of the cyclam molecules is given by the value of x in half-reaction (3). It follows that $C_{OH} = xC_c$. Thus,

$$i_{OH} = FAxC_c(D_{OH})^{1/2} (\pi t)^{-1/2} \quad (6)$$

or

$$i_{OH} = 0.5 \text{ x } (\frac{D_{OH}}{D_c})^{1/2} i_1 \quad (7)$$

and

$$i_2 = i_1 + i_{OH} - 0.5xi_1 \quad (8)$$

where $0.5xi_1$ represents the diminishment of i_{OH} by the reaction between OH^- and H^+ ions in the diffusion layer. Thus, the ratio of the plateau currents for the two waves in pulse polarograms such as the one in Figure 4.4B is given by

$$i_2/i_1 = 1 + 0.5x(\frac{D_{OH}}{D_c})^{1/2} - 0.5x. \quad (9)$$

From the pK_a values listed above, the calculated value of x for the 0.5 mM cyclam solution of Figure 4.4B is 1.3 which corresponds to a pH of 10.5. The measured pH of the solution matched this calculated value. The ratio of i_2/i_1 was calculated from Equation (9) using x = 1.3, $D_{OH} = 5.2 \times 10^{-5}$ cm^2 s^{-1} and $D_c = 6.5 \times 10^{-6}$ cm^2 s^{-1}. The calculated ratio of 2.2 matched the measured value of 2.2. Good agreement was obtained at other concentrations of cyclam in the range from 0.2 to 2.0 mM (Table 4.1).

The analysis presented here applies only to unbuffered solutions of cyclam. In the presence of suitable buffers the voltammetry of cyclam contains only a single peak because

no net formation of OH^- ions results from the presence of the cyclam ligand. This result was also confirmed in this work.

4.5 *Conclusions*

The differences in the voltammetry exhibited by $Hg(cyclam)^{2+}$ and the uncoordinated cyclam ligand at mercury electrodes in unbuffered solutions are well accounted for by the acid-base chemistry of the cyclam ligand and the unusually large diffusion coefficient of OH^- ions in water. The analysis provided in this study should apply to all basic ligands which form complexes with Hg^{2+}. Such ligands would be expected to yield double peaks in anodic voltammetry at mercury electrodes. The voltammetric behavior to be expected from the uncoordinated cyclam ligand at mercury electrodes is important in this present study as well as other studies[6] of transition metal-cyclam complexes as catalysts where it has been proposed that the free cyclam ligand is released during catalytic cycles.

Chapter 4 References

1. Beley, M.; Collin, J.-P.; Ruppert, R.; Sauvage, J.-P. *J. Am. Chem. Soc.* **1986**, *108*, 7461.

   Beley, M.; Collin, J.-P.; Ruppert, R.; Sauvage, J.-P. *J. Chem. Soc., Chem. Commun.* **1984**, 1315.

   Collin, J.-P.; Jouaiti, A.; Sauvage, J.-P. *Inorg. Chem.* **1988**, *27*, 1986.

2. Lovecchio, F.V.; Gore, E.S.; Busch, D.H. *J. Am. Chem. Soc.* **1974**, *96*, 3109.

   Jubran, N.; Ginzburg, G.; Cohen, H.; Meyerstein, D. *J. Chem. Soc., Chem. Commun.* **1982**, 517.

3. Balazs, G.B.; Anson, F. C. *J. Electroanal. Chem.* **1992**, *322*, 325.

4. Taniguchi, I.; Nakashima, N.; Matsushita, K.; Yasukouchi, K. *J. Electroanal. Chem.* **1987**, *224*, 199.

   Taniguchi, I.; Shimpuku, T.; Yamashita, K.; Ohtaki, H. *J. Chem. Soc., Chem. Commun.* **1990**, 915.

5. Fujihira, M.; Nakamura, Y.; Hirata, Y.; Akiba, U.; Suga, K. *Denki Kagaku*, **1991**, *59*, 532.

6. Fujihira, M.; Hirata, Y.; Suga, K. *J. Electroanal. Chem.* **1990**, *292*, 199.

7. Kodama, M.; Kimura, E., *J. Chem. Soc. Dalton*, **1976**, 2335.

8. Balazs, G.B.; Anson, F.C. *J. Electroanal. Chem*, in press.

9. Deming, R.L.; Allred, A.L.; Dahl, A.R.; Herlinger, A.R.; Kestner, A.W.; Mark, O. *J. Am. Chem. Soc.***1976**,*98*, 4132.

10. Kirowa-Eisner, E.; Osteryoung, J. *Anal. Chem.* **1978**, *50*, 1062.

11. Bard, A.J.; Faulkner, L.R. Electrochemical Methods; Wiley and Sons: New York, 1980, p 186.

12. Thöm, V.J.; Hosken, G.D.; Hancock, R.D.; *Inorg. Chem.* **1985**, *24*, 3378.

13. Hinz, F. P.; Margerum, D. W. *Inorg. Chem.* **1974**, *4*, 2941.

Table 4.1 Ratio of anodic plateau currents in normal pulse polarograms for the oxidation of Hg in the presence of cyclam.

[Cyclam], mM	x[a]	i_2/i_1 (Exp.)[b]	i_2/i_1 (Calc.)[c]
0.2	1.5	2.3	2.4
0.5	1.3	2.2	2.2
1.0	1.1	2.0	2.0
2.0	0.94	1.9	1.9

a. Average number of protons bound to each cyclam molecule.

b. Ratio of the plateau currents measured from polarograms such at the one in Figure 4.4B.

c. Current ratio calculated from Equation 9.

Chapter 5

Kinetics and Mechanism of the Electrocatalytic Reduction of Carbon Dioxide

5.1 *Introduction*

Previous work on the electrocatalytic reduction of CO_2 by Sauvage and co-workers[1-3] and Fujihira and co-workers[4,5] suggested that $Ni(cyclam)^{+}_{ads}$ is an efficient and selective catalyst for the aqueous reduction of CO_2 to CO at a mercury electrode. By a more thorough investigation of this and related systems, further evidence to support this conclusion is detailed in the previous chapters of this thesis. Chapter two discusses the electrochemistry of $Ni(cyclam)^{2+}$ and related compounds at mercury and reveals that the adsorption of $Ni(cyclam)^{+}$ is not as straightforward as previously proposed.[1,4] In chapter three, the electrochemistry of $Ni(cyclam)^{2+}$ in the presence of CO_2 and CO is studied in detail. Although the overall results of this section agree with those of Sauvage[1,2] and Fujihira,[4,5] there are several important conclusions which differ. Chapter four investigates the electrochemistry of cyclam at mercury electrodes, as this free ligand species was proposed to be detectable under certain experimental conditions.[4]

Several key issues have not yet been addressed with regard to the electrocatalytic reduction of CO_2, either in this thesis or in previous studies.[1-5] Although an overall catalytic cycle was proposed by Sauvage in one of these studies[1], some of the results presented in this thesis require that modifications to the cycle be made. In addition, the kinetics of the overall reaction have yet to be determined. Chapter five addresses these issues, and serves as a unifying chapter for the entire thesis.

5.2 *Experimental*

5.2.1 Materials

Cyclam (Aldrich) was recrystallized from *p*-dioxane. Tetramethylcyclam (TMC, Aldrich), was used as received. $Ni(cyclam)Cl_2$ and $Ni(cyclam)(ClO_4)_2$ were prepared according to the method of Bosnich *et al.*[6] Each was recrystallized twice from

methanol/diethyl ether and dried *in vacuo* at 60 °C for 24 hours. The synthesis of *trans* I $Ni(TMC)(ClO_4)_2$ was performed following literature procedures.[7] $Ni(dimethylcyclam)(ClO_4)_2$ and $Ni(monomethylcyclam)(ClO_4)_2$ were synthesized by an undergraduate research fellow following literature procedures.[8,9] *Cis*-$Ni(cyclam)Cl_2$ was prepared according to the method of Billo.[10] $KClO_4$ was prepared by the addition of $HClO_4$ to a solution of KOH. All aqueous solutions were prepared from analytic grade reagents; distilled water was further purified by passage through a Barnstead Organopure contaminant removal system. Solutions were buffered by either acetate, borate or an appropriate concentration of HCl or KOH; $KClO_4$ was added if necessary to provide a total ionic strength of 0.1 M. Prepurified argon was bubbled through a solution of V(II) to remove residual oxygen. Saturated CO_2 solutions were prepared by bubbling CO_2 gas (Matheson, 99.9% purity) through the solutions. Less concentrated solutions were obtained by the addition of appropriate amounts of acid to Na_2CO_3 or by the addition of Na_2CO_3 to a solution buffered at a pH of 4 to 6. Saturated CO solutions were prepared by bubbling CO gas (Matheson, 99.9% purity) through the solution.

5.2.2 Electrochemical Measurements

Triply distilled Hg (Bethlehem Instrument Co.) was used in a Brinkman model #410 Hanging Mercury Drop Electrode (HMDE). The surface area of this electrode was 0.027 cm^2 as determined by weight, averaging a large number of drops. Controlled potential reductions were performed with a mercury pool electrode (surface area of 4 cm^2) instead of the HMDE. Most experiments were done in 0.1 M $KClO_4$ as supporting electrolyte utilizing a conventional two compartment electrochemical cell. Buffered solutions were of sufficient capacity so that the pH did not shift significantly during the course of a given experiment; this requirement necessitated the use of ionic strengths of greater than 0.1 M for more concentrated CO_2 solutions. Solutions were deaerated by

bubbling with argon for at least 15 minutes prior to each experiment and a blanket of argon was kept over the solution during the course of the experiments.

Cyclic voltammograms were obtained with a Princeton Applied Research (PAR) Model 173 Potentiostat and a PAR Model 175 programmer. RDE voltammetry was done with a Pine Instruments Model RDE 3 potentiostat. All experiments were carried out at ambient laboratory temperature, 22 ±2 °C. All potentials were measured with respect to a saturated calomel reference electrode (SCE).

5.3 *Results and Discussion*

5.3.1 Summary of Aqueous CO_2 Chemistry

Since the electrocatalytic reduction of CO_2 as described[1-5] occurs in an aqueous medium, a discussion of the chemistry of this substrate in water is provided. Extensive research has been devoted to this topic[11] and only a brief summary will be given here.

Carbon dioxide, when dissolved in unbuffered media, exists in an equilibrium with the hydrated species (carbonic acid) as given in Equation (1).

$$CO_2 + H_2O \rightleftharpoons H_2CO_3 \qquad K=1.6 \times 10^{-3} \qquad (1)$$

The small value of the equilibrium constant indicates that only a small fraction of aqueous CO_2 is present in the hydrated form. Carbonic acid is a relatively weak acid and can dissociate as illustrated by Equations (2) and (3).

$$H_2CO_3 \rightleftharpoons H^+ + HCO_3^- \qquad pK_a = 6.15 \qquad (2)$$

$$HCO_3^- \rightleftharpoons H^+ + CO_3^{2-} \qquad pK_a = 9.92 \qquad (3)$$

The values for the pK_a's given are those for H_2CO_3 in a solution with an ionic strength of 0.1 M, which is the typical unbuffered medium used in the electrochemical reduction of CO_2. At a given pH, the fraction of the total of each species present can be calculated; a distribution diagram is shown in Figure 5.1. The catalytic activity of each species will be discussed further in Section 5.3.3.

5.3.2 Stoichiometry of the Electrochemical Reduction of CO_2

The overall reaction for the electrochemical reduction of CO_2 to CO in water is expressed by Equation (4).

$$CO_2 + 2e^- + H_2O \longrightarrow CO + 2OH^- \qquad (4)$$

In unbuffered media, this reduction causes an increase in the pH of the solution at the electrode surface. This leads to an apparent paradox, since one of the products of the reduction, OH^-, can react with CO_2 in several ways. At a pH of less than 8, the mechanism of this reaction is via direct hydration[11] (Equations (5), (6) and (7)).

$$CO_2 + H_2O \rightleftharpoons H_2CO_3 \qquad (5)$$

$$H_2CO_3 + OH^- \longrightarrow HCO_3^- + H_2O \qquad (6)$$

$$HCO_3^- + OH^- \longrightarrow CO_3^{2-} + H_2O \qquad (7)$$

Reactions (6) and (7) occur instantaneously, but because of the slowness of the hydration of CO_2, the overall rate law (pseudo first order) is given by Equation (8).[11]

$$\frac{-d[CO_2]}{dt} = k_{CO_2}[CO_2] \qquad k_{CO_2} = 0.03\ sec^{-1} \qquad (8)$$

At a pH of greater than 10, the direct reaction of CO_2 with OH^- is the dominant mechanism for the neutralization of CO_2 (Equations (9) and (10)).[11]

Figure 5.1 Distribution of carbon dioxide species as a function of pH.

(o = hydrated CO_2 (H_2CO_3), ■ = HCO_3^-, Δ = CO_3^{2-})

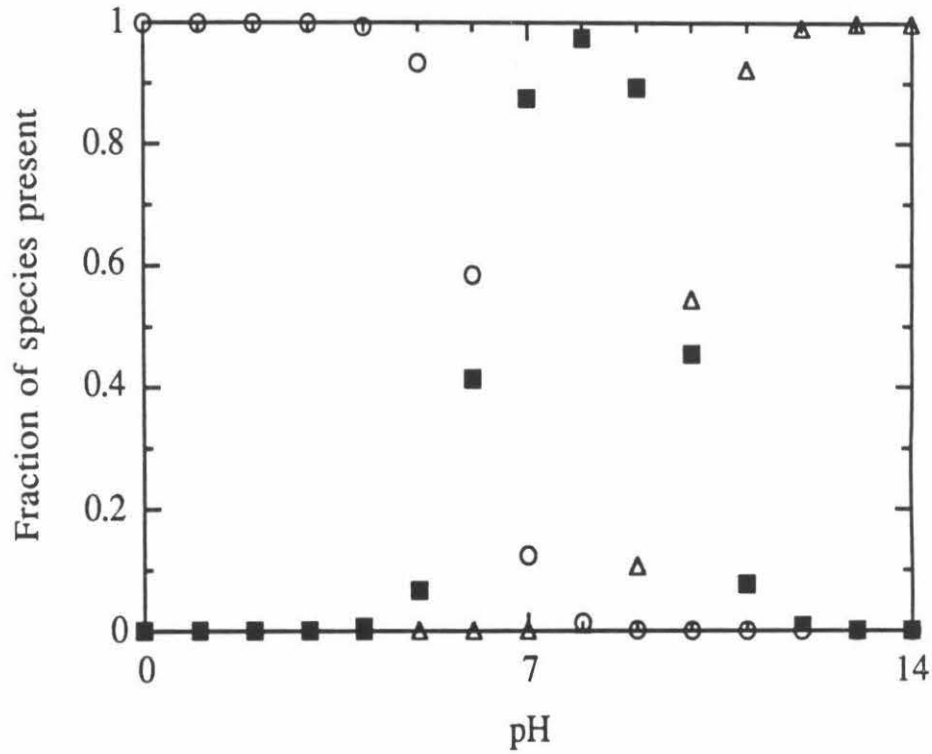

$$CO_2 + OH^- \longrightarrow HCO_3^- \qquad (9)$$

$$HCO_3^- + OH^- \longrightarrow CO_3^{2-} + H_2O \qquad (10)$$

Reaction (10) occurs instantaneously; the rate law for reaction (9) is given by Equation (11).

$$\frac{-d[CO_2]}{dt} = k_{OH^-}[OH^-][CO_2] \qquad k_{OH^-} = 8500\ M^{-1}\ sec^{-1} \qquad (11)$$

The reduction of CO_2 results in the production of OH^- ions at the electrode surface which in turn can react with the CO_2 molecules diffusing to the electrode. This neutralization of CO_2 results in the formation of HCO_3^- and/or CO_3^{2-}, both of which have been shown by previous studies[1] and by this work to be inactive towards catalytic reduction by $Ni(cyclam)^+_{ads}$. The important question is whether the OH^- ions diffusing away from the electrode surface have sufficient time to react with CO_2 in the diffusion layer extending outward from the electrode surface. In unbuffered solutions, the pH at the electrode surface can increase to almost 13 for saturated solutions of CO_2. If there is sufficient time for reaction (9) to occur, CO_2 will be neutralized. Given a rate constant of 8500 M^{-1} sec^{-1}, the question is whether the rate is fast enough so that OH^- ions have sufficient time to react with CO_2 as it crosses the diffusion layer. An exact calculation of this time for different experimental techniques and conditions is beyond the scope of this thesis, but conclusions can be drawn by comparing the peak currents for the reduction of CO_2 in buffered and unbuffered media. Figure 5.2 is a plot of the cyclic voltammetry peak current for the reduction of CO_2 in these two media as a function of the square root of the scan rate. Virtually no difference is seen at the faster potential scan rates between the two solutions, leading to the conclusion that OH^- ions do not have sufficient time while crossing the diffusion layer to react extensively with the CO_2 molecules diffusing to the electrode surface. At the slower scan rates, the peak currents for the unbuffered case are

Figure 5.2 Cyclic voltammetric current for the reduction of 10 mM CO_2 in 0.1 M $KClO_4$ (o) and in an acetate buffer at pH 4.5 (Δ) at a HMDE. Concentration of $Ni(cyclam)^{2+}$ is 0.2 mM.

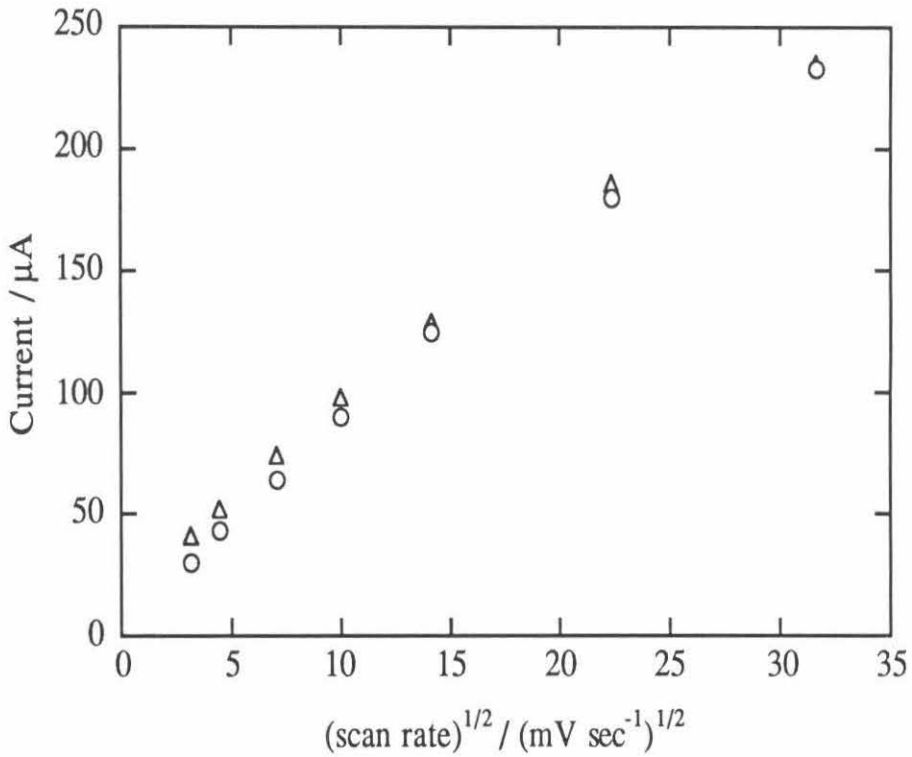

lower than those for the buffered case. This is not unexpected, as the diffusion layer requires longer times to cross at slower scan rates and the OH^- has sufficient time to reduce significantly the flux of CO_2 molecules arriving at the electrode. The lack of an expected linearity of these plots will be discussed later in Section 5.3.7.

The above experiment demonstrates that, on the CV time scale, reactions (9) and (10) cause a noticeable reduction of the catalytic CO_2 reduction current only at the slowest scan rates. As noted in chapter two, there is no effect of the solution pH on the quantity of the catalyst adsorbed and it is therefore impossible that the rate of CO_2 reduction is affected by a change in the quantity of catalyst adsorbed at higher pH's. In addition, the formation of the precipitate $Ni(cyclam)^0$-CO as noted in chapter three also showed no pH dependence. The diminishment of CO_2 reduction current at low scan rates is caused solely by the simple fact that fewer reducible CO_2 species arrive at the electrode surface.

Whether by accident or design, previous studies[1-5] have utilized buffered media (pH <8) and no mention was made of these effects. Fortunately, the annihilation of the reactant, CO_2, with one of the products of the reduction, OH^-, occurs much more slowly at a pH less than eight (Equations (5), (6) and (7)) and is therefore unable to cause any diminishment of the flux of CO_2 to the electrode surface. This conclusion is intuitive to which anyone who has ever tried to titrate CO_2 directly with OH^- using a visual indicator can attest .

The above analysis has considered only the situation around the electrode surface, specifically, within the diffusion layer. Since the effect of OH^- ions on CO_2 reduction is noticeable in cyclic voltammetry at slower scan rates, an interesting question is what happens in the bulk of the unbuffered solution? In other words, does the product of the electrochemical reduction of CO_2 eventually cause the reduction process to stop before all of the CO_2 is reduced to CO? If it is assumed that OH^- has sufficient time to react with CO_2 completely, then reaction (4) will proceed to an extent which can be calculated.

Because of the occurrence of reactions (9) and (10), the overall reaction for CO_2 reduction in the bulk of solution is given by Equation (12).

$$3CO_2 + 2e^- + H_2O \longrightarrow CO + 2HCO_3^- \qquad (12)$$

This reaction results in the production of only one CO molecule for every three CO_2 molecules present; the other two CO_2 molecules are rendered inactive towards reduction by their conversion to HCO_3^- and/or CO_3^{2-}. Reaction (12) is two-thirds of an electron per CO_2 overall, but still two-electron with regard to CO formation.

An experiment was conducted to test the above hypothesis. Performing a controlled potential electrolysis at -1.4 V in a tightly sealed cell, a known quantity of CO_2 in an unbuffered solution was reduced until the current had decreased to the background level. The amount of gas over the liquid was kept as small as possible to minimize the loss of CO_2 from solution; in addition, the electrolysis was allowed to proceed for a time sufficient to allow any CO_2 which escaped in the gas above the solution to diffuse back and be reduced. For this particular experiment, a value of (n) for the reduction of CO_2 was measured as 0.69, which is very close to the theoretical value of two-thirds expected based on Equation (12). In addition, the pH of the solution increased from the value expected given the initial concentration of CO_2 present to the value expected for a solution of HCO_3^- with a concentration two-thirds of the initial CO_2 concentration.

The overall result of the bulk reduction of CO_2 in unbuffered media is an increase in the pH until the point where all "CO_2" species are present as HCO_3^- or CO_3^{2-}, at which time the reduction stops, as these species are not catalytically reducible by $Ni(cyclam)^+_{ads}$ (Section 5.3.4). The pH at which this occurs is estimated from Figure 5.1 to be approximately 8, where the concentration of CO_2 is negligible.

5.3.3 Passivation of Catalytic Activity

The results of chapter three and of Section 5.3.2 above contain an unusual facet. One of the products of the electrocatalytic reduction of CO_2, CO, renders the catalytic surface inactive; the other product, OH^- ions, renders the substrate inactive. As demonstrated in chapter three, the reduction of $Ni(cyclam)^{2+}$ under CO results in the formation of an insoluble $Ni(cyclam)^0$-CO species. This $Ni(cyclam)^0$-CO species precipitates on the electrode surface and renders it inactive towards catalytic CO_2 reduction. In addition, the potential for the reduction of $Ni(cyclam)^{2+}$ under CO to $Ni(cyclam)^0$-CO is approximately equal to that of the catalytic reduction of CO_2. These two facts taken together result in a steady decrease in the catalytic reduction current for CO_2 with time, even under conditions when the flux of CO_2 to the electrode surface is constant. And, as illustrated in Section 5.3.2 above, if the time required for CO_2 to cross the diffusion layer extending outward from the electrode surface is long enough, OH^- can convert the active substrate, CO_2, into an inactive one, HCO_3^- or CO_3^{2-}. An intriguing question at this time is whether it is the accumulation of OH^- ions around the electrode and not the formation of a precipitate on the electrode surface that causes the drop in the CO_2 catalytic current with time (Figure 3.10).

To address this question, an experiment was done in buffered media whereby a rotating disc electrode was scanned to increasingly negative potentials in the presence of $Ni(cyclam)^{2+}$ and CO_2. An acetate buffer at pH 4.5 was chosen for the low background current, as well as the fact that at this pH, all of the carbon dioxide is present as discrete CO_2 molecules. An analogous experiment done in the absence of a buffer (Figure 3.10) exhibited an unexpected, dramatic decrease in the CO_2 reduction current with time. In the buffered solution, the current at the RDE decreased with time, but at a much slower rate. Also, the current did not decrease to zero as it did in the unbuffered case.

Another experiment done with a stationary mercury electrode in a solution buffered at pH 4.5 was done to determine if the passivation of the electrode surface by the precipitate could be reversed and the catalytic activity restored. In unbuffered solutions, it was found that reactivation of a previously passivated electrode surface could occur if the electrode was poised at potentials of -1.0 V (or positive of this) for long periods of time (Figure 3.11). In the buffered solution, minimal potential pauses (less than 10 seconds) were necessary before the start of the second scan in order to reactivate the catalytic behavior completely. There are several reasons that can explain the results of the rotating and stationary electrode voltammetry discussed above.

One possibility is that the passivating agent, the precipitate Ni(cyclam)^0-CO, does not form at pH 4.5, or is immediately oxidized by protons (which are in much greater concentration in the buffered solution versus the unbuffered). To examine this possibility, a controlled potential electrolysis of Ni(cyclam)$^{2+}$ under CO was done at a mercury pool electrode to check for the formation of the precipitate Ni(cyclam)^0-CO. In buffered solutions, the precipitate formed on the mercury pool, but at a much slower rate than was observed in an unbuffered solution. Under an atmosphere of CO_2, no precipitate was observed, even after electrolysis for one hour. At this point, it is not known why no precipitate formed under an atmosphere of CO_2. Presumably, its rate of formation under CO_2 at pH 4.5 is not sufficiently greater than its rate of decomposition to provide visual evidence of the precipitate. Another possibility to explain the voltammetry in buffered solutions is that the passivation of the electrode surface and consequent decrease in catalytic current for CO_2 reduction is due entirely to the reduction in the flux of CO_2 to the electrode surface as shown in Equations (9) and (10).

Since the cyclic voltammetry of CO_2 reduction shows almost no difference in buffered versus unbuffered solutions as seen in the previous section, the latter possibility is not likely to be the cause of the reduced electrode passivation in buffered solutions. This

factor, coupled with the much slower appearance of Ni(cyclam)^0-CO in buffered solutions, points to the conclusion that almost all of the passivation of the electrode surface is due to the precipitation of Ni(cyclam)^0-CO. In buffered solutions, where the formation of this species occurs more slowly, the passivation effect is less noticeable and less complete. Indeed, the slower rate of formation may be overshadowed by the oxidation of Ni(cyclam)^0-CO to Ni(cyclam)$^+$ (Section 3.3.1) resulting in the partial adsorption of the catalyst, $Ni(cyclam)^+_{ads}$.

5.3.4 Binding of CO_2 to Ni(cyclam)$^{2+}$ and Ni(cyclam)$^+$

When considering the mechanism for the catalytic reduction of CO_2, the coordination of the substrate to the catalyst must be considered. Since the adsorbed catalyst has been well characterized in chapter two, a discussion of the binding of CO_2 to the catalyst is now appropriate. In previous studies on the electrochemical reduction of CO_2 with Ni(cyclam)$^{2+}$ as a catalyst, it was only briefly mentioned that the coordination of CO_2 to Ni(cyclam)$^+$ is favored if the latter species is adsorbed on the electrode surface. No additional detail was given, other than a brief mentioning of the possibility of hydrogen bonding between the hydrogen on the amine of the cyclam and the nucleophilic oxygen of the CO_2.

Although CO_2 is a relatively weak ligand, several studies have investigated the binding of CO_2 to transition metal complexes.[12-18] In addition, organometallic reactions involving CO_2 have been well documented.[19-22] CO_2 can coordinate in one of three ways: (1) Lewis acid site of carbon (C coordination), (2) Lewis base site of oxygen (end-on coordination), and (3) η^2 coordination to the C=O bond (side-on coordination). Most studies of the binding of CO_2 to transition metal complexes have indicated that the coordination is by mode (1), i.e., to the carbon, with the electrophilic carbon favoring

highly basic metal centers. Coordination mode (2) typically occurs only for metal centers of higher oxidation states.

In this work as well as others, very little evidence was obtained to support the existence of CO_2 coordination to Ni(cyclam)$^{2+}$. The absorption spectrum of Ni(cyclam)$^{2+}$ does not change in the presence of CO_2, while CO_2 has been shown to result in large absorption changes for similar macrocycles of cobalt and nickel.[12,13,18] In another study,[14] CO_2 was shown to have a high affinity for Co(I) tetraazamacrocycles and a relatively low affinity for either the Ni(II) or Ni(I) analogs. In a more comprehensive work by Lewis and co-workers,[15] binding constants for a series of macrocycles of Co(I) and Ni(I) were studied by measuring the shift in the reduction potential of the metal center as a function of the concentration of CO_2. Factors such as redox potential, ligand structure and solvent were correlated to the binding constants. In all of these studies, the electronic environment around the metal played a key role in the affinity of the complex for CO_2. The ligand structure and degree of unsaturation increased the basicity of the metal center, thus making the reduction potential more negative. Since CO_2 typically coordinated through the electrophilic carbon atom, electron rich centers are desirable for strong coordination. It is not surprising that Ni(cyclam)$^{2+}$, with a fully saturated ligand and lacking a highly basic metal center, would have a low affinity for CO_2.

In a detailed theoretical study of the binding of CO_2 to nickel tetraamine complexes,[23] the calculated binding energies for CO_2 to the Ni(II) center were extremely negative and it was concluded that Ni(II) tetraamine complexes do not coordinate CO_2 to any significant extent. Additional evidence for the lack of coordination of CO_2 to Ni(cyclam)$^{2+}$ can be inferred by considering the electrochemistry of Ni(TMC)$^{2+}$ as discussed in chapter two. When the electrochemistry of this species in the presence and absence of CO_2 was compared, the presence of CO_2 was found to have no effect on the Ni(TMC)$^{2+/+}$ redox potential. Although the steric hindrance to the metal center of

$Ni(TMC)^{2+}$ is greater than that of $Ni(cyclam)^{2+}$, no difference was noted between the *trans* I and *trans* III isomers of $Ni(TMC)^{2+}$ or between these species and $Ni(MMC)^{2+}$. If steric hindrance were the only factor preventing the binding of CO_2 to $Ni(TMC)^{2+}$, one would expect to see differences between these ligands.

In the theoretical studies by Sakaki,[23] it was demonstrated that CO_2 can coordinate to a Ni(I) tetraamine, but only if an anionic ligand is coordinated trans to the CO_2. For these calculations, F^- was used as this anionic ligand. Although F^- is perhaps not the best choice to represent the mercury metal surface such as would be present with $Ni(cyclam)^{+}_{ads}$, it was suggested that the presence of a negatively charged electrode surface would also enable CO_2 to coordinate to the Ni(I) tetraamine. From calculations of the orbital energies of the hypothetical complexes, the most favorable coordination of CO_2 to the metal center was determined to be through the carbon atom (mode (1)), and that this bond was as strong as the usual coordinate bond. The explanation for this mode of coordination can be found by a consideration of the molecular orbitals for CO_2 and $Ni(I)(NH_3)_4F$ (the model compound). The molecular orbital diagrams for $Ni(II)(NH_3)_4$ and $Ni(I)(NH_3)_4F$ is shown in Figure 5.3. A mixing of the calculated orbitals for CO_2 and for $Ni(I)(NH_3)_4F$ is shown in Figure 5.4. The HOMO of the Ni(I) center is a singly occupied d_{xy} orbital; however, this orbital is important only for NH_3 coordination. The fully occupied d_z2 orbital extends toward the CO_2, favoring σ interaction with the π^* orbitals of CO_2. Coordination of an anion axial to the bound CO_2 has two effects. One, it neutralizes the positive charge of Ni(I) to reduce charge dipole interaction, and two, it increases the charge transfer from Ni(I) to CO_2 by raising the energy of the Ni(I) d_z2 orbital. Some backbonding from the Ni(I) metal center to the π^* orbital of CO_2 was calculated to exist, but this type of bonding was weaker than the Ni(I)-C σ bond.

The proposal by Sauvage[1] that hydrogen bonding stabilizes the coordination of CO_2 to the Ni(I) center is also verified in this theoretical work.[23] In addition, protonation

Figure 5.3 Molecular orbital diagram of $Ni(II)(NH_3)_6$, $Ni(II)(NH_3)_4F$, $Ni(I)(NH_3)_4F$ (from reference 23).

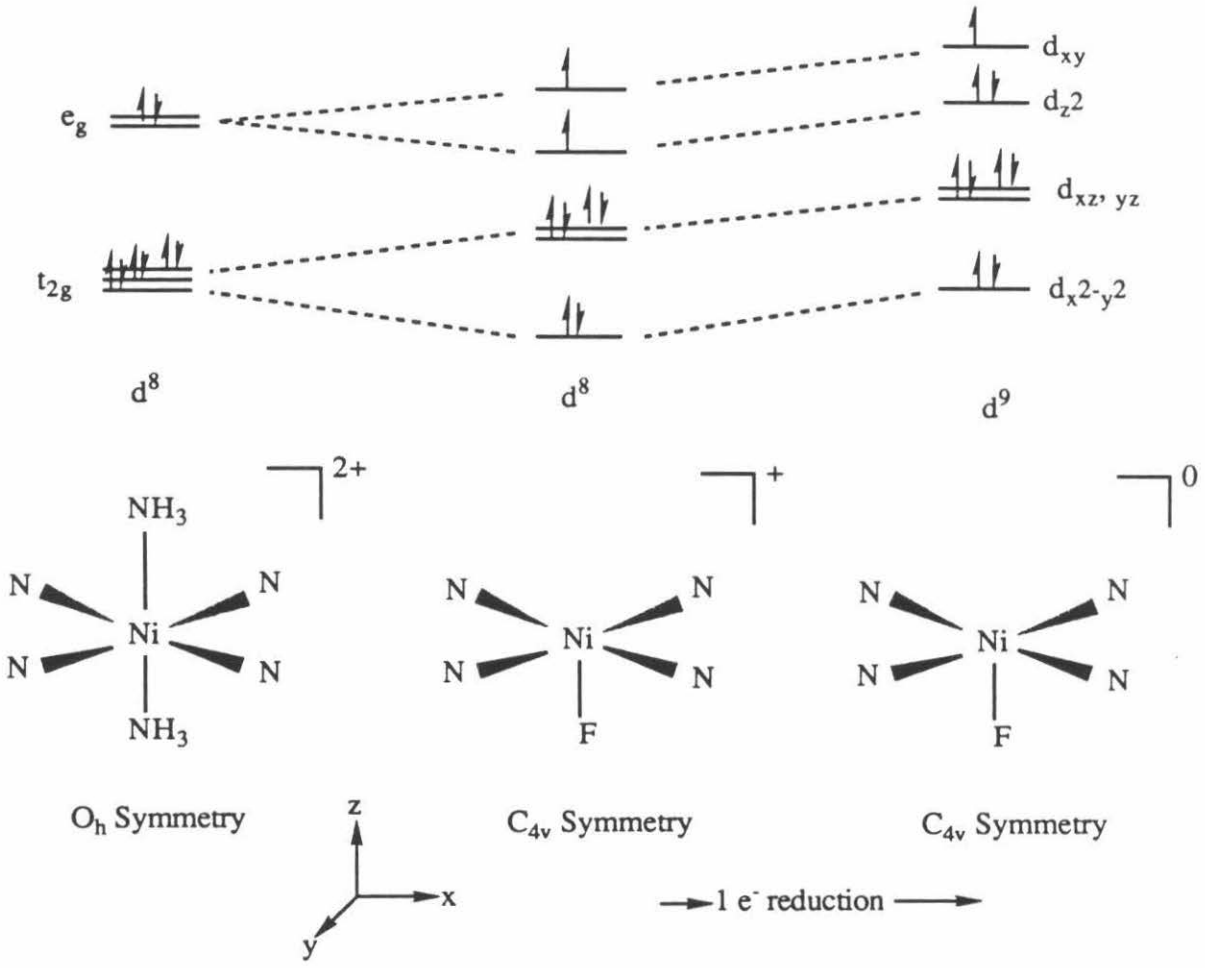

Figure 5.4 Molecular orbital mixing of $Ni(I)(NH_3)_4F$ and CO_2 (from reference 23).

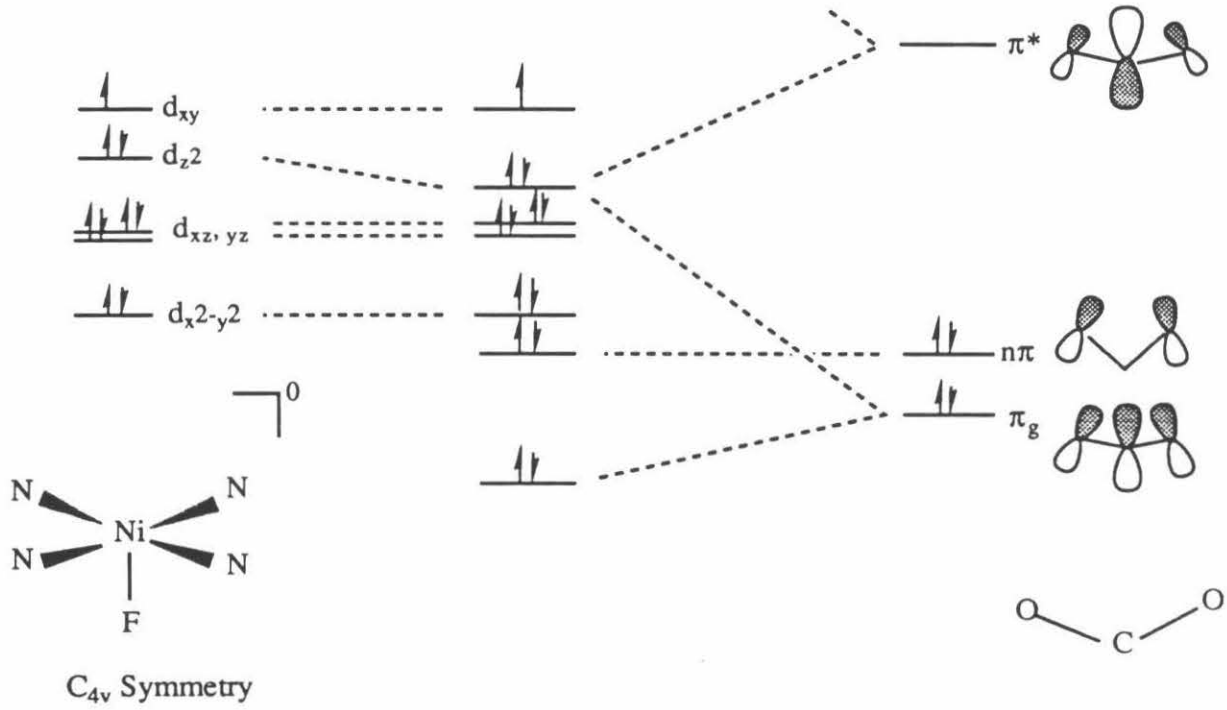

of the CO_2 coordinated species occurs at the terminal oxygen of the CO_2 and further stabilizes the structure. Again, the presence of the tetraamine ligand and of the anionic ligand axial to CO_2 increases the charge transfer from Ni(I) to the proton further. As a result of the protonation of the complex, the C=O bond is weakened and OH^- is able to dissociate, a conclusion which agrees with the proposed mechanism (Figure 5.5).

The research of Sauvage and co-workers[1] demonstrated that HCO_3^- and CO_3^{2-} are inactive towards reduction using $Ni(cyclam)^+_{ads}$ as a catalyst, a result which was verified in this work. Catalytic CO_2 reduction current is observed only when the pH of the solution is sufficiently low such that most carbon dioxide is present as aqueous CO_2. If the solution is buffered to pH values of between 5 and 7, a CO_2 reduction current is seen which corresponds to the concentration of aqueous CO_2 (Figure 5.1). At pH values greater than 7, no CO_2 reduction current is observed. Since coordination of CO_2 is through the carbon atom, the absence of catalytic reduction of HCO_3^- or CO_3^{2-} is most likely due to sterics. That is, the structure of HCO_3^- and CO_3^{2-} are such that the orbital overlap between the carbon and the Ni(I) metal center is insufficient for a stable coordination to occur. An alternative explanation is that the uniqueness of CO_2 coordination to $Ni(cyclam)^+_{ads}$ is due to solvation effects. Aqueous CO_2 exists as distinct CO_2 molecules, whereas HCO_3^- and CO_3^{2-} are solvated to a much greater extent. It is possible that this extra degree of solvation is sufficient to prevent the binding of these species to $Ni(cyclam)^+_{ads}$.

5.3.5 Binding of CO to $Ni(cyclam)^{2+}$ and $Ni(cyclam)^+$

So far, only the binding of CO_2 to the catalyst $Ni(cyclam)^+_{ads}$ has been discussed. In order to complete the catalytic cycle, a consideration of the extent of binding of CO to the catalyst is also necessary.

Figure 5.5 Postulated mechanistic cycle for the aqueous electrocatalytic reduction of CO_2 to CO by $Ni(cyclam)^{2+}$ (from reference 1).

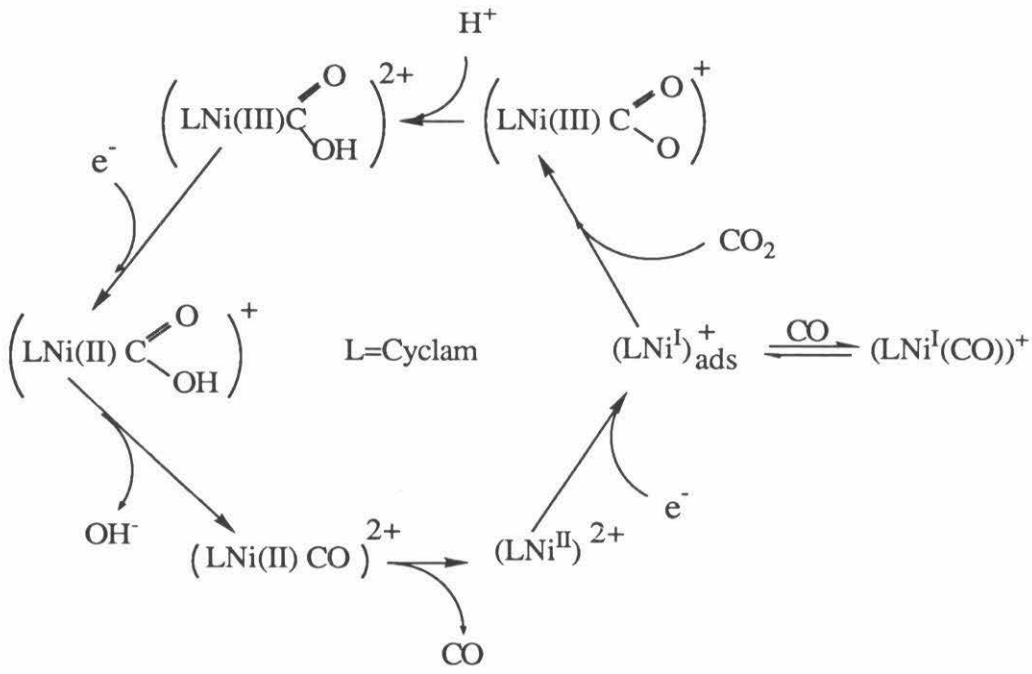

CO is a ubiquitous ligand and its coordination to transition metal macrocycles has been studied in much depth.[23-26] Gagné and Ingle[25] found that CO reacted with a Ni(II) radical or Ni(I) to produce a five coordinate carbonyl species. Fujita *et al.*[26] investigated the binding of CO to a variety of macrocyclic Ni(I) complexes. In all of the studies, it was found that the Ni(I) center was pushed out of the plane of the nitrogens of the ligand, resulting in a distortion of the ligand geometry. It was proposed that the more flexible ligands, such as those with unsaturation, could better adjust to the core size change. The basicity of the ligand was found to have a smaller effect on the stability of the NiL^{+}-CO complex. In the present study, no evidence was found for the coordination of CO to $Ni(cyclam)^{2+}$ or $Ni(TMC)^{2+}$; however, CO does coordinate to $Ni(TMC)^{+}$, as seen in Section 3.3.2. Since the Ni(I) center lies outside of the plane of the ligand, no significant ligand rearrangement is necessary and CO can coordinate in the manner shown by the ligands above.

In the theoretical work by Sakaki,[23] the binding of CO to a Ni(II) tetraamine was reaffirmed. The Ni - CO distance was rather long (2.4 Å) and the binding energy small. This weak CO coordination occurs as a result of weak backbonding from a Ni(II) d_{π} orbital to the empty CO π^* orbitals. In the mechanism proposed by Sauvage (Figure 5.5), the CO rapidly dissociates from the Ni(II) adduct formed after the reduction of the Ni(III) carboxylate species. The choice of a Ni(II) tetraamine for theoretical calculations of the extent of CO binding would seem logical and thus only the binding of a Ni(II) metal center to CO was considered.

In chapter three of this thesis, the reduction of $Ni(cyclam)^{2+}$ in the presence of CO has been shown to result in the formation of $Ni(cyclam)^{+}$-CO and $Ni(cyclam)^{0}$-CO. Although no binding studies were done, the coordination of CO is fairly strong as evidenced by the shift in the reduction potentials. A controlled potential electrolysis of

$Ni(cyclam)^{2+}$ under CO resulted in the change of the solution color from light yellow ($Ni(cyclam)^{2+}$) to lime green ($Ni(cyclam)^{+}$-CO) and the formation of an insoluble ($Ni(cyclam)^{0}$-CO) species. Under CO_2, these results were also noted except that the rate of formation of these carbonyl species was slower. The greenish colored solution was also noted by Sauvage,[1] and was also attributed to the formation of Ni(I) carbonyl species.

The above discussion addresses only the solution $Ni(cyclam)^{+}$-CO species but the catalyst for the electrochemical reduction of CO_2 is $Ni(cyclam)^{+}$ adsorbed on the electrode surface. No direct experimental work has been done on the coordination of CO to $Ni(cyclam)^{+}_{ads}$, but the chronocoulometric assays for $Ni(cyclam)^{+}_{ads}$ detailed in chapter three provide insight. These data indicate that the presence of CO has no effect on the quantity of $Ni(cyclam)^{+}$ adsorbed on the mercury electrode at potentials as negative as -1.3 V. In addition, CO has no effect on the prepeak seen at -1.3 V, and thus the presence of CO has no effect on the rearrangement of the adsorbed complex at the potential of the prepeak.

The most conclusive evidence that CO does not bind to $Ni(cyclam)^{+}_{ads}$ to any appreciable extent can be found in the results of the cyclic voltammograms shown in Figure 5.6. In this experiment, cyclic voltammograms of $Ni(cyclam)^{2+}$ were taken in two CO_2 saturated solutions, identical except that one solution was also saturated with CO. If CO were affecting the adsorption of $Ni(cyclam)^{+}$ in any way, differences between these two cyclic voltammograms should be evident. As can be seen in Figure 5.6, only a modest difference is noted, a result which indicates that CO does not significantly affect the coordination of CO_2 to $Ni(cyclam)^{+}_{ads}$. The same result was obtained with normal pulse polarography. If CO_2 coordinates much more strongly to $Ni(cyclam)^{+}_{ads}$ than CO does, the same results would also be possible; however, this is unlikely, due to the fact that CO is a much better ligand, especially to lower valency metal centers. The much better π acceptor capability of CO, and thus the increased backbonding from the metal center to CO, would

Figure 5.6 Cyclic voltammogram of the catalytic reduction of CO_2 at a HMDE in 0.1 M $KClO_4$. Concentration of CO_2 is 1.0 mM; concentration of $Ni(cyclam)^{2+}$ is 1.0 mM. Scan rate is 200 mV sec^{-1}. Solid line is solution initially saturated with argon, dashed line is solution initially saturated with CO.

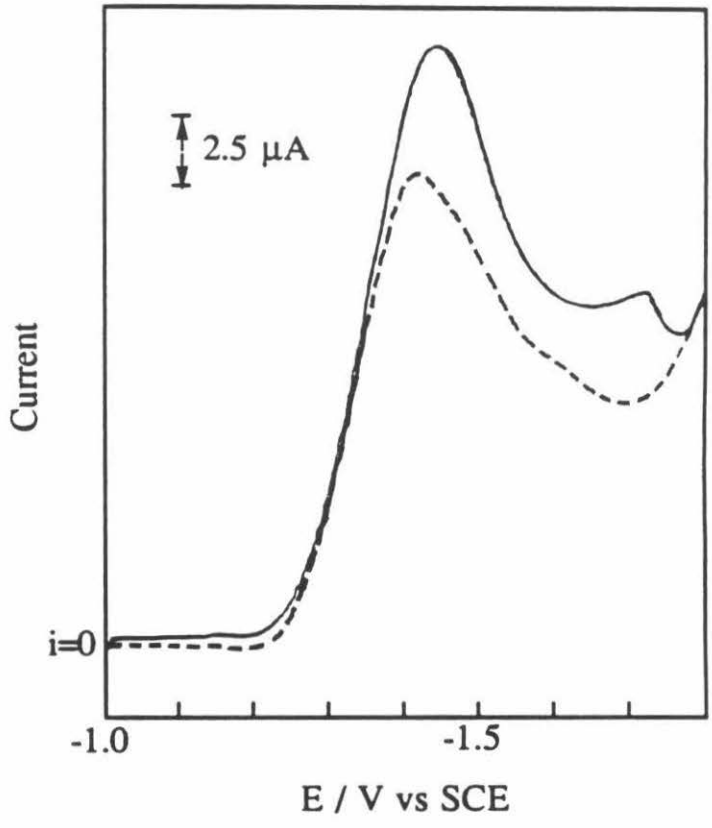

create a much stronger bond than that which is involved in CO_2 coordination. Evidently, the factors which enable CO_2 to coordinate strongly to $Ni(cyclam)^+_{ads}$ prevent the coordination of CO. In effect, adsorbed and solution $Ni(cyclam)^+$ are opposites in this regard. $Ni(cyclam)^+_{ads}$ coordinates CO_2 but not CO, and $Ni(cyclam)^+_{soln}$ coordinates CO but not CO_2.

5.3.6 Mechanism of the Electrocatalytic Reduction of CO_2

The mechanism proposed by Sauvage[1] for the electrochemical reduction of CO_2 as catalyzed by $Ni(cyclam)^+_{ads}$ (Figure 5.5) is not totally incompatible with the results presented in that research and with the evidence discussed in this thesis. Similar mechanisms have been proposed for the photochemical reduction[27] of CO_2 to CO as catalyzed by $Ni(cyclam)^+$ and for the electrochemical reduction[28] of CO_2 as catalyzed by Pd phosphine complexes. The theoretical calculations by Sakaki[23] suggest that all of the species in Figure 5.5 are theoretically possible from a molecular orbital energy analysis. However, several of the mechanistic steps require further clarification or modification. An analysis of each step is presented below, starting with the $Ni(cyclam)^{2+}$ species in solution.

As demonstrated in chapter two of this work, $Ni(cyclam)^{2+}$ is reductively adsorbed to $Ni(cyclam)^+$ over a potential range from -0.6 to 1.6 V. This adsorption process occurs in two stages; the first step requires a rearrangement of the complex before adsorption can occur. At the potential of the prepeak seen in the cyclic voltammetry, a ligand rearrangement occurs which allows the further adsorption of up to a full monolayer of $Ni(cyclam)^+$ on the electrode surface. In the proposed catalytic cycle (Figure 5.5), the presence of CO leads to the formation of unadsorbable $Ni(cyclam)^+$-CO. However, the chronocoulometric assays for $Ni(cyclam)^+_{ads}$ in the presence of CO demonstrate unequivocally that $Ni(cyclam)^+$ is not desorbed at potentials positive of the prepeak seen in cyclic voltammetry. The electrocapillary data of Fujihira[4] would seem to indicate the

desorption of Ni(cyclam)$^+$ under CO at potentials negative of -1.7 V. Although the research described in this thesis cannot directly refute this assertion, it is not believed that the desorption of the catalyst as caused by the formation of unadsorbable Ni(cyclam)$^+$-CO has an effect on the catalytic reduction of CO_2 at potentials where this reaction proceeds at a significant rate. In fact, at lower concentrations of CO_2 (<1 mM), the rate of CO_2 reduction is diffusion controlled (Section 3.3.3), indicating that the catalyst is fully active at potentials as negative as -1.5 V.

The adsorbed Ni(cyclam)$^+$ binds CO_2 in an oxidative addition step to produce a Ni(III)cyclam$^+$-CO_2 adduct. As shown by Sakaki,[23] this is a viable species and the presence of an anionic ligand (or negatively charged electrode) axial to the CO_2 further strengthens the CO_2 bond. The formation of a Ni(cyclam)-CO_2 adduct is reasonable but the existence of Ni in a +3 oxidation state at the very negative potentials where catalytic CO_2 reduction can occur is unlikely. Ni(III)cyclams are known[29] and the redox potential for the Ni(cyclam)$^{3+/2+}$ couple has been established as +0.67 V. In the mechanism[27] for the photochemical reduction of CO_2, a Ni(III)cyclam hydride formation step is included, leading to the formation of hydrogen. In contrast, for the electrochemical reduction of CO_2, no hydrogen was detected. It is therefore unlikely that a Ni(III) hydride is present since this latter species is a typical precursor for the formation of hydrogen.

Although the formal oxidation state of the nickel center is subject to interpretation, it is more reasonable to think of the catalyst-CO_2 adduct as existing with nickel in the +1 oxidation state. As shown by Sakaki[23], the model compounds used for the theoretical studies demonstrate that the species Ni(I)cyclam-CO_2 is stable. Also demonstrated was the fact that protonation of this species occurs readily and thus the formation of a carboxylate is the next logical step in the mechanism. The weakening and subsequent breaking of the C-O bond releases OH^-, leaving Ni(II)cyclam-CO on the surface. No evidence has been presented in this thesis or in previous studies for the existence of a Ni(II)cyclam-CO

species (adsorbed or not). CO is released and since Ni(II)cyclam is not stable on the electrode surface at these potentials, it is immediately reduced to $Ni(cyclam)^{+}_{ads}$, completing the catalytic cycle. Ni(I)cyclam-CO species are not present in the cycle since they are sufficiently stable in water to be observable on the time scale of cyclic voltammetry and to provide visual evidence (change in solution color).

It has been shown that, with slight modifications, the mechanistic scheme as described by Sauvage[1] is compatible with the available data on this system. An overall scheme incorporating these changes and adding the new research covered in this thesis is shown in Figure 5.7.

Several other issues require further clarification at this point. Both Sauvage and Fujihira attempted to correlate the dependence of the observed CO_2 reduction current on the concentration of $Ni(cyclam)^{2+}$ in solution. No firm correlation could be made between the two variables, other than to say that there is a "weak" or an "isotherm-like" dependence of the catalytic current on the solution of $Ni(cyclam)^{2+}$. Since the active catalyst is adsorbed $Ni(cyclam)^{+}$, a more useful comparison would be between the peak CO_2 reduction current and the activity of $Ni(cyclam)^{+}_{ads}$. A determination of the activity of the surface catalyst is beyond the scope of this thesis; the surface coverage of $Ni(cyclam)^{+}_{ads}$ is used instead. Such a comparison is shown in Figure 5.8. The general trend of increased CO_2 reduction current at higher catalyst concentrations is expected, but no exact correlation is obtained, indicating that the surface coverage as measured in the absence of the substrate is not a true indicator of catalyst activity. There are several possible reasons for this assessment. The formation of the precipitate $Ni(cyclam)^{0}$-CO on the electrode could reduce the activity of $Ni(cyclam)^{+}_{ads}$, either by physically blocking the electrode, or by shifting the equilibrium between $Ni(cyclam)^{2+}$ and $Ni(cyclam)^{+}_{ads}$. Alternatively, under certain conditions such as a high rate of CO_2 reduction, the formation of hydroxide ion might be able to

Figure 5.7 Modified mechanistic cycle for the aqueous electrocatalytic reduction of CO_2 to CO as catalyzed by $Ni(cyclam)^{2+}$.

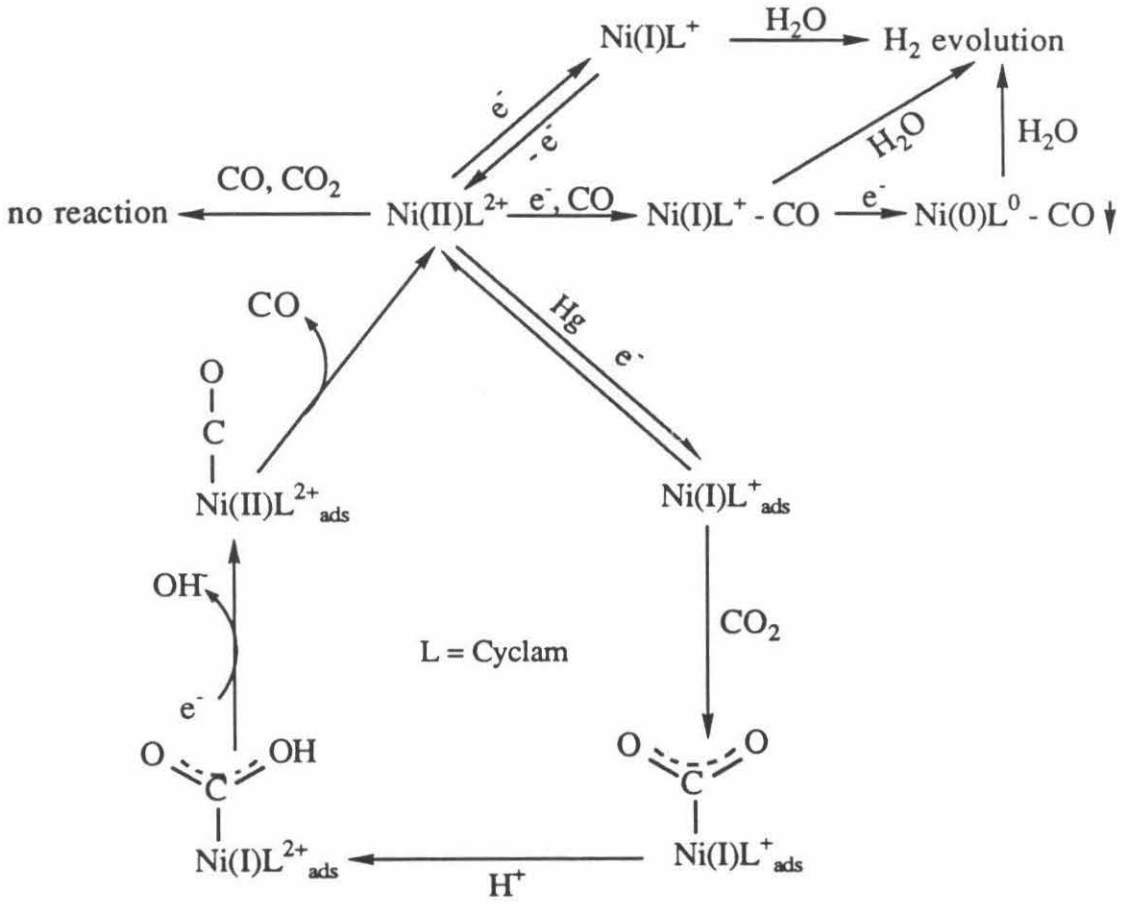

Figure 5.8 Plot of peak CO_2 catalytic reduction current versus quantity of catalyst present on the electrode surface for solution concentrations of $Ni(cyclam)^{2+}$ from 1 μM to 2 mM. CO_2 reduction currents are from cyclic voltammetry of CO_2 saturated solutions; scan rate is 100 mV sec^{-1}. Quantity of adsorbed catalyst determined from chronocoulometry (Chapter 2).

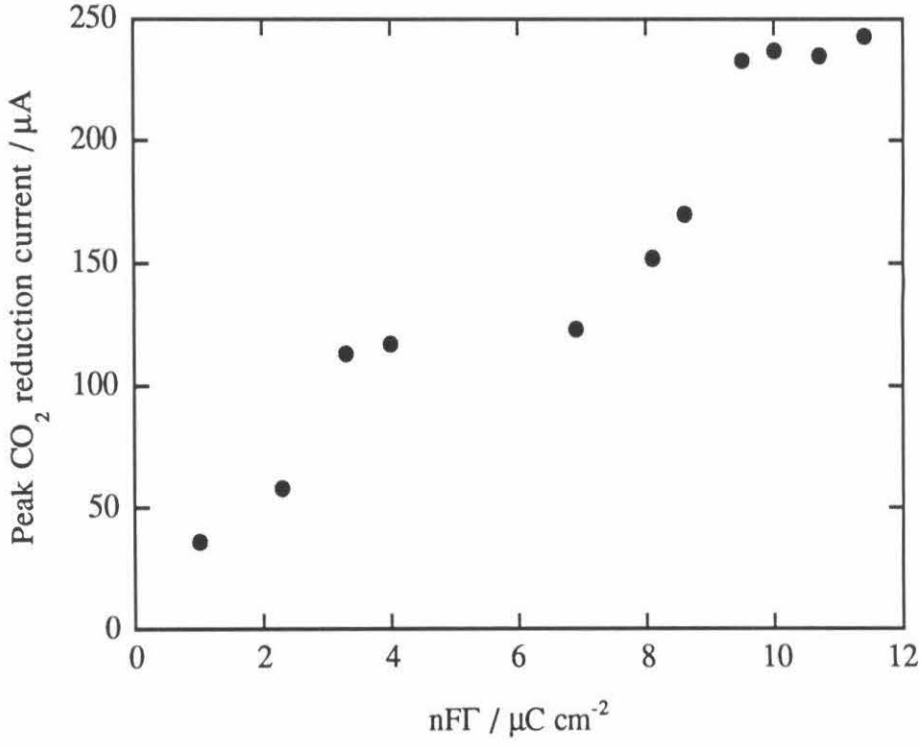

sufficiently decrease the CO_2 reduction rate so that any correlation such as that expected for Figure 5.8 would not be obtained.

Another question involves the correlation between the potential of the prepeak and the onset of CO_2 reduction as seen in cyclic voltammetry. Both Sauvage[1] and Fujihira[4] asserted that the adsorption process symbolized by the prepeak produced the active catalyst, $Ni(cyclam)^{+}_{ads}$. It was not mentioned why CO_2 reduction (albeit slow) was observable at potentials positive of this prepeak. As demonstrated in chapter two of this thesis, the prepeak represents the double layer charging adjustment accompanying a surface rearrangement of an already adsorbed $Ni(cyclam)^{+}$ species. But if the catalyst is present at potentials positive of the prepeak, why doesn't catalytic reduction of CO_2 occur at these potentials? One possibility is that the rearrangement of the $Ni(cyclam)^{+}_{ads}$ species which occurs at -1.3 V is necessary in order for it to be catalytically active, either for steric or electronic reasons. However, this explanation cannot explain why some catalytic activity is observed at potentials positive of the prepeak. Another possibility is that the potential at which the $Ni(cyclam)^{+}_{ads}$-CO_2 adduct is reduced is coincidentally the same potential as that of the prepeak. The latter is the most likely reason; additional evidence for this claim can be obtained by considering the catalytic CO_2 reduction ability for other Ni(II)cyclam derivatives. For all of the derivatives of cyclam considered in this work, the potential at which CO_2 reduction occurs is approximately the same as illustrated in Table 5.1. Even though many of these compounds exhibit adsorption of NiL^{+} on the electrode surface at potentials quite positive of the CO_2 reduction peak, the reduction of CO_2 occurs at approximately -1.45 V.

Research investigating the catalytic activity of Ni(cyclam)+ towards N_2O[30] and NO_3^-[31] showed that the reduction of these substrates occurred at potentials different from that observed for CO_2 reduction. In one case,[30] the catalysis occurred at potentials positive

of the prepeak, in the other,[31] the catalysis occurred negative of the prepeak. These results are further evidence that CO_2 reduction is dependent on the electrode potential and not on the existence of a particular form of $Ni(cyclam)^{+}_{ads}$.

5.3.7 Kinetics of the Electrocatalytic Reduction of CO_2

Although it was desirable to perform a detailed kinetic study of this system and extract useful kinetic parameters, most efforts towards this goal were stymied. The appearance of a $Ni(cyclam)^{0}$-CO precipitate under all conditions where CO_2 was catalytically reduced prevented the measurement of accurate currents, either with rotating or stationary electrodes. Another problem encountered was the formation of CO gas bubbles at the electrode surface when the reduction was attempted with CO_2 concentrations greater than approximately 1 mM (the solubility of CO in water is only 1 mM and CO_2 is 40 mM). As mentioned in Section 5.3.2, OH^- ion production at the surface of the electrode may interfere with the flux of reactant under certain conditions.

It was noted in the cyclic voltammetry of the reduction that the peak currents for the catalytic reduction of CO_2 did not increase linearly with the potential scan rate. Under normal conditions, this result would be expected if the overall kinetics of the reaction were limiting the rates. However, the deviation of the scan rate was found to become progressively worse as the concentrations of CO_2 or of $Ni(cyclam)^{2+}$ were increased. It would be expected that an increase in the amount of the catalyst would increase the rate of reaction but the opposite was found to be true. The kinetics of the reaction appear to be intertwined with the effects noted above.

In an attempt to salvage the kinetic investigations, all further experiments were done under conditions which would reduce these effects. Solutions buffered at pH 4.5 to 5 were used to eliminate any possible reduction in CO_2 flux due to OH^- ions. The concentration of $Ni(cyclam)^{2+}$ was less than 1 mM so that the formation of $Ni(cyclam)^{0}$-CO on the electrode

surface was minimized. It was also desired to keep the concentration of the substrate CO_2 as low as possible but the electrocatalytic activity of $Ni(cyclam)^{+}_{ads}$ towards proton reduction generally made this difficult. A rotating disc electrode was employed as this method is the most convenient for obtaining kinetic information. The results of this experiment are shown in Figure 5.9. In all cases, the experimental current matched that which was calculated from the Levich equation.[32] This result implies that, at these rotation rates, the kinetics of the reduction are sufficiently fast so that mass transport of the substrate to the electrode is limiting the rate, not the binding of CO_2 to the catalyst or the rate of subsequent steps. Normally, the electrode rotational rate would be increased until a deviation from the "Levich line" was obtained. For this system, all attempts at increased rotational speeds resulted in a wave which was not resolvable from the background current response and it was difficult to accurately measure the CO_2 reduction current. This was probably due to the electrode itself, as it was noted that the mercury on the electrode disc was no longer uniformly coating the surface.

Despite these limitations, some conclusions can be drawn. From the results above, it is apparent that the catalytic reduction of CO_2 proceeds at diffusion controlled rates under conditions where the previously mentioned difficulties do not occur. The results of Sauvage *et al.*[1] indicate that the turnover frequency for the catalyst is quite high, approximately 1000 h^{-1} and that the catalytic activity remains even after 8000 turnovers. Also, the results of Fujihira *et al.*[4] showed that the rate constant, k_{cat}, was potential dependent. The initial rate of reduction increased with increasingly negative potentials; the mechanism shown in Figure 5.7 is consistent with this observation. This result implies that it is the electron transfer step which is limiting the rate of the reduction.

Figure 5.9 Plot of the experimental (o) and calculated (Δ) peak currents in the voltammogram for the reduction of CO_2 at a rotating disc electrode. Solution is acetate buffer; [Ni(cyclam)$^{2+}$] is 0.5 mM, [CO_2] is 1 mM.

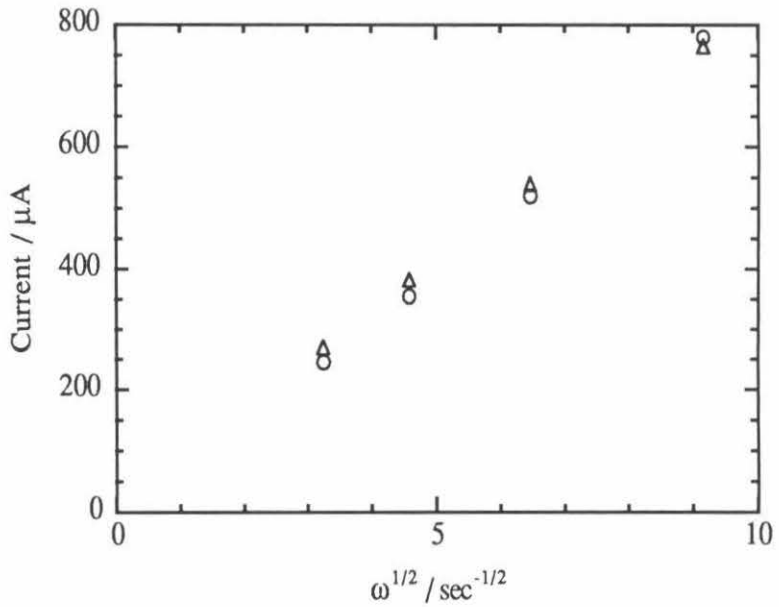

5.3.8 Selectivity and Efficiency of the Catalyst, Ni(cyclam)$^{2+}$

In this study and others,[1-5] Ni(cyclam)$^{+}$ has been shown to be a selective and efficient catalyst for the electrochemical reduction of CO_2. Ni(cyclam)$^{+}$ also catalyzes the reduction of water or protons, as evidenced by the positive shift of their reduction potentials. In the presence of CO_2, these reactions are effectively suppressed, a result which demonstrates that the selectivity of the catalyst towards CO_2 reduction is excellent. The catalyst is quite efficient as well; the results of this study demonstrate that the reduction of CO_2 proceeds at a diffusion-controlled rate under conditions where there are no extraneous factors.

Since the studies of Fischer and Eisenberg,[33] a number of studies on the electrocatalytic reduction of CO_2 using transition metal complexes have appeared and are referenced in chapter one of this thesis. Of all of the complexes, Ni(cyclam)$^{2+}$ appears to be the most selective in terms of production of CO over the competing hydrogen evolution reaction. The uniqueness of Ni(cyclam)$^{2+}$ is due in part to its stability and steric configuration. Ni(cyclam)$^{+}$ is exceptionally stable, even in strongly acidic media;[34] this stability is due to the macrocyclic effect[35] and to the precise fit of the nickel metal center in the fourteen membered cyclam ring.[36] Fujihira *et al.*[4] suggested that Ni(cyclam)$^{2+}$ may demetalate when reduced, especially under CO. However, chapter three demonstrates that this conclusion is in error. Ni(cyclam)$^{+}$ and Ni(cyclam)$^{+}$-CO are unstable in water, but only because of their relatively slow oxidation to Ni(cyclam)$^{2+}$ by protons or water.

The steric bulk of the ligand also plays an important role in the selectivity of the catalyst. In all of the earlier studies of transition metal catalysis of CO_2 reduction (Chapter one), the addition of bulky groups on the cyclam ring lowered the efficiency of the catalyst. As can be seen from Table 5.1, the methyl groups on the amines of the ring drastically lower the peak CO_2 reduction current. In addition, this added steric bulk decreased the

selectivity of $Ni(TMC)^+$ for CO production over that of hydrogen.[1] It was proposed that this was due to the inability of CO_2 molecules to coordinate to $Ni(TMC)^+$ due to their larger size, whereas the smaller H^+ or H_20 species could coordinate. In another study by Sauvage and co-workers,[3] a $Ni_2(biscyclam)^{4+}$ species was investigated with regard to CO_2 and H_2O reduction. It was found that while $Ni(cyclam)^{2+}$ and $Ni_2(biscyclam)^{4+}$ are similar with respect to CO_2 reduction, $Ni_2(biscyclam)^{4+}$ was a much better catalyst for the evolution of hydrogen. The involvement of dihydride intermediates of the type Ni(H)-Ni(H) might be responsible for these results.

5.4 *Conclusions*

In this thesis, a mechanism has been proposed (Figure 5.7) which is compatible with the available data, both in this work and in previous experimental[1-5] and theoretical[23] studies. Although the electrochemical reduction of CO_2 as catalyzed by $Ni(cyclam)^+_{ads}$ is a much more complex system than previously described,[1-5] it is nonetheless quite efficient and selective. It would be informative to pursue several aspects of this system in more detail, and these areas are a good basis for future studies.

The structure of the $Ni(cyclam)^+$ complex on the mercury electrode surface is not definitively known at this time. Surface spectroscopic techniques, such as Raman or IR, would be helpful in establishing the configuration of the surface bound catalyst. CO_2 reduction can occur at potentials where the rearrangement represented by the small prepeak seen in the cyclic voltammetry of $Ni(cyclam)^{2+}$ (Figure 2.1) has not yet occurred, but it would still be helpful to identify what changes are associated with this rearrangement.

Although the kinetic studies discussed in Section 5.3.7 were less than exhaustive because of experimental limitations, further efforts in this area might prove informative.

Because of the negative potentials associated with the catalytic CO_2 reduction, the mercury coated RDE was not the best option as its background response obscured the response for the catalytic reduction of CO_2. It is believed that a pure mercury electrode, such as a HMDE or DME, would exhibit superior resolution. Any kinetic currents should be measured before the accumulation of the precipitate Ni(cyclam)^0-CO on the electrode surface affects the results. The most promising technique would be a potential step experiment in which the current is measured as soon as possible after the step.

Chapter 5 references

1. Beley, M.; Collin, J.-P.; Ruppert, R.; Sauvage, J.-P. *J. Am. Chem. Soc.* **1986**, *108*, 7461.
2. Beley, M.; Collin, J.-P.; Ruppert, R.; Sauvage, J.-P. *J. Chem. Soc., Chem. Commun.* **1984**, 1314.
3. Collin, J.-P.; Jouaiti, A.; Sauvage, J.-P. *Inorg. Chem.* **1988**, *27*, 1986.
4. Fujihira, M.; Hirata, Y.; Suga, K. *J. Electroanal. Chem.* **1990**, *292*, 199.
5. Fujihira, M.; Nakamura, Y.; Hirata, Y.; Akiba, U.; Suga, K. *Denki Kagaku* **1991**, *59*, 532.
6. Bosnich, B.; Tobe, M.L.; Webb, G.A. *Inorg. Chem.* **1965**, *8*, 1102,1109.
7. Barefield, E.K.; Wagner, F. *Inorg. Chem.* **1973**, *12*, 2435.
8. Wagner, F.; Barefield, E.K. *Inorg. Chem.* **1976**, *15*, 408.
9 Ciampolini, M.; Fabbrizzi, L.; Licchelli, M.; Perotti, A.; Pezzini, F.; Poggi, A. *Inorg. Chem.* **1986**, *25*, 4131.
10. Billo, E.J. *Inorg. Chem.* **1981**, *20*, 4019.
11. Stumm, W.; Morgan, J.J.; Aquatic Chemistry: An Introduction Emphasizing Chemical Equilibria in Natural Waters; Wiley and Sons: New York, 1981.
    Kern, D.M. *J. Chem. Ed.* **1960**, *37*, 14.
    Butler, J.N.; Carbon Dioxide Equilibria and Their Applications; Addison-Weseley: Cambridge, MA, 1982.
12. Creutz, C.; Scharwz, H.A.; Wishart, J.F.; Fujita, E.; Sutin, N. *J. Am. Chem. Soc.* **1989**, *111*, 1153.
13. Fujita, E.; Szalda, D.; Creutz, C.; Sutin, N. *J. Am. Chem. Soc.* **1988**, *110*, 4870.
14. Gangi, D.A.; Durand, R.R. *J. Chem. Soc., Chem. Commun.* **1986**, 697.
15. Schmidt, M.H.; Miskelly, G.M.; Lewis, N.S. *J. Am. Chem. Soc.* **1990**, *112*, 3420.

16. Gambarotta, S.; Arena, F.; Floriani, C.; Zanazzi, P.F. *J. Am. Chem. Soc.* **1982**, *104*, 5082.

17. Fachinetti, G.; Floriani, C.; Zanazzi, P.F. *J. Am. Chem. Soc.* **1978**, *100*, 7405.

18. Creutz, C.; Schwarz, H.A.; Wishart, J.F.; Fujita, E.; Sutin, N. *J. Am. Chem. Soc.* **1991**, *113*, 3361.

19. Darensbourg, D.J.; Kudaroski, R.A. *Adv. Organometallic Chem.* **1983**, *22*,129.

20. Vol'pin, M.E.; Kolomnikov, I.S. *Pure Appl. Chem.* **1973**, *33*, 576.

21. Vol'pin, M.E. *Pure Appl. Chem.* **1972**, *30*, 607.

22. Collman, J.P.; Hegedus, L.S.; Norton, J.R.; Finke, R.G.; Principles and Applications of Organotransition Metal Chemistry; University Science Books: Mill Valley, CA, 1987, p. 204.

23. Sakaki, S. *J. Am. Chem. Soc.* **1992**, *114*, 2055.

24. Cotton, F.A.; Wilkinson, G.; Advanced Inorganic Chemistry; Wiley and Sons: New York, 1988.

25. Gagné, R.R.; Ingle, D.M. *Inorg. Chem.* **1981**, *20*, 420.

26. Furenlid, L.R.; Renner, M.W.; Szalda, D.J.; Fujita, E. *J. Am. Chem. Soc.* **1991**, *113*, 883.

27. Craig, C.A.; Spreer, L.O.; Otvos, J.W.; Calvin, M. *J. Phys. Chem.* **1990**, *94*, 7957.

28. DuBois, D.L.; Miedaner, A.; Haltiwanger, R.C. *J. Am. Chem. Soc.* **1991**, *113*, 8753.

29. Busch, D.H.; Pillsbury, D.G.; Lovecchio, F.V.; Tait, A.M.; Hung, Y.; Jackels, S.; Rakowski, M.C.; Schammel, W.P.; Martin, L.Y. in Electrochemical Studies of Biological Systems, Sawyer, D.T., Ed.; ACS Symp. Ser. 38., Washington, 1977.

30. Taniguchi, I.; Shimpuku, T.; Yamashita, K.; Ohtaki, H. *J. Chem. Soc., Chem. Commun.* **1990**, 915.

31. Taniguchi, I.; Nakashima, N.; Matsushita, K.; Yasukouchi, K. *J. Electroanal. Chem.* **1987**, *224*, 199.

32. Bard, A.J.; Faulkner, L.F. Electrochemical Methods; Wiley and Sons: New York, 1980, p. 280.

33. Fischer, B.; Eisenberg, R. *J. Am. Chem. Soc.* **1980**, *102*, 7361.

34. Busch, D.H. *Acc. Chem. Res.* **1978**, *11*, 392.

35. Cabbiness, D.K.; Margerum, D.W. *J. Am. Chem. Soc.* **1970**, *92*, 2151.

36. Jubran, N.; Cohen, H.; Meyerstein, D. Israel J. Chem. 1985, 25, 118.

Bosnich, B.; Mason, R.; Pauling, P.J.; Robertson, G.B.; Tobe, M.L. *Chem. Commun.* **1965**, 97.

Adam, K.R.; Antolovich, M.; Brigden, L.G.; Lindoy, L.F. *J. Am. Chem. Soc.* **1991**, *113*, 3346.

Thöm, V.J.; Fox, C.C.; Boeyens, J.C.A.; Hancock, R.D. *J. Am. Chem. Soc.* **1984**, *106*, 5947.

Table 5.1 Summary of peak potentials and currents obtained from cyclic voltammetry of CO_2 reduction as catalyzed by various Ni(II) tetraazamacrocycles. 0.1 M $KClO_4$ solutions saturated with CO_2, concentration of NiL^{2+} is 1 mM. Scan rate is 100 mV sec^{-1}.

Ni(II) macrocycle	Peak Potential, V vs SCE	Peak Current, μA
$Ni(cyclam)^{2+}$	-1.41	200
cis-$Ni(cyclam)^{2+}$	-1.41	78
$Ni(MMC)^{2+}$	-1.40	110
$Ni(DMC)^{2+}$	-1.36	15
$Ni(TMC)^{2+}$	-1.53	7